# Cubic Polynomial Maps with Periodic Critical Orbit, Part I

John Milnor

March 6, 2008

**Dedicated to JHH:**

Julia sets looked peculiar—
Unruly and often unrulier—
Till young Hubbard with glee
Shrank each one to a tree
And taught us to see them much trulier.

***This will be a discussion of the dynamic plane and the parameter space for complex cubic maps which have a superattracting periodic orbit. It makes essential use of Hubbard trees to describe associated Julia sets.***

## 1 Introduction.

The parameter space for cubic polynomial maps has complex dimension 2. Its non-hyperbolic subset is a complicated fractal locus which is difficult to visualize or study. One helpful way of exploring this space is by means of complex 1-dimensional slices. This note will pursue such an exploration by studying maps belonging to the complex curve $\mathcal{S}_p$ consisting of all cubic maps with a superattracting orbit of period $p$. Here $p$ can be any positive integer.

A preliminary draft of this paper, based on conversations with Branner, Douady and Hubbard, was circulated in 1991 but not published. The present version tries to stay close to the original; however, there has been a great deal of progress in the intervening years. (See especially (Faught 92), (Branner and Hubbard 92), (Branner 93), (Roesch 99, 06), and (Kiwi 06).) In particular, a number of conjectures in the original have since been proved; and new ideas have made sharper statements possible.

We begin with the period 1 case. Section 2 studies the dynamics of a cubic polynomial map $F$ which has a superattracting fixed point, and whose Julia set $J(F)$ is connected. The filled Julia set of any such map consists of a central Fatou component bounded bounded by a Jordan curve, together with various ***limbs*** sprouting off at internal angles which are explicitly described.

(See Figures 2, 3. This statement was conjectured in the original manuscript and then proved by Faught.) Section 3 studies the parameter space $\mathcal{S}_1$ consisting of all (monic, centered) cubic maps with a specified superattractive fixed point, and provides an analogous description of the non-hyperbolic locus in $\mathcal{S}_1$. (See Figure 4.) Section 4 makes a more detailed study of hyperbolic components in $\mathcal{S}_1$. Section 5 begins the study of the period $p$ case, describing the geometry of the complex affine curve $\mathcal{S}_p$ consisting of maps with a marked critical point of period $p$. This is a non-compact complex 1-manifold; but can be made into a compact complex 1-manifold $\overline{\mathcal{S}}_p$ by adjoining finitely many ***ideal points***. There is a conjectured cell subdivision of $\overline{\mathcal{S}}_p$ with a 2-cell centered at each ideal point, and with the union of all ***simple closed regulated curves*** as 1-skeleton. To each quadratic map $Q(z) = z^2 + c$ with period $p$ critical orbit, there is associated a 2-cell $\mathbf{e}_Q$. Section 6 describes a conjectural canonical embedding of the filled Julia set $K(Q)$, cut open along its minimal Hubbard tree, into this 2-cell. (However, there are many other 2-cells which cannot be described in this way.) This paper concludes with an Appendix which discusses ***Hubbard trees***, following (Poirier 93), and also describes the slightly modified ***puffed-out*** Hubbard trees.

## 1A. Basic Concepts and Notations.

Any polynomial map $F : \mathbb{C} \to \mathbb{C}$ of degree $d \geq 2$ is affinely conjugate to one which is ***monic*** and ***centered***, that is, of the form

$$F(z) \;=\; z^d + c_{d-2}z^{d-2} + \cdots + c_0\ .$$

This normal form is unique up to conjugation by a $(d-1)$-st root of unity, which replaces $F(z)$ by $G(z) = \omega\, F(z/\omega)$ where $\omega^{d-1} = 1$, and replaces the Julia set $J(F)$ by the rotated Julia set $J(G) = \omega\, J(F)$.

The set $\mathcal{P}(d)$ of all such monic, centered maps forms a complex $(d-1)$-dimensional affine space. A polynomial $F \in \mathcal{P}(d)$ belongs to the ***connectedness locus*** $\mathcal{C}(\mathcal{P}(d))$ if its Julia set $J(F)$ is connected, or equivalently if the orbit of every critical point is bounded. This connectedness locus is always a compact cellular subset of $\mathcal{P}(d)$. This was proved by (Branner and Hubbard 88) for the cubic case, and by (Lavaurs 89) for higher degrees. (See also (Branner 86). By definition, following (Brown 60), a subset of some Euclidean space $\mathbb{R}^n$ is ***cellular*** if its complement in the sphere $\mathbb{R}^n \cup \infty$ is an open topological cell.)

A polynomial map $F$ is ***hyperbolic*** if the orbit of every critical point converges to an attracting cycle. (See for example (Milnor 06, §19).) The set $\mathcal{H}$ consisting of all hyperbolic maps in $\mathcal{C}(\mathcal{P}(d))$ is a disjoint union of open topological cells, each containing a unique post-critically finite map which will be called its ***center***. (Compare (Milnor 92b).) Thus every critical orbit of such a center map is either periodic or eventually lands on a periodic critical orbit. One noteworthy special case is the ***principal hyperbolic component*** $\mathcal{H}_0 \subset \mathcal{C}(\mathcal{P}(d))$, centered at the map $z \mapsto z^d$, and consisting of all $F \in \mathcal{H} \subset \mathcal{P}(d)$ such that $J(F)$ is a Jordan curve. (For a study of $\mathcal{H}_0$ in the degree 3 case, see (Petersen and TanLei 04).)

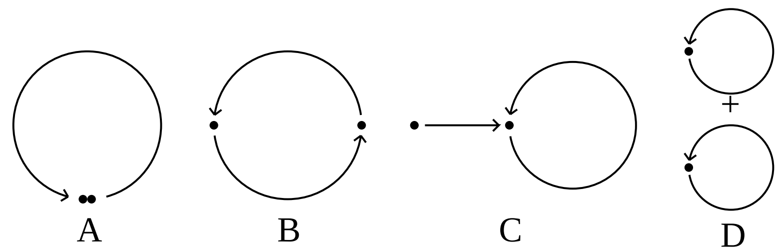

Figure 1: Schematic diagrams for the four classes of cubic hyperbolic components. Each dot represents a critical point (or the Fatou component containing it), and each arrow represents some iterate of $F$.

Hyperbolic components in $\mathcal{C}(\mathcal{P}(3))$ fall into four distinct types as follows. (Compare (Milnor 92a).) For components of the first three types, the corresponding maps have just one attracting periodic orbit, and hence just one cycle of periodic Fatou components.

**A. Adjacent Critical Points**, with both critical points in the same periodic Fatou component.

**B. Bitransitive**, with the two critical points in different Fatou components belonging to the same periodic cycle.

**C. "Capture"**, with just one critical point in the cycle of periodic Fatou components. The orbit of the other critical point must eventually land in (or be "captured by") this cycle.

**D. Disjoint Attracting Orbits**, with two distinct attracting periodic orbits, each of which necessarily attracts just one critical orbit.

**Remark 1.1. Outside the Connectedness Locus.** There are many hyperbolic components in $\mathcal{P}(3)$ which belong to the complement of the connectedness locus. These will be called ***escape components***, since they consist of hyperbolic maps for which at least one critical orbit "escapes to infinity," so that the Julia set is disconnected.

One such component, called the ***shift locus***, has an extremely complicated topological structure. (Compare (Blanchard *et al.* 91).) It consists of maps for which the Julia set is isomorphic to a one-sided shift on three symbols. (More generally, a polynomial or rational map of degree $d$ belongs to the ***shift locus*** if its Julia set is isomorphic to the one-sided shift on $d$ symbols. A completely equivalent condition is that all of its critical points on the Riemann sphere belong to the immediate basin of a common attracting fixed point, which must be the point at infinity in the polynomial case.)

For maps in the remaining escape components in $\mathcal{P}(3) \smallsetminus \mathcal{C}(\mathcal{P}(3))$, there is only one critical point in the basin of infinity, while the other critical point belongs to the immediate basin of a bounded attracting periodic orbit. We will give a rough classification of these components in Section5.

Here is a rough picture of the complement $\mathcal{P}(3) \smallsetminus \mathcal{C}(\mathcal{P}(3))$. (See (Branner 93).) Take a large sphere centered at the origin in the space $\mathcal{P}(3) \cong \mathbb{C}^2$. Then each escape hyperbolic component with an attracting orbit intersects this 3-sphere in an embedded solid torus, which forms one interior component of a

"***Mandelbrot torus***", that is, a product of the form (Mandelbrot set)$\times$(circle). There are countably many such Mandelbrot-tori, and also many connected components without interior, for example solenoids or circles, corresponding to polynomials whose Julia set is a Cantor set which contains one critical point. If we remove all of these Mandelbrot-tori, solenoids, etc., from the 3-sphere, then what is left are points of the shift locus. (Compare Remark 4.1 and Figure 15.)

**Remark 1.2. Quadratic Rational Maps.** (Compare (Rees 90, 92, 95), (Milnor 93).) In a suitable parameter space for quadratic rational maps, there are again four different types of hyperbolic components. One of these is the shift locus as described above. (In the terminology of Rees, this is of Type I.) The remaining three are precise analogues of Types B, C, D (or in Rees's terminology, Types II, III, IV).

**Caution:** I have used the term "capture component" for components of Type C, even for quadratic rational maps. However, extreme care is needed, since the term "***capture***" is often used with a completely different meaning. See for example (Wittner 88), (Rees 92), and (Luo 95), where this word refers instead to a procedure for modifying the dynamics of a quadratic polynomial to yield a quadratic rational map.

**Definition 1.3. The Moduli Space $\hat{\mathcal{P}}(3)/\mathcal{I}$.** We are interested in cubic maps for which one of the two critical points has a periodic orbit. Hence it is convenient to work with the space $\hat{\mathcal{P}}(3)$ consisting of monic centered cubic maps together with a ***marked critical point*** $a$. Since there are two possible choices for the marked point, this space $\hat{\mathcal{P}}(3)$ is a 2-fold ramified covering of $\mathcal{P}(3)$. Each $F \in \hat{\mathcal{P}}(3)$ can be written in ***Branner-Hubbard normal form*** as

$$F(z) \;=\; z^3 - 3a^2 z + b\,, \tag{1}$$

with critical points $a$ and $-a$. Thus $\hat{\mathcal{P}}(3)$ could be identified with the complex coordinate space $\mathbb{C}^2$, using $a,\, b$ as coordinates. However, for the purposed of this paper, it will be more convenient to use coordinates $(a, v)$ where $a$ is the marked critical point and

$$v \;=\; F(a) \;=\; b - 2a^3$$

is the corresponding critical value. We will write

$$F(z) \;=\; F_{a,v}(z) \;=\; z^3 \;-\; 3a^2 z \;+\; (2a^3 + v)\,, \tag{2}$$

and will use the notations $\hat{\mathcal{H}}_0 \subset \mathcal{C}(\hat{\mathcal{P}}(3)) \subset \hat{\mathcal{P}}(3)$ for the corresponding principal hyperbolic component and connectedness locus in the complex $(a, v)$-plane.

It is not hard to check that two distinct maps $F_{a,v}$ and $F_{a',\,v'}$ in $\hat{\mathcal{P}}(3)$ are affinely conjugate, in a conjugacy which carries the marked critical point $a$ to the marked critical point $a'$, if and only if $a' = -a$ and $v' = -v$, with conjugacy $z \mapsto -z$. Thus we define the ***canonical involution*** $\mathcal{I}$ of $\hat{\mathcal{P}}(3)$ to be the correspondence $F(z) \mapsto -F(-z)$, taking $F_{a,v}$ to $F_{-a,\,-v}$ and rotating the associated Julia set by 180° degrees. The quotient $\hat{\mathcal{P}}(3)/\mathcal{I}$ can be described as the ***moduli space***, consisting of all affine conjugacy classes of cubic polynomials with marked critical point. (Thus I distinguish between a "parameter space," whose elements are actual maps, and a "moduli space" made up of conjugacy classes of maps.) A complete set of conjugacy class invariants for a polynomial $F$ with marked critical point is provided by the numbers $a^2$ and $v^2$, together with a choice of square root $av = \pm\sqrt{a^2v^2}$ which is needed to specify the choice of marking. Thus $\hat{\mathcal{P}}(3)/\mathcal{I}$ can be identified with an algebraic variety in $\mathbb{C}^3$, with coordinates $a^2$, $v^2$, $av$ satisfying a homogeneous quadratic equation. This variety has a mild singularity at the origin.

One special feature of cubic maps is that for each critical point there is a uniquely defined ***co-critical point*** which has the same image under $F$. Using the normal form of Equation (1) or (2), the marked point $a$ has co-critical point $-2a$, while $-a$ has co-critical point $+2a$. (Even if we don't use this normal form, the critical points, co-critical points, and their center of gravity will still lie in arithmetic progression along a straight line in the $z$-plane.)

# 2 Maps with critical fixed point: the Julia set.

Before trying to understand configurations in parameter space, it is important to study the $z$-plane. We first consider the case of a superattracting orbit of period one. That is, using the normal form $F(z) = z^3 - 3a^2z + 2a^3 + v$, we consider maps satisfying $F(a) = a$, or in other words[1]

$$v \;=\; a\,, \qquad\qquad F(z) \;= F_{a,a}(z) \;=\; z^3 - 3a^2z + (2a^3 + a)\,. \qquad (3)$$

The locus of all such maps is denoted by $\mathcal{S}_1$. Let $U_a$ be the ***immediate attracting basin*** of the superattracting point $a$ under this map $F$. Thus $U_a$ is a simply connected bounded open neighborhood of $a$.

Let $\mathcal{C}(\mathcal{S}_1) = \mathcal{S}_1 \cap \mathcal{C}(\hat{\mathcal{P}}(3))$ be the connectedness locus within $\mathcal{S}_1$. If $F \in \mathcal{C}(\mathcal{S}_1)$, then the filled Julia set $K(F)$ (the complement of the attracting basin of infinity) is a compact connected subset of the $z$-plane. We divide the discussion into two cases, according as the ***free critical point*** $-a$ does or does not belong to the immediate basin $U_a \subset K(F)$.

**Case 1 (Hyperbolic of Type A):** Suppose that $F \in \mathcal{S}_1 \cap \hat{\mathcal{H}}_0$. In other words, suppose that $F$ belongs to the unique hyperbolic component of Type A within $\mathcal{S}_1$, so that the other critical point $-a$ also belongs to the immediate basin $U_a$ of the superattracting point $a$. In this case, the dynamics is quite well understood. The Julia set $J(F) = \partial K(F)$ is a Jordan curve. The bounded component of its complement is the attractive basin $U_a$, and the unbounded component is the attractive basin of infinity. Furthermore, the

[1] An extra motive for studying this particular family of maps is the close relationship between this family of cubic maps and the family of rational maps which arise from cubic polynomial equations via Newton's method. See (TanLei 97).

map $F$ restricted to $U_a$ is conformally conjugate to a Blaschke product of the form $\Psi(w) = e^{2\pi it}w^2(r-w)/(1-rw)$, with $t \in \mathbb{R}/\mathbb{Z}$ and $0 \le r < 1$; and this conformal conjugacy extends homeomorphically over the closure $\overline{U}_a$. The map $F$ is uniquely determined, up to affine conjugacy, by the parameter $e^{2\pi it}r$, which varies over the open unit disk $\mathbb{D}$; however, $F$ does not depend holomorphically on this parameter. (A holomorphic parametrization will be described in Lemma 3.6.)

**Case 2 (Everything Else):** For the rest of this section we will concentrate on the more difficult case where $F \in \mathcal{C}(\mathcal{S}_1)\smallsetminus\hat{\mathcal{H}}_0$. *In other words, we will assume that both critical points have bounded orbits, and that the free critical point $-a$ lies outside the immediate basin $U_a$ of the superattracting critical point $a$.* Then there is a unique ***Böttcher isomorphism*** from the basin $U_a$ onto the open unit disk which conjugates $F$ to the squaring map $w \mapsto w^2$, that is

$$\beta \,:\, U_a \xrightarrow{\cong} \mathbb{D} \qquad \text{with} \qquad \beta(F(z)) \;=\; \beta(z)^2\,. \tag{4}$$

(See for example (Blanchard 84) or (Milnor 06).) According to (Faught 92) (see also (Roesch 99, 06), the boundary $\partial U_a$ is locally connected, and in fact is a simple closed curve. By a well known theorem of Carathéodory, this implies that the Böttcher map extends uniquely to a homeomorphism

$$\beta \,:\, \overline{U}_a \;\to\; \overline{\mathbb{D}}$$

from the closure of $U_a$ to the closed unit disk. (See for example (Milnor 06, §17.16).) In particular, each point $z$ of the boundary $\partial U_a$ can be uniquely labeled by its ***internal angle*** $t \in \mathbb{R}/\mathbb{Z}$, where $z = \beta(e^{2\pi it})$. (Angles are always measured in fractions of a full turn.)

Making use of Faught's result, we will prove the following.

**Theorem 2.1.** *If $F \in \mathcal{C}(\mathcal{S}_1)$ with $-a \notin U_a$, then the filled Julia set $K(F)$ is equal to the union of the topological disk $\overline{U}_a$ with a collection of compact connected sets $K_t$, where $t$ ranges over a countably subset $\Lambda$ of the circle $\mathbb{R}/\mathbb{Z}$. Furthermore*

**(i)** *The $K_t$ are pairwise disjoint, and each $K_t$ intersects $\overline{U}_a$ in the single boundary point $\beta(e^{2\pi it})$.*

**(ii)** *There is a preferred element $t_0 \in \Lambda$ such that the free critical point $-a$ belongs to $K_{t_0}$.*

**(iii)** *The angle $t$ belongs to this index set $\Lambda \subset \mathbb{R}/\mathbb{Z}$ if and only if $2^n t \equiv t_0 \pmod{\mathbb{Z}}$ for some integer $n \ge 0$.*

**(iv)** *For $t \not\equiv t_0 \pmod{\mathbb{Z}}$, the map $F$ carries $K_t$ homeomorphically onto $K_{2t}$. However, $F$ carries $K_{t_0}$ onto the entire filled Julia set $K(F)$.*

By definition, $K_t$ is the ***limb*** which is attached to $\overline{U}_a$ at the point $\beta(e^{2\pi it})$ with internal angle $t$, and $K_{t_0}$ is the ***critical limb***.

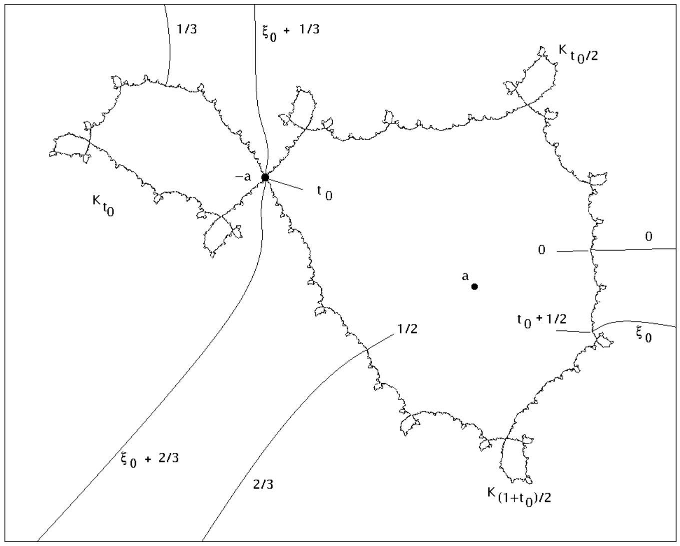


Figure 2: Julia set for an $F \in \mathcal{S}_1$ on the boundary of $\hat{\mathcal{H}}_0$ with non-periodic internal angle. Note that there is no limb at the critical value. The two rays which land at the critical point fold together to a single ray. (In this particular example, the critical internal angle is $t_0 = .34326\cdots$, and the external angle at the co-critical point is $\xi_0 = .95884\cdots$.)

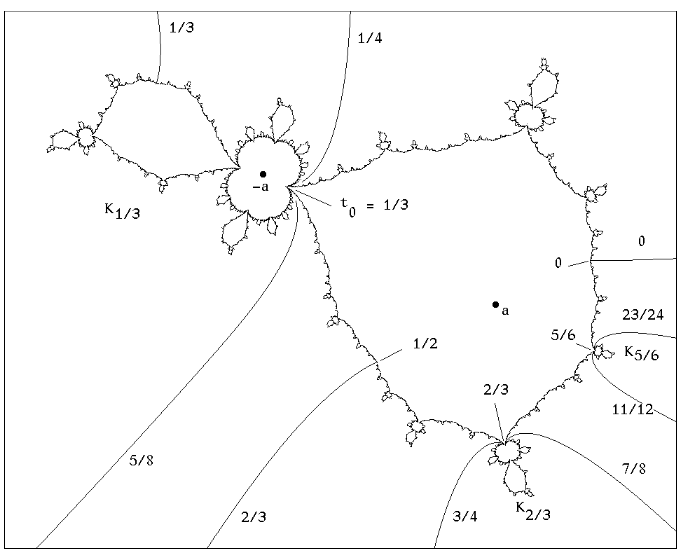


Figure 3: *Julia set for a map* $F \in \mathcal{S}_1$ *on the boundary of* $\hat{\mathcal{H}}_0$ *with periodic internal angle* $t_0 = 1/3$.

In fact, there are two rather different cases. In the simplest case (Figure 2), the critical angle $t_0$ is not periodic under angle doubling. In other words, $t_0$ is either irrational, or rational with even denominator. The critical limb $K_{t_0}$ then maps homeomorphically onto the entire filled Julia set, and the free critical point $-a$ is precisely equal to the boundary point $\beta(e^{2\pi i t_0}) \in \partial U_a$. Furthermore, the map $F$ itself, considered as a point in parameter space, belongs to the boundary $\partial\hat{\mathcal{H}}_0$ of the principal hyperbolic component.

On the other hand, if the critical angle $t_0$ is periodic under angle doubling, then $-a$ lies strictly outside of $\overline{U}_a$. In this case, the critical limb $K_{t_0}$ is the union of an "inner" part which maps onto the critical value limb $K_{2t_0}$ by a 2-fold branched covering, and an "outer" part which maps homeomorphically onto $K(F) \smallsetminus K_{2t_0}$. The map $F$ may belong to the boundary $\partial\hat{\mathcal{H}}_0$ (compare Figure 3), or it may lie completely outside the closure of $\hat{\mathcal{H}}_0$.

The proof of Theorem 2.1 will be based on a comparison between internal angles, measured at the critical fixed point $a$, and external angles, measured at infinity. Note that internal angles multiply by two under the map $F$, while external angles multiply by three. Equality between angles will be denoted by the symbol $\equiv$ with $\pmod{\mathbb{Z}}$ understood.

**Definition 2.2.** Angles $t_1, \ldots, t_k$ are in ***positive cyclic order*** if it is possible to choose representatives $\hat{t}_j \in \mathbb{R}$ so that $\hat{t}_1 < \cdots < \hat{t}_k < \hat{t}_1 + 1$. For any $t_1 \not\equiv t_2$ in $\mathbb{R}/\mathbb{Z}$, the ***open interval*** $\boldsymbol{(}t_1, t_2\boldsymbol{)}$ will mean the set of all angles $t \in \mathbb{R}/\mathbb{Z}$ for which $t_1, t, t_2$ are in positive cyclic order. The corresponding ***closed interval*** $\boldsymbol{[}t_1, t_2\boldsymbol{]}$ is defined to be the closure of $\boldsymbol{(}t_1, t_2\boldsymbol{)}$. Note that these intervals have ***length*** equal to $\mathbf{frac}(t_2 - t_1)$, where $\mathbf{frac} : \mathbb{R}/\mathbb{Z} \to [0, 1)$ maps each point of the circle $\mathbb{R}/\mathbb{Z}$ to its unique representative in the half-open interval.

**Basic Construction.** For each rational angle $\tau \in \mathbb{Q}/\mathbb{Z}$, the internal ray of angle $\tau$ lands at a point

$$\beta(e^{2\pi i \tau}) \in \partial U_a \subset J(F)$$

which is periodic or preperiodic under $F$. It follows that $\beta(e^{2\pi i \tau})$ is also the landing point of at least one external ray $\mathcal{R}_\xi \subset \mathbb{C} \smallsetminus K(F)$ which is periodic or preperiodic. (See for example (Milnor 06, §18.11 and §18.12).) There can be at most finitely many such rays, so we can make an explicit choice $\xi = \xi(\tau)$ by choosing the largest one in cyclic order, measured from the internal ray which lands at this same point. The identity

$$\xi(2\,\tau) \;\equiv\; 3\,\xi(\tau) \tag{5}$$

then follows easily.

**Definition 2.3.** Let $G : \mathbb{C} \to [0, \infty)$ be the Green's function (= canonical potential function) which vanishes precisely on $K(F)$. Given two rational internal angles $\tau_0 \not\equiv \tau_1$ in $\mathbb{Q}/\mathbb{Z}$, and given some equipotential curve $G = G_0 > 0$, define the ***quadrilateral*** $\mathcal{Q} = \mathcal{Q}(\tau_0, \tau_1, G_0)$ to be the compact simply connected region in $\mathbb{C} \smallsetminus U_a$ which is bounded by three edges in the Fatou set and one edge in the Julia set, as follows.

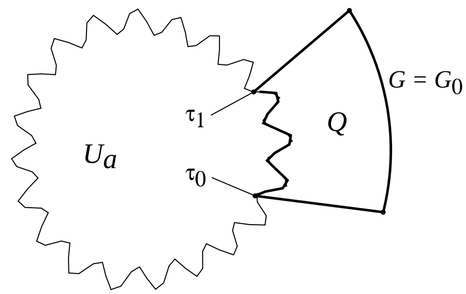


Figure 4: *Sketch of the quadrilateral* $\mathcal{Q} = \mathcal{Q}(\tau_0, \tau_1, G_0)$.

**(a)** The segments of the external rays $\mathcal{R}_{\xi(\tau_0)}$ and $\mathcal{R}_{\xi(\tau_1)}$ defined by the potential inequality $G \le G_0$.

**(b)** The segment of the equipotential curve $G = G_0$ which lies between these two external rays so that the external angle lies in the closed interval $[\,\xi(\tau_0),\, \xi(\tau_1)\,]$.

**(c)** The segment of the boundary $\partial U_a$ consisting of all $\beta(e^{2\pi i t})$ with $t \in [\,\tau_0,\, \tau_1\,]$.

Note that this quadrilateral $\mathcal{Q}$ contains all limbs which are attached to $\overline{U}_a$ at internal angles strictly between $\tau_0$ and $\tau_1$ in cyclic order.

**Lemma 2.4.** *Now suppose that the length* $\mathbf{frac}(\tau_1 - \tau_0)$ *of the interval* $(\tau_0, \tau_1)$ *of internal angles is less than* $1/2$*, and also that the length of the corresponding interval* $(\xi(\tau_0), \xi(\tau_1))$ *of external angles satisfies*

$$\mathbf{frac}\Big(\xi(\tau_1) - \xi(\tau_0)\Big) \; < \; 1/3\,. \tag{6}$$

*Then the quadrilateral* $\mathcal{Q} = \mathcal{Q}(\tau_0, \tau_1, G_0)$ *contains no critical point, and maps biholomorphically onto the quadrilateral* $\mathcal{Q}' = \mathcal{Q}(2\,\tau_0,\, 2\,\tau_1,\, 3\,G_0)$*. But if*

$$\mathbf{frac}\Big(\xi(\tau_1) - \xi(\tau_0)\Big) \; > \; 1/3\,, \tag{7}$$

*with* $\mathbf{frac}(\tau_1 - \tau_0) < 1/2$ *as above, then* $\mathcal{Q}$ *contains the free critical point* $-a$*, and maps onto the entire region* $\{G \le 3\,G_0\}$*. In this case, points in* $\mathcal{Q}'$ *have two preimages in* $\mathcal{Q}$*, counted with multiplicity, while the remaining points in the region* $\{G \le 3\,G_0\}$ *have only one preimage.*

**Proof.** Let $z_0$ be any point of $\mathbb{C}$ which does not belong to the image $F(\partial\mathcal{Q})$ of the boundary of $\mathcal{Q}$. By the Argument Principle, the number of solutions to the equation $F(z) = z_0$ with $z \in \mathcal{Q}$, counted with multiplicity, is equal to the winding number of $F(\partial\mathcal{Q})$ around $z_0$. If we are in the case of Equation (6), then it is not hard to check that $F$ maps this boundary homeomorphically onto the boundary $\partial\mathcal{Q}'$. Hence this winding number is $+1$ for $z_0$ in the interior of $\mathcal{Q}'$, and zero for $z_0$ outside. For the case of Equation (7), the argument is similar, but now the image $F(\partial\mathcal{Q})$ consists of a circuit around $\partial\mathcal{Q}'$, together with a circuit around the entire equipotential $G = 3\,G_0$.

To check for the presence of critical points, we use a form of the Riemann-Hurwitz formula. Choose a cell subdivision of $F(\mathcal{Q})$, with $\mathcal{Q}'$ as subcomplex (if it is not the entire image), and with $F(-a)$ as vertex if $-a \in \mathcal{Q}$. Then each cell in $F(\mathcal{Q})$ lifts up to either a single cell in $\mathcal{Q}$ if it lies outside of $\mathcal{Q}'$, or if it is equal to the vertex $F(-a)$, or to two cells in $\mathcal{Q}$. Computing the Euler characteristic,

$$\chi \;=\; \sum_{n=0}^{2}(-1)^n(\text{number of } n \text{ cells}) \;=\; +1$$

for both $\mathcal{Q}$ and $F(\mathcal{Q})$, we find easily that $-a \in \mathcal{Q}$ if and only if we are in the second case (7). (Furthermore, the critical value $F(-a)$ then belongs to $\mathcal{Q}'$. A similar argument shows that the third case $\xi(\tau_1) \in \big(\,\xi(\tau_0) + \frac{2}{3},\ \xi(\tau_0) + 1\,\big)$ cannot occur.) $\square$

**Proof of Theorem 2.1.** For each internal angle $t \in \mathbb{R}/\mathbb{Z}$, define $K_t$ to be the intersection of all quadrilaterals $\mathcal{Q}(\tau_0,\, \tau_1,\, G_0)$ for which $t \in \big(\,\tau_0,\, \tau_1\,\big)$ and $G_0 > 0$. Then $K_t$ can be described as the intersection of a nested sequence of compact, connected, non-vacuous sets, and hence is itself compact, connected, and non-vacuous.

For every $t$, it is easy to check that the intersection $K_t \cap \overline{U}_a$ consists of the single point $\beta(e^{2\pi i t})$. For countably many choices of $t$, we will see that $K_t$ is much larger than this single intersection point. The following statement follows immediately from Lemma 2.4.

> *For each $t \not\equiv t_0$, the map $F$ carries $K_t$ homeomorphically onto $K_{2t}$. However, $F$ carries $K_{t_0}$ onto the entire filled Julia set $K(F)$.*

In particular, if $2^n t \equiv t_0$, then it follows that $F^{\circ(n+1)}$ maps $K_t$ onto $K(F)$, so that $K_t$ contains infinitely many points. To complete the proof of Theorem 2.1, we need only prove a converse statement:

> *If $2^n t \not\equiv t_0$ for all $n \neq 0$, then $K_t$ consists of the single point $\beta(e^{2\pi i t})$.*

Define the ***angular width*** $\Delta\xi(\mathcal{Q})$ of a quadrilateral $\mathcal{Q} = \mathcal{Q}(\tau_0,\, \tau_1,\, G_0)$, to be the length of the interval $\big(\,\xi(\tau_0),\ \xi(\tau_1)\,\big) \subset \mathbb{R}/\mathbb{Z}$; and define the angular width $\Delta\xi(K_t)$ of the set $K_t$ to be the infimum of $\Delta\xi(\mathcal{Q})$ over all quadrilaterals $\mathcal{Q}$ which contain $K_t$. In other words, this angular width

$$0 \;\le\; \Delta\xi(K_t) \;<1$$

is the infimum, over all open intervals $\big(\,\tau_0,\, \tau_1\,\big)$ which contain $t$, of the length of the interval $\big(\,\xi(\tau_0),\ \xi(\tau_1)\,\big)$. (Intuitively, this is just the infimum of $\xi(\tau_1) - \xi(\tau_0)$.)

**Lemma 2.5.** *This angular width satisfies*

$$\Delta\xi(K_{2\,t}) \;=\; 3\Delta\xi(K_t) \qquad \textit{for} \qquad t \not\equiv t_0\,,$$

but

$$\Delta\xi(K_{2\,t_0}) \;=\; 3\,\Delta\xi(K_{t_0}) \,-\, 1\,.$$

**Proof.** The congruence $\Delta\xi(K_{2\,t_0}) \equiv 3\,\Delta\xi(K_{t_0}) \pmod{\mathbb{Z}}$ follows immediately from Equation (5), and the more precise statement then follows from Lemma 2.4. □

To complete the proof of Theorem 2.1, consider any angle $t$ such that $K_t$ contains more than one point. Since the boundary of the connected set $K_t$ is contained in the Julia set, and since repelling periodic points are dense in the Julia set, it follows that $K_t$ contains many repelling periodic points. Each of these must be the landing point of an external ray, and it follows easily that $\Delta\xi(K_t) > 0$.

But if this were true with $2^n t \not\equiv t_0$ for all $n \geq 0$, then it would follow inductively from Lemma 2.5 that

$$\Delta\xi(K_{2^n t}) \;=\; 3^n\Delta\xi(K_t) \;\to\infty \quad \text{as} \quad n\to\infty\,.$$

which is clearly impossible. This shows that $K_t$ contains more than one point if and only if some forward image is equal to the critical limb $K_{t_0}$, which proves Theorem 2.1. □

Next we will show that each limb is separated from the rest of $K(F)$ by two external rays. Recall that $\Lambda \subset \mathbb{R}/\mathbb{Z}$ is the countable set consisting of all $t$ such that $2^n t \equiv t_0$ for some $n \geq 0$. For each internal angle $t$, consider the closed intervals $[\,\xi(\tau_0),\, \xi(\tau_1)\,]$ of external angles which are associated with quadrilaterals $\mathcal{Q}(\tau_0,\, \tau_1,\, G_0)$ such that $t \in (\,\tau_0,\, \tau_1\,)$. If $t \in \Lambda$, then evidently these closed intervals intersect in an interval, to be called $[\,\xi^-(t),\, \xi^+(t)\,]$, with length equal to the angular width $\Delta\xi(K_t) > 0$. On the other hand, if $t \notin \Lambda$, so that $\Delta\xi(K_t) = 0$, then a similar argument show that the intervals $[\,\xi(\tau_0),\, \xi(\tau_1)\,]$ intersect in a single point $\xi(t)$.

**Theorem 2.6.** *For each $t \in \Lambda$, the two external rays $\mathcal{R}_{\xi^{\pm}(t)}$ both land at the point of attachment $\beta(e^{2\pi i t})$ for the limb $K_t$, and these rays together with their landing point, separate $K_t$ from the rest of $K(F)$. For $t \notin \Lambda$, the external ray $\mathcal{R}_{\xi(t)}$ lands at $\beta(e^{2\pi i t})$, and no other ray accumulates at this point.*

**Proof.** First suppose that $t \notin \Lambda$. Then it follows from the proof of Theorem 2.1 that $K_t$ consists of the single point $\beta(e^{2\pi i t})$, and that $\Delta\xi(K_t) = 0$. This means that we can find quadrilaterals $\mathcal{Q}(\tau_0,\, \tau_1,\, G_0)$ such that the open interval $(\,\tau_0,\, \tau_1\,)$ is arbitrarily small, and contains $t$, and such that the interval $[\,\xi(\tau_0),\, \xi(\tau_1)\,]$ of exterior angles is also arbitrarily small. Taking the intersection of $[\,\xi(\tau_0),\, \xi(\tau_1)]$ over all such quadrilaterals, we clearly obtain a single exterior angle $\xi(t)$. Let $X_t \subset J(F)$ be the set of all accumulation points for the corresponding external ray $\mathcal{R}_{\xi(t)}$. For every $t' \not\equiv t$, the set $X_t$ is separated from $K_{t'}$ by some rational external ray. Hence $X_t$ must consist of the singleton $K_t$, as required. Similarly, for any $\xi' \not\equiv \xi(t)$, the ray $\mathcal{R}_{\xi'}$ is separated from $K_t$ by some rational external ray, and hence cannot accumulate on $K_t$.

Now suppose that $t \in \Lambda$. If $t_0$ is not periodic under angle doubling, then $2t_0 \notin \Lambda$, so that there is a single ray $\mathcal{R}_{\xi(2t_0)}$ landing at the critical value $F(-a)$. Since $F$ carries a neighborhood of $-a$ to a neighborhood of $F(-a)$ by a 2-fold branched covering, it follows that exactly two rays land at $-a = \beta(e^{2\pi i t_0})$.

On the other hand, if $t_0$ is periodic, then the point of attachment $\beta(e^{2\pi i t_0})$ is a periodic point of rotation number zero in the Julia set, and there are exactly two ways of accessing $\beta(e^{2\pi i t_0})$ from $\mathbb{C} \setminus K(F)$, or in other words, exactly two prime ends of $\mathbb{C} \setminus K(F)$ which map to $\beta(e^{2\pi i t_0})$. Hence, again there must be exactly two external rays which land on $\beta(e^{2\pi i t_0})$. (See for example (Milnor 06, §§17, 18).) In either case, these two rays, together with their common landing point, must separate at least one limb from $U_a$. Since no other limb can have this property, it follows that these two rays must separate $K_{t_0}$ from the rest of $K(F)$. It is then easy to check that the two rays must be precisely $\mathcal{R}_{\xi^\pm(t_0)}$. The corresponding statement for an arbitrary limb $K_t$ then follows, since $F^{\circ n} : K_t \xrightarrow{\cong} K_{t_0}$ for some $n \geq 0$. $\square$

**Remark 2.7.** It follows easily that there is a canonical retraction from $\mathbb{C} \setminus \{a\}$ to the circle $\partial U_a$ which carries each limb to its point of attachment, and which takes a constant value on each internal or external ray. In particular, there is a canonical map $T : \mathbb{R}/\mathbb{Z} \to \mathbb{R}/\mathbb{Z}$ from external angles to internal angles with the following two properties:

- For any limb $K_t$ this map $\xi \mapsto T(\xi)$ takes the constant value $T(\xi) = t$ for $\xi$ in the interval $[\xi^-(t),\, \xi^+(t)]$ of length $\Delta\xi(K_t)$.
- Furthermore, $T$ is monotone of degree one, in the sense that it lifts to a monotone map $\hat{\xi} \mapsto \hat{T}(\hat{\xi})$ from $\mathbb{R}$ to $\mathbb{R}$, with $\hat{T}(\hat{\xi} + 1) = \hat{T}(\hat{\xi}) + 1$.

It is not difficult to compute the lengths $\Delta\xi(K_t)$ of these intervals of constancy.

**Lemma 2.8.** *If $2^n t \equiv t_0$ with $n \geq 0$ minimal, then*

$$\Delta\xi(K_t) \;=\; \Delta\xi(K_{t_0})/3^n\,, \quad \textit{where} \tag{8}$$

$$\Delta\xi(K_{t_0}) \;=\; \begin{cases} 1/3 & \text{if} \quad t_0 \quad \text{is not periodic under angle doubling,} \\ 3^{p-1}/(3^p - 1) & \text{if} \quad 2^p t_0 \equiv t_0 \pmod{\mathbb{Z}} \quad \text{with } p \geq 1 \text{ minimal.} \end{cases}$$

*In both cases, the sum of $\Delta\xi(K_t)$ over all $t \in \mathbb{R}/\mathbb{Z}$ is precisely equal to $+1$. In other words, almost every external angle $\xi$ belongs to such an interval of constancy.*

Thus the set of $\xi$ such that the external ray $\mathcal{R}_\xi$ lands on the boundary $\partial U_a$ has measure zero.

**Proof of Lemma 2.8.** The Equation (8) follows immediately from Lemma 2.5. Suppose first that $t_0$ is not periodic under angle doubling (Figure 2). Then for each $n \ge 0$ there are exactly $2^n$ distinct solutions $t$ to the congruence $2^n t \equiv t_0$, and $\Delta\xi(K_t) = \Delta\xi(K_{t_0})/3^n$ for each one of these solutions. Summing over all $n$ and all solutions, we get

$$\sum_t \Delta\xi(K_t) \;=\; \Delta\xi(K_{t_0}) \sum_{n\ge 0} 2^n/3^n \;=\; 3\,\Delta\xi(K_{t_0})\,. \tag{9}$$

We have $\Delta\xi(K_{t_0}) \ge 1/3$ by Lemma 2.5; but the sum (9) must be $\le 1$ since the sum of the lengths of subintervals of $\mathbb{R}/\mathbb{Z}$ cannot be greater than one. Thus $\Delta\xi(K_{t_0})$ is exactly 1/3, and the sum is exactly one.

Now suppose that $2^p t_0 \equiv t_0$ with $p \ge 0$ minimal (Figure 3). Then by Lemma 2.5,

$$\Delta\xi(K_{2t_0}) \;=\; 3\Delta\xi(K_{t_0}) - 1,$$

hence

$$\Delta\xi(K_{2^n t_0}) \;=\; 3^{n-1}(3\Delta\xi(K_{t_0}) - 1) \;\text{ for }\; 1 \le n \le p.$$

In particular,

$$\Delta\xi(K_{t_0}) \;=\; \Delta\xi(K_{2^p t_0}) \;=\; 3^{p-1}(3\Delta\xi(K_{t_0}) - 1)\,,$$

hence we can solve for the required expression

$$\Delta\xi(K_{t_0}) \;=\; \frac{3^{p-1}}{3^p - 1}\,.$$

It then follows by Lemma 2.5 that

$$\Delta\xi(K_{2^n t_0}) \;=\; \frac{3^{n-1}}{3^p - 1} \qquad \text{for} \qquad 1 \le n \le p\,. \tag{10}$$

(Curiously enough, the sum of these angular widths (10) over all angles $2^n t_0$ in the periodic orbit is always precisely 1/2.) For each $t$ with $\Delta\xi(K_t) > 0$, let $m \ge 0$ be the smallest integer such that $2^m t \equiv 2^n t_0$ for some angle $2^n t_0$ in the periodic orbit. Then $\Delta\xi(K_t) = 3^{n-m-1}/(3^p - 1)$. Summing over all such $t$, we see that

$$\sum_t \Delta\xi(K_t) \;= \sum_{n=1}^{p} \frac{3^{n-1}}{3^p - 1}\Big(1 + 1/3 + 2/9 + 4/27 + \cdots\Big) \;=\; 1,$$

as required. This proves Lemma 2.8 $\square$

The precise relationship between the internal argument $t$ and the external argument or arguments $\xi$ at a point of $\partial U_a$ can be described more explicitly as follows. According to Remark 2.7, the correspondence $\xi \mapsto t = T(\xi)$ is a well defined, continuous, and monotone map of degree one from the circle $\mathbb{R}/\mathbb{Z}$ to itself. However, it turns out to be easier to describe the inverse function

$t \mapsto \xi = T^{-1}(t)$, which is monotone, but has a jump discontinuity at $t$ for every limb $K_t$. Recall that the mapping $F$ doubles internal arguments and triples external arguments. Hence it is often convenient to describe $t$ by its base 2 expansion, but to describe $\xi$ by its base 3 expansion, which we write as $\xi = .x_1x_2x_3\cdots$ (base 3) $= \sum x_i/3^i$ with $x_i \in \{0,1,2\}$.

Suppose, to fix our ideas, that the internal argument $t_0$ of the principal limb satisfies $0 < t_0 < 1/2$. Let us start with the unique fixed point on the circle $\partial U_a$, with internal argument zero. Since $U_a$ is mapped onto itself by $F$, the corresponding external argument must be either zero or $1/2$. Applying the involution $\mathcal{I} : (a, v) \mapsto (-a, -v)$ if necessary, we may assume that this point has external argument zero. (See 3.)

**Lemma 2.9.** *With these hypotheses, the correspondence*

$$t \ \mapsto \ \xi = \xi_{t_0}(t) = T^{-1}(t) = .x_1x_2x_3\cdots$$

*is obtained by setting $x_m$ equal to either $0$, $1$, or $2$ according as $2^mt$ belongs to the interval $[0\,,\,t_0]$, $[t_0\,,\,1/2]$, or $[1/2\,,\,1]$ modulo one.*

Thus there is a jump discontinuity whenever $2^mt$ lies exactly at the boundary between two of these intervals. When $1/2 < t_0 < 1$, the statement is similar, except that we use the intervals

$$[0,\,1/2], \quad [1/2,\,t_0], \quad \text{and} \quad [t_0,\,1].$$

In the case where the fixed point on $\partial U_a$ has external argument $1/2$, we must add $1/2$ to the value of $\xi$ described above.

**Proof of Lemma 2.7.** Consider the three pre-images of the fixed point which has internal and external arguments zero. One is the point itself, one must lie in the principal limb, by Theorem 2.1, and the third must be the unique point on $\partial U_a$ which has internal argument $1/2$. The corresponding external arguments must be $0$, $1/3$ and $2/3$ respectively. Given a completely arbitrary internal argument $t$, we can now compute the corresponding external argument $\xi = T^{-1}(t)$, simply by following its orbit under $F$. $\square$

**Remark 2.10. The Non-Periodic Case.** (Figure 2.) In the case of a critical angle $t_0$ which is not periodic under doubling, the map $F$ is uniquely determined by $t_0$ (up to the involution $\mathcal{I}$), and we can give a much more precise description of $K(F)$. If $2^nt \equiv t_0$, then the map $F^{\circ(n+1)}$ carries the limb $K_t$ homeomorphically onto $K(F)$. Let

$$f_t \ : \ K(F) \ \xrightarrow{\cong} \ K_t$$

be the inverse homeomorphism. Then $f_t$ carries each limb $K_{t'}$ onto a ***secondary limb*** $f_t(K_{t'}) \subset K_t$, to be denoted by $K_{t\,t'}$. More generally, for any finite sequence of limbs $K_{t_1}, K_{t_2}, \ldots, K_{t_m}$, we can form an ***$m$-th order limb***

$$f_{t_1} \circ f_{t_2} \circ \cdots \circ f_{t_m}(K(F)),$$

which will be denoted briefly by

$$K_{t_1 t_2 \cdots t_m} \;\subset\; K_{t_1 t_2 \cdots t_{m-1}} \;\subset\; \cdots \;\subset K_{t_1 t_2} \;\subset\; K_{t_1}\,.$$

Each of these higher order limbs contains an associated Fatou component

$$f_{t_1} \circ f_{t_2} \circ \cdots \circ f_{t_m}(U_a)\,,$$

and every Fatou component within $K(F)$ is uniquely determined by such a list $t_1,\, t_2,\, \ldots t_m$ with $m \ge 0$. Note that

$$F(K_{t_1 t_2 \cdots t_m}) \;=\; K_{2t_1\, t_2 \cdots t_m} \quad \text{for} \quad t_1 \not\equiv t_0$$

but

$$F(K_{t_0 t_1 \cdots t_m}) \;=\; K_{t_1 \cdots t_m}\,,$$

with similar formulas for the associated Fatou components. (Here $t_0$ is the fixed critical angle, but $t_1, \ldots t_m$ can be the internal angles for arbitrary limbs.)

It seems natural to conjecture that $K(F)$ is locally connected in this situation, and in particular that the diameter of the $m$-th order limb $K_{t_1 \cdots t_m}$ tends to zero as $m \to \infty$.

**Remark 2.11. The Periodic Case.** For periodic $t_0$ the situation is much more complicated, since there may be Cremer points or other difficulties. However, if we consider only maps $F$ which belong to the boundary $\partial\hat{\mathcal{H}}_0$ of the principal hyperbolic component, as in Figure 3, then the situation is well understood. In this case, the point of attachment $\beta(e^{2\pi i t_0})$ is parabolic, of period $p \ge 1$, with rotation number zero, and the Julia set is certainly locally connected. (Compare (TanLei and Yin 96).) In fact, this parabolic $F$ is the root point of a hyperbolic component which has Hubbard tree with an easily described topological model, consisting of the line segment between the two critical vertices 0 and $e^{2\pi i t_0}$, together with the images of this line segment under the map $z \mapsto z^2$. (See, for example, the top three examples in Figure 35, which represent "puffed-out" versions of three such trees.)

# 3 Parameter Space: The curve $\mathcal{S}_1$.

Consider the set of all cubics having a critical fixed point. Using the normal form (2), we define the ***superattracting period one curve*** $\mathcal{S}_1$ to be the one-parameter subspace of $\hat{\mathcal{P}}(3)$ consisting of all $F = F_{a,a} \in \hat{\mathcal{P}}(3)$ for which the critical value $v = F(a)$ is equal to $a$, so that the marked critical point $a$ is a fixed point. (In §5 and §6, we will study the analogous curve $\mathcal{S}_p$, consisting of cubics with a marked critical point of period $p$.) Evidently the curve $\mathcal{S}_1 \subset \hat{\mathcal{P}}(3)$ is canonically biholomorphic to the complex $a$-plane. We will sometimes use the abbreviated notation $F_a$ for a point in $\mathcal{S}_1$.

The boundary of the intersection $\mathcal{C}(\hat{\mathcal{P}}(3)) \cap \mathcal{S}_1$ (considered as a subset of the $a$-plane) is shown in Figure 5. Since there is only one free critical point in this family, much of the Douady-Hubbard theory concerning the parameter space for quadratic polynomials carries over with minor changes. However, there are new difficulties. (Faught 92) proved locally connectivity, modulo local connectivity of the Mandelbrot set, and showed that all hyperbolic components in $\mathcal{S}_1$ are bounded by Jordan curves. See (Roesch 06) for a simplified proof, for a generalization of these results to higher degrees, and for a proof that the limbs which branch off from the principal hyperbolic component have diameters tending to zero.

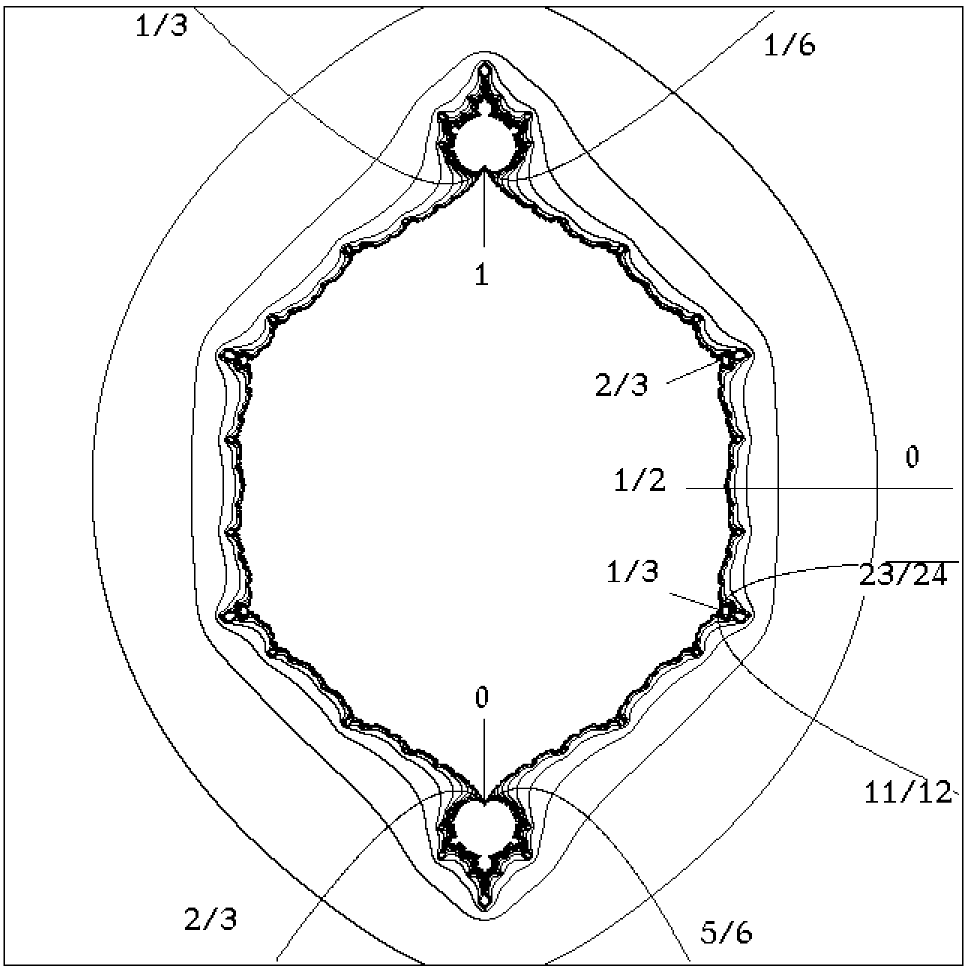


Figure 5: The non-hyperbolic locus in $\mathcal{S}_1$, projected into the $a$-plane. The connectedness locus $\mathcal{C}(\hat{\mathcal{P}}(3)) \cap \mathcal{S}_1$ consists of this non-hyperbolic locus together with the bounded components of its complement.

Recall that the ***canonical involution*** $\mathcal{I}$ of $\hat{\mathcal{P}}(3)$ takes the pair $(a, v)$ to $(-a, -v)$, preserving equation (3). It corresponds to the linear conjugation

$F(z) \mapsto -F(-z)$; and clearly preserves the subsets $\hat{\mathcal{H}}_0 \subset \mathcal{C}(\hat{\mathcal{P}}(3))$ and $\mathcal{S}_1$. Geometrically, its effect is to rotate the Julia set of $F$ by $180°$, and to add $1/2$ to all external angles. Note that the curve $\mathcal{S}_1$ has uniformizing parameter $a$, while the quotient curve $\mathcal{S}_1/\mathcal{I}$ has uniformizing parameter $a^2$. (Figures 5, 6.) We will sometimes use the abbreviated notation $F = F_a$ to indicate the dependence of $F \in \mathcal{S}_1$ on the parameter $a$.

**Remark 3.1.** Alternatively, we could equally well work with the affinely conjugate normal form

$$z \;\mapsto\; F(z+a) - a \;=\; z^3 + 3az^2\,,$$

with superattracting fixed point at the origin. More generally, for any fixed constant $\mu$, we can look at the complex curve $\mathrm{Per}(1;\,\mu)$ consisting of all cubic maps

$$z \;\mapsto\; z^3 + 3\alpha z^2 + \mu z\,,$$

having a fixed point of multiplier $\mu$ at the origin. The cases where $\mu \neq 1$ is a root of unity are of particular importance, since these curves contain regions which border on two different hyperbolic components within the ambient space $\hat{\mathcal{P}}(3)$. Note that the canonical involution, which maps the function $F(z)$ to $-F(-z)$, sends each $\mathrm{Per}(1;\,\mu)$ onto itself, changing the sign of $\alpha$. In general, the connectedness locus in $\mathrm{Per}(1;\,\mu)$ varies by an isotopy as $\mu$ varies within the open unit disk, but changes topology as $\mu$ tends to a limit on the unit circle. However, there is one noteworthy exception:

**Conjecture 3.2.** *The connectedness locus in the quotient* $\mathrm{Per}(1;\,\mu)/\mathcal{I}$ *tends to a limit without changing topology, as* $\mu \to 1$.

In fact the limiting configuration in $\mathrm{Per}(1;\,1)/\mathcal{I}$, as shown in Figure 8, looks topologically very much like the corresponding configuration in Figure 6, although the geometrical shapes are different.

# 3A. Maps Outside of the Connectedness Locus.

We begin the analysis of the curve $\mathcal{S}_1$ with the following analogue of a well known result of (Douady and Hubbard 82).

**Lemma 3.3.** *The connectedness locus* $\mathcal{C}(\mathcal{S}_1) = \mathcal{S}_1 \cap \mathcal{C}(\hat{\mathcal{P}}(3))$ *in* $\mathcal{S}_1$ *is a cellular set. Furthermore, there is a canonical conformal diffeomorphism from the complement* $\mathcal{E} = \mathcal{S}_1 \smallsetminus \mathcal{C}(\mathcal{S}_1)$ *onto* $\mathbb{C} \smallsetminus \overline{\mathbb{D}}$.

By definition, $\mathcal{E}$ will be called the ***escape region*** in $\mathcal{S}_1$. (More generally, when discussing the curve $\mathcal{S}_p$ of maps with critical orbit of period $p > 1$, we will see that there are always two or more connected escape regions.)

**Proof of Lemma 3.3.** First consider some fixed polynomial $F = F_{a,a}$ in $\mathcal{S}_1$. Then $F : \mathbb{C} \to \mathbb{C}$ is conjugate, throughout some neighborhood of infinity, to

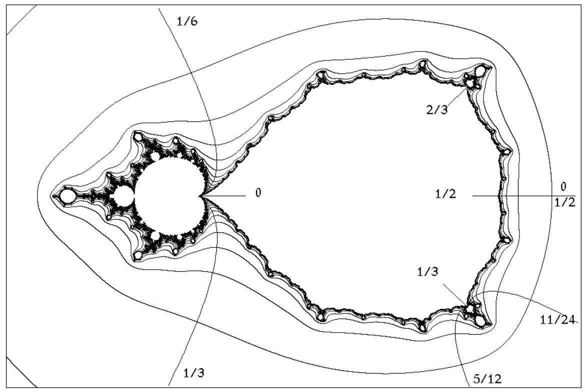


Figure 6: Non-hyperbolic locus in the quotient plane $\mathcal{S}_1/\mathcal{I}$, with parameter $a^2$.

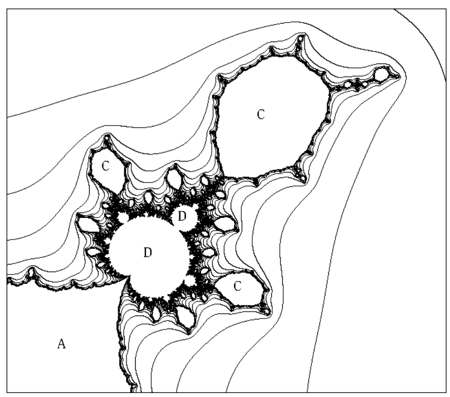


Figure 7: Detail of Figure 6 showing the $2/3$-limb. (For labels, see §4.)

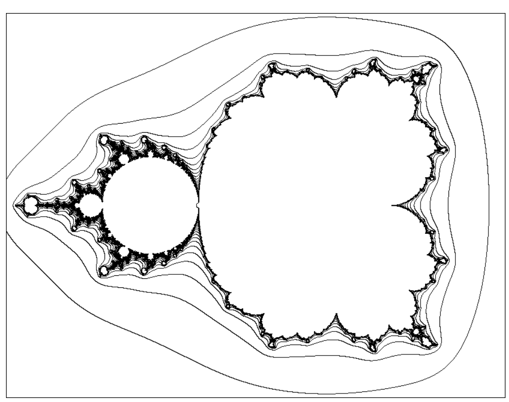

Figure 8: Configuration analogous to Figure 6 in the plane $\mathrm{Per}(1;\,1)/\mathcal{I}$ of maps with a fixed point of multiplier $+1$.

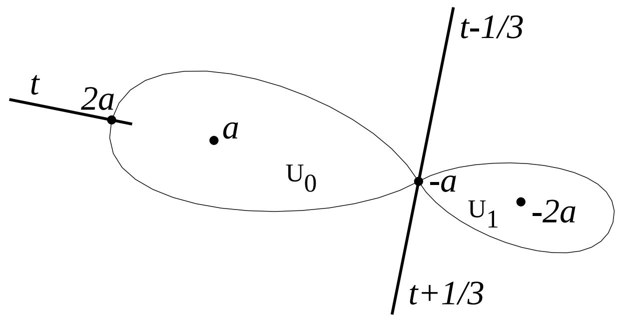


Figure 9: Sketch in the dynamic plane for a map with one escaping critical orbit. The equipotential and the external rays through the escaping critical point $-a$ and through its co-critical point $2a$ are shown, with the rays labeled by their angles.

the map $w \mapsto w^3$. In other words, there exists a ***Böttcher diffeomorphism*** $z \mapsto \beta_F(z)$, defined and holomorphic throughout a neighborhood of infinity, satisfying the identity

$$\beta_F(F(z)) \ = \beta_F(z)^3\,.$$

(See for example (Milnor 06) In fact $\beta_F$ is unique up to sign, and can be normalized by the requirement that $\beta_F(z) \sim z$ as $|z| \to \infty$. If we draw an equipotential through the free critical point $-a$, as illustrated in Figure 9, then $\beta$ is well defined everywhere in the region outside this equipotential, and maps this exterior region diffeomorphically onto the complement of a suitable disk centered at the origin. It is not well defined at the critical point $-a$ itself, but does extend smoothly through a neighborhood of the co-critical point $2a$. Thus (following Branner and Hubbard) we can define the map $\widehat{\beta}:\ \mathcal{E} \to \mathbb{C} \smallsetminus \overline{\mathbb{D}}$ by setting

$$\widehat{\beta}(F) \ = \ \beta_F(2a) \qquad \text{where} \qquad F \ = \ F_{a,a}\,.$$

(We may also use the alternate notation $\widehat{\beta}(a)$ for $\widehat{\beta}(F_{a,a})$.)

It is not hard to check that $\widehat{\beta}$ is holomorphic and locally bijective, and that $|\widehat{\beta}(F)|$ converges to $+1$ as $F$ converges towards the connectedness locus. In order to show that it is a covering map, we must describe its behavior near infinity. Note that the orbit of $2a$ under $F$ is given by

$$F\ :\ 2a \ \mapsto\ 4a^3 + a \ \mapsto\ \cdots \ \mapsto\ 4^{3^{k-1}} a^{3^k} + (\text{lower order terms}) \ \mapsto\ \cdots\,.$$

The asymptotic formula

$$\widehat{\beta}(F_{a,v}) \ \sim\ \sqrt[3]{4}\, a \qquad \text{as} \qquad |a| \to \infty \tag{11}$$

follows easily. Thus $\widehat{\beta}:\ \mathcal{E} \to \mathbb{C} \smallsetminus \overline{\mathbb{D}}$ is proper and locally bijective. Since it has degree one near infinity, it follows that it is a conformal isomorphism, as required. $\square$

Using this description of the escape region $\mathcal{E} \subset \mathcal{S}_1$, we can talk about ***external rays*** $\mathcal{R}_\xi(\mathcal{E})$ within this escape region in parameter space. The reader should take care, since we will discuss external rays $\mathcal{R}'_\xi(F)$ for the Julia set $J(F)$ at the same time.

**Definition 3.4.** The map $F = F_{a,a}$ belongs to the ray $\mathcal{R}_t(\mathcal{S}_1)$ in parameter space if and only if the corresponding dynamic ray $\mathcal{R}'_t(F)$ passes through the co-critical point $2a$. It then follows that the ray $\mathcal{R}'_{3t}(F)$ passes through the critical value $F(2a) = F(-a)$, and hence that two rays $\mathcal{R}'_{t\pm 1/3}(F)$ must crash together at the free critical point $-a$ (Figure 9).

Note that the intersection $\mathcal{C}(\hat{\mathcal{P}}(3)) \cap \mathcal{S}_1$ is not known to be locally connected,[2] so that we do not know that these external rays in parameter space land at well defined points of $\mathcal{C}(3)$. However, we can prove the following.

**Lemma 3.5.** *If the number $\xi \in \mathbb{Q}/\mathbb{Z}$ is periodic under tripling (or in other words if its denominator is relatively prime to 3), then the two external rays $\mathcal{R}_{\xi+1/3}(\mathcal{S}_1)$ and $\mathcal{R}_{\xi-1/3}(\mathcal{S}_1)$ both land at well defined points of the connectedness locus. Furthermore, for either one of these two landing maps $F$, the Julia set $J(F)$ contains a parabolic periodic point, namely the landing point of the periodic external ray $\mathcal{R}'_\xi(F)$.*

**Proof.** (Compare (Goldberg and Milnor 93, Appendices B, C).) Let $F \in \mathcal{C}(3)$ be any accumulation point of the ray $\mathcal{R}_{\xi\pm 1/3}(\mathcal{S}_1)$. Then the ray $\mathcal{R}'_\xi(F)$ must land at a well defined periodic point in $J(F)$, which a priori can be either repelling or parabolic. (See for example (Milnor 06).) If it were repelling, then for any nearby map $F_1 \in \mathcal{S}_1$ the corresponding ray $\mathcal{R}'_\xi(F_1)$ would land at a nearby periodic point. However, as noted above, for $F_1$ in the ray $\mathcal{R}_{\xi\pm 1/3}(\mathcal{S}_1)$ this ray $\mathcal{R}'_\xi(F_1)$ must crash into the critical point $-a$, and hence cannot land. Thus $F$ must have a parabolic cycle, with period dividing the period of $\xi$.

On the other hand, the set of all $F = F_a \in \mathcal{S}_1$ having a parabolic cycle of bounded period forms an algebraic variety. Since it is not the whole curve $\mathcal{S}_1$, it must be finite. But the collection of all accumulation points for the ray $\mathcal{R}_{\xi\pm 1/3}(\mathcal{S}_1)$ must be connected, so this set of accumulation points can only be a single point. $\square$

## 3B. Maps in $\hat{\mathcal{H}}_0$.

An argument quite similar to the proof of Lemma 3.3 applies to the principal hyperbolic component $\hat{\mathcal{H}}_0$, intersected with $\mathcal{S}_1$. In fact we will show that the quotient $(\hat{\mathcal{H}}_0 \cap \mathcal{S}_1)/\mathcal{I}$ is canonically biholomorphic to the unit disk.

We suppose that $F = F_a$ belongs to the principal hyperbolic component $\hat{\mathcal{H}}_0$, or in other words we suppose that the immediate basin $U_a$ contains both critical points. If $a \neq 0$, then as in the discussion in §2 there is a unique

[2] As noted at the beginning of this section, Faught showed that this set is locally connected if and only if the Mandelbrot set is locally connected.

Böttcher coordinate $w = \beta(z) = \beta_a(z)$ which maps some neighborhood of $z = a$ biholomorphically onto a neighborhood of $w = 0$, and which conjugates $F$ to the squaring map $w \mapsto w^2$, so that, as in Equation 4

$$\beta_a(F(z)) = \beta_a(z)^2 .$$

Since $F \in \hat{\mathcal{H}}_0$ we cannot extend this Böttcher coordinate throughout the basin $U_a$. For this basin will also contain the co-critical point $-2a$, which satisfies $F(-2a) = F(a) = a$. Evidently $\beta_a(z) = \pm\sqrt{\beta_a(F(z))}$ cannot be defined as a single valued function in a neighborhood of $-2a$. However an argument quite similar to the proof of Lemma 3.3 shows the following.

**Lemma 3.6.** *There is a canonical conformal isomorphism $\eta$ from the quotient space $(\hat{\mathcal{H}}_0 \cap \mathcal{S}_1)/\mathcal{I}$ onto the open unit disk. More explicitly, if $F = F_a \in \hat{\mathcal{H}}_0 \cap \mathcal{S}_1$, then the Böttcher coordinate $z \mapsto w = \beta_a(z)$, which initially is defined only in a neighborhood of $z = a$, can be analytically continued to a neighborhood of the other critical point $z = -a$ in such a way that the resulting correspondence $a \mapsto \beta_a(-a) \in \mathbb{D}$ is well defined, holomorphic and even, as $F_a$ varies through the region $\hat{\mathcal{H}}_0 \cap \mathcal{S}_1$. This correspondence induces the required conformal isomorphism $\eta : a^2 \mapsto \beta_a(-a)$.*

Thus the dynamical behavior of the critical point $-a$ under the map $F_a$ is just like that of the point $w_a = \beta_a(-a)$ under the squaring map. Intuitively we can say that $F_a$ is obtained from the squaring map by "enramifying" the point $w_a$.

**Proof of Lemma 3.6.** We continue to assume that $a \neq 0$. Note first that the absolute value $|\beta_a(z)|$ extends as a well defined function of $z$ throughout the basin $U_{F_a}$. This extended function will be smooth except at points which map precisely onto $a$ under some iteration of $F_a$, and will have non-zero gradient except at points which map onto $-a$ under some iteration of $F_a$. For any $0 < r \leq 1$, let $C_r$ be that component of the open set $\{z \in U_{F_a} : |\beta_a(z)| < r\}$ which contains the superattracting point $a$. Evidently there is a largest value of $r$ so that $\beta_a$ extends to a conformal diffeomorphism from $C_r$ onto the open disk $\{w : |w| < r\}$. We claim that the boundary $\partial C_r$ must contain the critical point $-a$. For if $z$ is any non-critical boundary point of $C_r$, then using Equation (4) there exists a unique holomorphic extension of $\beta_a$ to a neighborhood of $z$. Hence, if $|\beta_a(-a)| \neq r$ there would be no obstruction to a holomorphic extension to a larger neighborhood. In fact, we claim that $\beta_a$ extends homeomorphically over the closure $\overline{C}_r$ (and holomorphically over a neighborhood of $\overline{C}_r$). Here we must rule out the possibility that $\partial C_r$ consists of two loops, one inside the other, meeting at the point $-a$. But this configuration is easily excluded by the maximum modulus principle.

In this way, we see that the map $\beta = \beta_a$ takes a well defined value at the critical point $-a$. Thus we obtain a well defined point

$$a \mapsto w_a = \beta_a(-a) \in \mathbb{D}$$

whose dynamical properties under the squaring map are the same as those of $-a$ under $F_a$. Evidently this image point $w_a$ will not be changed if we apply the involution $\mathcal{I}$. Hence it can be considered as a holomorphic function $w_a = \eta(a^2)$. Here $a$ ranges over all non-zero parameters for which the associated map $F_a$ belongs to $\mathcal{S}_1 \cap \hat{\mathcal{H}}_0$. As $a \to 0$, a brief computation shows that $\eta(a^2) \sim -\sqrt{12}\,a^2$. Hence the apparent singularity at $a=0$ is removable. Since this correspondence $\eta : a^2 \mapsto \beta_a(-a)$ is well defined and holomorphic, it suffices to show that $\eta$ is a proper map of degree one from a region in the $a^2$-plane onto the open unit disk. First consider a boundary point $F_a$ of the region $\mathcal{S}_1 \cap \hat{\mathcal{H}}_0$. Then as noted earlier the Böttcher mapping from the immediate basin $U_{F_a}$ onto the unit disk has no critical points, and in fact is a conformal diffeomorphism. In particular, $\beta_a^{-1}$ can be defined as a single valued function on the disk of radius $1-\epsilon$, for any $\epsilon > 0$. This last property must be preserved under any small perturbation of $F_a$, and it follows that $|\beta_b(-b)| > 1-\epsilon$ for any $F_b \in \hat{\mathcal{H}}_0$ sufficiently close to $F_a$. Thus $\eta$ is a proper map from $(\hat{\mathcal{H}}_0 \cap \mathcal{S}_1)/\mathcal{I}$ onto $\mathbb{D}$. Since $\eta^{-1}(0)$ is the single point $0$, with $\eta'(0) = -\sqrt{12} \neq 0$, it follows that $\eta$ is a conformal diffeomorphism. $\square$

## 3C. Maps outside of $\hat{\mathcal{H}}_0$.

In analogy with Lemma 2.4 in the dynamic plane, we have the following result in parameter space.

**Lemma 3.7.** *The conformal diffeomorphism* $\eta : (\mathcal{S}_1 \cap \hat{\mathcal{H}}_0)/\mathcal{I} \xrightarrow{\cong} \mathbb{D}$ *of Lemma 3.6 extends to a continuous map*

$$\overline{\eta} : \mathcal{S}_1/\mathcal{I} \to \overline{\mathbb{D}}$$

*which maps each* $F_{\pm a} \in \mathcal{S}_1/\mathcal{I}$ *outside of* $\hat{\mathcal{H}}_0/\mathcal{I}$ *to the point* $e^{2\pi i t_0}$*, where* $t_0$ *is the internal argument for the principal limb of* $F_a$ *or of* $F_{-a}$*.*

Intuitively, each $F_{\pm a}$ outside of $\hat{\mathcal{H}}_0/\mathcal{I}$ should belong to a limb which is attached to the boundary of $\hat{\mathcal{H}}_0/\mathcal{I}$, and we want to map it to the corresponding point of the circle $\partial\mathbb{D}$.

**Proof of Lemma 3.7.** Fixing some $F \in \mathcal{S}_1 \cap (\mathcal{C}(3) \smallsetminus \hat{\mathcal{H}}_0)$, choose two rational angles $t_\ell < t_0 < t_r$ close to $t_0$. Then the critical point $-a$ is contained in the sector bounded by the two extended rays $\widehat{\mathcal{R}}_{t_\ell}$ and $\widehat{\mathcal{R}}_{t_r}$. Without loss of generality, we may assume that these extended rays meet $\partial U_a$ at repelling periodic points, since there can be at most finitely many parabolic points. Evidently this situation will be preserved under a small perturbation of $F$. This proves that the correspondence $F \mapsto e^{2\pi i t_0}$ is continuous as $F$ varies over $\mathcal{C}(3) \smallsetminus \hat{\mathcal{H}}_0$. (It is conjectured that this correspondence is not only continuous, but actually locally constant away from the boundary of $\hat{\mathcal{H}}_0$. Compare Lemmas 3.9 and 3.10.) If we perturb $F = F_a$ into $\hat{\mathcal{H}}_0$, then a similar argument, using the construction from Lemma 3.3, shows that $\overline{\eta}(F_{\pm a})$ depends continuously on $a$. $\square$

In analogy with the discussion above, let us define the ***limb*** $\mathcal{C}_t$, attached to $(\mathcal{S}_1 \cap \overline{\mathcal{H}}_0)/\mathcal{I}$ at internal angle $t$, to be the set $\overline{\eta}^{-1}(e^{2\pi i t})$. In other words, $F_{\pm a}$

belongs to $\mathcal{C}_t$ if and only if the principal limb of the filled Julia set $K(F_a)$ is attached at internal angle $t$, so that $-a \in K_t \subset K(F_a)$. *By abuse of language, we may say that the map $F_a$ belongs to the limb $\mathcal{C}_t$, although properly speaking it is the unordered pair $\{F_a\,,\,F_{-a}\}$ which belongs to $\mathcal{C}_t$.*

According to Faught, the principal hyperbolic component $\mathcal{S}_1 \cap \hat{\mathcal{H}}_0$ in $\mathcal{S}_1$ is bounded by a Jordan curve, so that $\overline{\eta}$ maps $(\mathcal{S}_1 \cap \overline{\mathcal{H}}_0)/\mathcal{I}$ homeomorphically onto $\overline{\mathbb{D}}$. (We cannot be sure that the connectedness locus $\mathcal{C}(\mathcal{S}_1)$ in $\mathcal{S}_1$ is locally connected, since it contains many copies of the Mandelbrot set. However Faught showed that such Mandelbrot copies are the only possible source of non-local-connectivity.) It follows that the limb $\mathcal{C}_t \subset (\mathcal{S}_1 \cap \mathcal{C}(3))/\mathcal{I}$ has more than one point if and only if the angle $t$ is periodic under doubling, or in other words if and only if $t$ is rational with odd denominator. Compare Figure 6, in which the 0-limb to the left, the $1/3$-limb to the lower right, and the $2/3$-limb (Figure 7) to the upper right are clearly visible.

In analogy with Lemmas 2.8 and 2.9, let us describe the relationship between internal and external angles in parameter space. *It will be convenient to measure internal arguments $t$ in the $a^2$-plane $\mathcal{S}_1/\mathcal{I}$, where we identify affinely conjugate polynomials, but to measure external arguments $\eta$ in the $a$-plane $\mathcal{S}_1$ where we make no such identification.* (Compare Figures 2, 3.)

**Lemma 3.8.** *The correspondence $t \mapsto \eta(t)$ between internal and external angles in parameter space can be expressed in terms of the corresponding function $t \mapsto \xi_{t_0}(t)$ in the dynamic plane (Lemma 2.9), by the formula $\eta(t) = \xi_t(t+\frac{1}{2})$. This function $t \mapsto \eta(t)$ is strictly monotone, increasing by $1/2$ as $t$ increases by $1$, and has a jump discontinuity at $t$ if and only if $t$ is periodic under the doubling map mod 1. In fact if $t$ has period $p$ under doubling then the discontinuity at $t$ is given by*

$$\Delta\eta(t) \;=\; \eta(t^+) - \eta(t^-) \;=\; \xi_t(\frac{1}{2}+t^+) - \xi_t(\frac{1}{2}+t^-) \;=\; \frac{1}{3(3^p-1)}\,.$$

For example the jump from $\xi_{1/3}(\frac{5}{6}^-) = 11/12$ to $\xi_{1/3}(\frac{5}{6}^+) = 23/24$ in Figure 3 corresponds exactly to the jump from $\eta(\frac{1}{3}^-) = 5/12$ to $\eta(\frac{1}{3}^+) = 11/24$ in Figure 6. (In fact the corresponding shapes in the Julia set and in parameter space are very similar! It would be interesting to explore this phenomenon.)

Note that the sum of these discontinuities,

$$\sum \left\{\frac{1}{3(3^p-1)} \;:\; 2^p t \equiv t\,,\; 0 \le t < 1\,,\; p \text{ minimal}\right\}$$

is equal to $1/2$. In fact, writing $(3^p-1)^{-1}$ as $3^{-p}+3^{-2p}+3^{-3p}+\cdots$, we can express this sum as

$$\frac{1}{3}\sum \left\{3^{-p} \;:\; 2^p t \equiv t\,,\; 0 \le t < 1\right\} \;=\; \frac{1}{3}\sum_1^\infty \frac{2^p-1}{3^p} \;=\; \frac{1}{3}\big(2-\frac{1}{2}\big) \;=\; \frac{1}{2}\,.$$

The proof of Lemma 3.8 is not difficult, and will be omitted. $\square$

Thus the correspondence $t \mapsto \xi_t(t+\frac{1}{2})$ is discontinuous precisely when $2^m(t+\frac{1}{2}) \equiv t \pmod 1$ for some $m \geq 0$, or in other words when $t = t_0$ is rational with odd denominator. *It is natural to conjecture that these are precisely the internal arguments at which some non-trivial limb $\mathcal{C}_t$ is attached to $\partial\hat{\mathcal{H}}_0 \cap \mathcal{S}_1$ within $\mathcal{C}(3) \cap \mathcal{S}_1$.* The points of attachment are of particular interest. These are the maps $F = F_a$ for which the periodic point $k(t) \in \partial U_a$ is parabolic, with multiplier equal to $+1$.

**Caution.** Although the boundary $\partial\hat{\mathcal{H}}_0 \cap \mathcal{S}_1$ is a topological circle, parametrized by the internal argument $t_0$, it definitely is not true that the corresponding Julia sets vary continuously with $t_0$. In fact the cases where $-a$ does or does not belong to $\overline{U}_a$ are presumably both everywhere dense along this circle.

Now suppose that we fix some angle $t_0$ which is periodic of order $p$ under doubling.

**Lemma 3.9.** *The two angles $\eta(t_0^-) = \xi_{t_0}(\frac{1}{2}+t_0^-)$ and $\eta(t_0^+) = \xi_{t_0}(\frac{1}{2}+t_0^+)$ are consecutive angles of the form $\frac{i}{3(3^p-1)}$. The corresponding external rays in parameter space land at a common map $F_0$ which has the following property. In the dynamic plane $\mathbb{C} \smallsetminus J(F_0)$, the external rays of argument $\eta(t_0^-)$ and $\eta(t_0^+)$ and the internal ray of argument $t_0+\frac{1}{2}$ all land at a common pre-periodic point $z_0$ in the Julia set. Furthermore, the multiplier $F^{\circ p\prime}(F(z_0))$ is equal to $+1$.*

These two external rays $\mathcal{R}_{\eta(t_0^-)}(\mathcal{S}_1)$ and $\mathcal{R}_{\eta(t_0^+)}(\mathcal{S}_1)$ cut off an open region $W(t_0) \subset \mathcal{S}_1$ which (following (Atela 92)) we may call the ***wake*** of the $t_0$-limb. It can be characterized as follows.

**Lemma 3.10.** *Every map $F \in W(t_0)$ has the property that the internal ray of argument $t_0+\frac{1}{2}$ for $F$, as well as the external rays of argument $\eta(t_0^-)$ and $\eta(t_0^+)$, all land at a common pre-periodic point in the Julia set $J(F)$. However, for any map $F \notin \overline{W}(t_0)$, the two external rays of argument $\eta(t_0^-)$ and $\eta(t_0^+)$ for $F$ land at distinct pre-periodic points.*

**Proof Outline for Lemmas 3.9 and 3.10.** To simplify the discussion and fix our ideas we will only describe the case $t_0 = 1/3$. The general case is not essentially different. As a first step, we must check that there exist maps $F \in \mathcal{S}_1$ which satisfy the condition that the internal ray $\mathcal{R}_{5/6}(F)$ and the two external rays $\mathcal{R}'_{11/12}(F)$ and $\mathcal{R}'_{23/24}(F)$ all land at a common point. For example any hyperbolic map in the $1/3$-rd limb will satisfy this condition. (Compare Figure 3.) Using the dynamics, it then follows that other triples such as $\mathcal{R}_{2/3}$, $\mathcal{R}'_{3/4}$, $\mathcal{R}'_{7/8}$ and $\mathcal{R}_{1/3}$, $\mathcal{R}'_{1/4}$, $\mathcal{R}'_{5/8}$ also have a common landing point. For a map satisfying this condition, since the two angles $1/4$ and $5/8$ differ by more than $1/3$, it follows that there must be a critical point, namely $-a$, lying in the region between the two rays $\mathcal{R}'_{1/4}(F)$ and $\mathcal{R}'_{5/8}(F)$.

On the other hand, there are also maps, such as $F(z) = z^3$, for which the two rays $\mathcal{R}'_{11/12}(F)$ and $\mathcal{R}'_{23/24}(F)$ land at distinct pre-periodic points. As we deform the map $F$ along some path in $\mathcal{S}_1$, how can we pass from one type of behavior to the other? If $F$ is a transition point which belongs to the connectedness locus, then at least one of these two rays must land at a pre-parabolic point

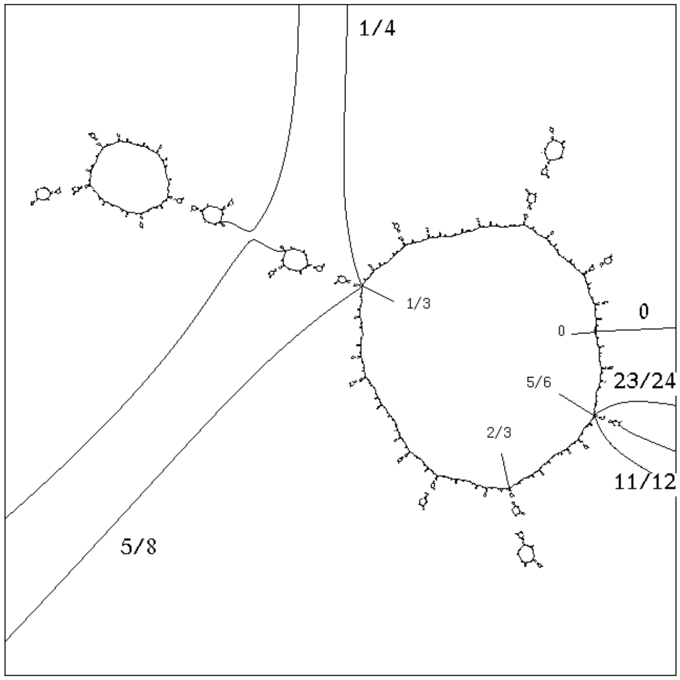


Figure 10: Julia set for a map which belongs to the wake $W(1/3)$, but not to the connectedness locus. (Compare Figure 5.) The unlabeled rays on the left pass close to the escaping critical point $-a$ and that on the right passes close to the co-critical point $2a$.

(that is a pre-periodic point whose orbit falls onto a parabolic cycle). Compare (Goldberg and Milnor 93, Appendix B). Note that there are only finitely many maps in $\mathcal{S}_1$ which possess parabolic cycles of the appropriate period and multiplier. On the other hand, for a transition outside of the connectedness locus, the critical point $-a$ must pass out of the region bounded by $\mathcal{R}'_{1/4}(F)$ and $\mathcal{R}'_{5/8}(F)$. Hence, at the transition point, one of these two rays must crash into the critical point $-a$. But this is exactly the defining property of a map $F$ which belongs to the external ray of angle $11/12$ respectively $23/24$ in parameter space. Thus the boundary between the two types of behavior is formed by these two external rays, each of which lands at a well defined map by Lemma 3.5, together with a finite set. Hence these two rays must land at a common map, as asserted in Lemma 3.9. The rest of the proof is straightforward. $\square$

# 4 Hyperbolic components in $\mathcal{S}_1$.

This section will present a more detailed, but partially conjectural, picture of the connectedness locus intersected with $\mathcal{S}_1$. Recall that a map in $\mathcal{C}(3)$ is called ***hyperbolic*** if the orbits of both critical points converge to attracting periodic orbits. The set of hyperbolic points forms a union of components of the interior of $\mathcal{C}(3)$. Conjecturally it constitutes the entire interior. It is shown in (Milnor 92b) that each hyperbolic component is an open topological 4-cell, which is canonically biholomorphic to one of four standard models. Furthermore, each hyperbolic component contains one and only one post-critically finite map, called its ***center*** . (A map is ***post-critically finite*** if the forward orbit of every critical point is either periodic, or eventually falls onto a periodic cycle which may be either repelling or superattracting. However, in the hyperbolic case, such a post-critical cycle must necessarily be superattracting.)

In the case of a hyperbolic component which intersects $\mathcal{S}_1$, clearly Type B cannot occur, and Type A occurs only for the principal hyperbolic component $\hat{\mathcal{H}}_0$. However, we will see that Type C and D both occur infinitely often (and all four types are important in studying maps with a periodic critical orbit of higher period). It is not difficult to check that for *any* hyperbolic component in the connectedness locus which intersects $\mathcal{S}_1$, the intersection is an open topological 2-cell which contains the center point. (Compare Lemma 3.6.) All of these hyperbolic components in $\mathcal{S}_1$ are bounded by Jordan curves. (See (Faught 92) or (Roesch 06).)

In the case of a *capture component*, we can be even more explicit. The closure $\overline{U}_a$ of the immediate basin of the fixed point $+a$ is homeomorphic to the disk $\overline{\mathbb{D}}$, using the Böttcher coordinate. There must be some first element in the orbit of the other critical point $-a$ which belongs to $\overline{U}_a$. *Using the Böttcher coordinate of this point, say $F^{\circ n}(-a)$, we obtain the required homeomorphism $a \mapsto \beta_a(F^{\circ n}(-a))$ from the closure of the capture component in $\mathcal{S}_1$ onto the closed unit disk.*

In the case of a component of type D (disjoint attracting orbits), we can make the much sharper statement. *If $F_0$ is the center map in the component, then by the Douady-Hubbard operation of "tuning", we obtain a copy $F_0 * M$ of the Mandelbrot set $M = \mathcal{C}(2)$ which is topologically embedded into $\mathcal{S}_1$.* ((Douady and Hubbard 85)). Compare the discussion in (Milnor 89).) In particular, there are infinitely many other hyperbolic components of type D which are canonically subordinated to the given one. When discussing such an embedded Mandelbrot set, we will always implicitly assume that it is maximal, ie., that $F_0 * M$ is not a subset of some strictly larger embedded Mandelbrot set. In other words, we assume that $F_0$ cannot itself be obtained by tuning some other center point of lower period.

The "directions" in which we can proceed from one hyperbolic component or embedded Mandelbrot set to any other, measured around the boundary of the component or Mandelbrot set, can be described quite explicitly as follows. (Note that Case B is excluded, since it does not occur in $\mathcal{S}_1$.)

**Case A.** From the hyperbolic component $\hat{\mathcal{H}}_0$ in $\mathcal{S}_1$, as discussed in §1, we can proceed outward in any direction $t \in \mathbb{R}/\mathbb{Z}$ which is rational with odd denominator, or equivalently is periodic under doubling. Components which are attached in this direction are said to belong to the ***limb*** $\mathcal{C}_t$. In particular, there is one copy of the Mandelbrot set which is immediately attached to $\hat{\mathcal{H}}_0$ in each such direction. We will use the notation $F_t * M$ for this "satellite" of

$\hat{\mathcal{H}}_0$ in the limb $\mathcal{C}_t \subset \mathcal{S}_1$ .

**Case C.** If $C$ is a capture component in the limb $\mathcal{C}_t$ , then we can go out from $C$ in any direction $\alpha$ which is a preimage of $t$ under doubling. In other words, $\alpha$ must satisfy $2^k\alpha \equiv t \mod 1$ for some $k \geq 0$ . (Compare Figure 11.) Here the "direction" from $C$ is measured using the Böttcher parametrization of the boundary $\partial C$ , as described above. One particular direction plays a special role: namely, the direction $\alpha = 2t$ , which leads from the component $C$ back towards the principal component $\hat{\mathcal{H}}_0$ .

**Case D.** From each embedded Mandelbrot set $F * M$ we can go out in any dyadic direction $\delta = m/2^k$ , measured around the Caratheodory loop $\delta \mapsto \gamma(\delta) \in \partial M$ which parametrizes the boundary of $M$ . (The number $\delta \in \mathbb{R}/\mathbb{Z}$ can be described as an external argument with respect to $M$ , but is certainly not an external argument with respect to the cubic connectedness locus.) Here the case $\delta = 0$ plays a special role, as the direction in which we must proceed from $F * M$ in order to get back to the principal hyperbolic component $\hat{\mathcal{H}}_0$ .

In particular, if we start out on some immediate satellite $F_t * M$ of the principal hyperbolic component, then at each dyadic boundary point $F_t * \gamma(\delta)$ , $\delta \neq 0$ , there is a capture component, which we will denote by $C(t, \delta)$ , immediately attached.

Thus the principal component $\hat{\mathcal{H}}_0$ has immediate satellites $F_t * M$ , and these have immediate satellites $C(t, \delta)$ . According to (Roesch 06): *These are the only examples of hyperbolic components or Mandelbrot sets in $\mathcal{S}_1$ which are immediately contiguous to each other.* If we exclude these cases, and if we exclude contiguous components within an embedded Mandelbrot set, then it is conjectured that we can pass from one hyperbolic component to another only by passing through infinitely many components, both of Type C and of Type D.

# 4A. Hubbard Trees.

(Compare §6 as well as the Appendix.) In order to partially justify this picture, let us describe Hubbard trees for the various hyperbolic components. The Hubbard tree for the center point $z \mapsto z^3$ of $\hat{\mathcal{H}}_0$ is of course just a single doubly-critical vertex.

The Hubbard tree $T(t)$ for the center point $F_t$ of the satellite $F_t * M$ can be described as follows. We assume that the argument $t \in \mathbb{Q}/\mathbb{Z}$ has period $n \geq 1$ under doubling modulo 1. *Then $T(t)$ consists of $n$ different edges radiating out from a central vertex at angles $t$, $2t$, $4t$, $\ldots$ modulo 1, as measured from some fixed base direction.* Here the central vertex $\mathbf{v}_0$ and the other endpoint $\mathbf{w}_0$ of the edge at angle $t$ are both critical, but all other vertices are non-critical. The canonical mapping $\tau$ from $T(t)$ to itself fixes the central vertex $\mathbf{v}_0$ and permutes the other vertices cyclically, carrying the vertex at angle $\alpha$ to the vertex at angle $2\alpha$ .

Now choose some dyadic angle $\delta = m/2^k \not\equiv 0$ in $\mathbb{Q}/\mathbb{Z}$ . Let $\gamma(\delta) \in M$ be the quadratic map at external argument $\delta$ in the Mandelbrot set, and let $T'(\delta)$

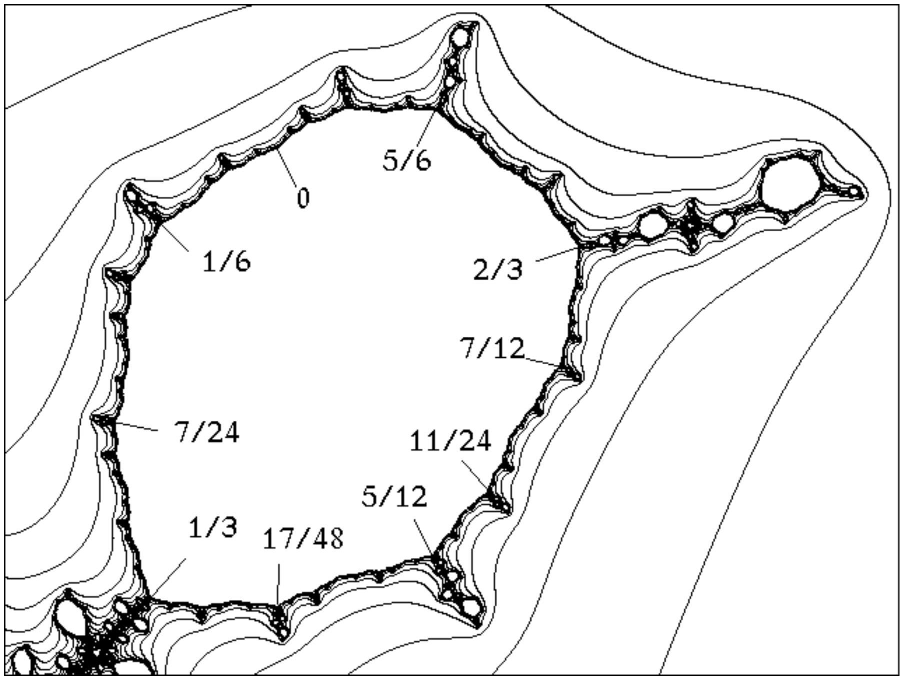


Figure 11: Detail of Figure 7, showing the capture component $C(2/3\,,\,1/2)$. (Here $2/3$ is the internal angle in $\hat{\mathcal{H}}_0$ at which a small Mandelbrot set is attached, and $1/2$ is the external angle with respect to this Mandelbrot set. The interior of this component $C(2/3\,,\,1/2)$ is parametrized by the Böttcher coordinate of $F^{\circ 3}(-a)$.

be its Hubbard tree. Thus the $(k+1)$-st forward image of the critical vertex in $T'(\delta)$ is a fixed vertex. If we tune $F_t$ by $\gamma(\delta)$, or equivalently if we tune $T(t)$ by $T'(\delta)$, then we obtain a new tree $T(t) * T'(\delta)$ for which the $(nk+1)$-st forward image $\mathbf{w}_{nk+1}$ of the "outer" critical point $\mathbf{w}_0$ is periodic of period $n$, lying at angle $2t$ from the central critical point $\mathbf{v}_0$. Thus for each edge of $T(t)$ it contains a complete copy of $T'(\delta)$, all of these copies being pasted together at the post-critical fixed point, which is now critical. (However, only the primary copy at angle $t$ contains another critical point.)

In order to obtain the tree $T(t, \delta)$ for the center of the satellite $C(t, \delta)$, we modify this construction very slightly as follows. As an angled topological tree with two marked critical points, $T(t, \delta)$ is identical with $T(t) * T'(\delta)$. However, $T(t, \delta)$ has fewer post-critical points, hence fewer vertices, and the canonical mapping from the tree to itself is changed so that the $nk$-th forward image $\mathbf{w}_{nk}$ of the outer critical point $\mathbf{w}_0$ maps to the central critical point $\mathbf{w}_{nk+1} = \mathbf{v}_0$. In other words, the edge $\mathbf{e}$ in the $t$-limb which leads out to $\mathbf{w}_{nk}$ is now to be mapped to a path in the $2t$-limb which leads all the way in to $\mathbf{v}_0$. (Figure 12, 13, 14.)

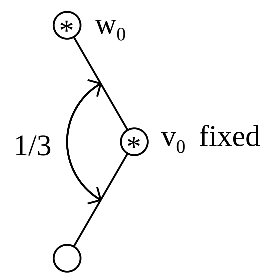


Figure 12: Tree for the center point $F_{1/3}$ of the satellite $F_{1/3} * M$ at internal angle $1/3$. Critical points are indicated by stars, and vertices in the Fatou set by small circles.

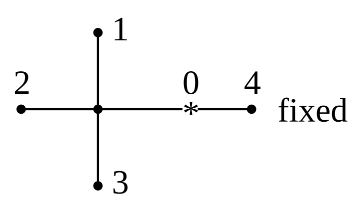


Figure 13: Tree for the quadratic map $\gamma(1/8)$ with external angle $1/8$ in the Mandelbrot set. The post-critical vertices are numbered so that $0 \mapsto 1 \mapsto 2 \mapsto \cdots$.

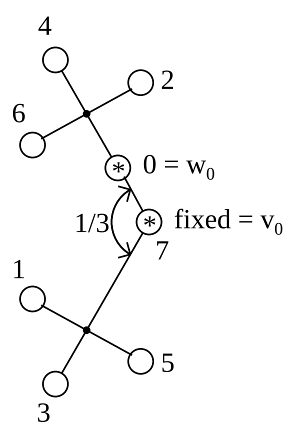


Figure 14: Tree for the center of the capture component $C(1/3\,,\,1/8)$ in $\mathcal{S}_1$ which is attached to $F_{1/3} * M$ at the point $F_{1/3} * \gamma(1/8)$.

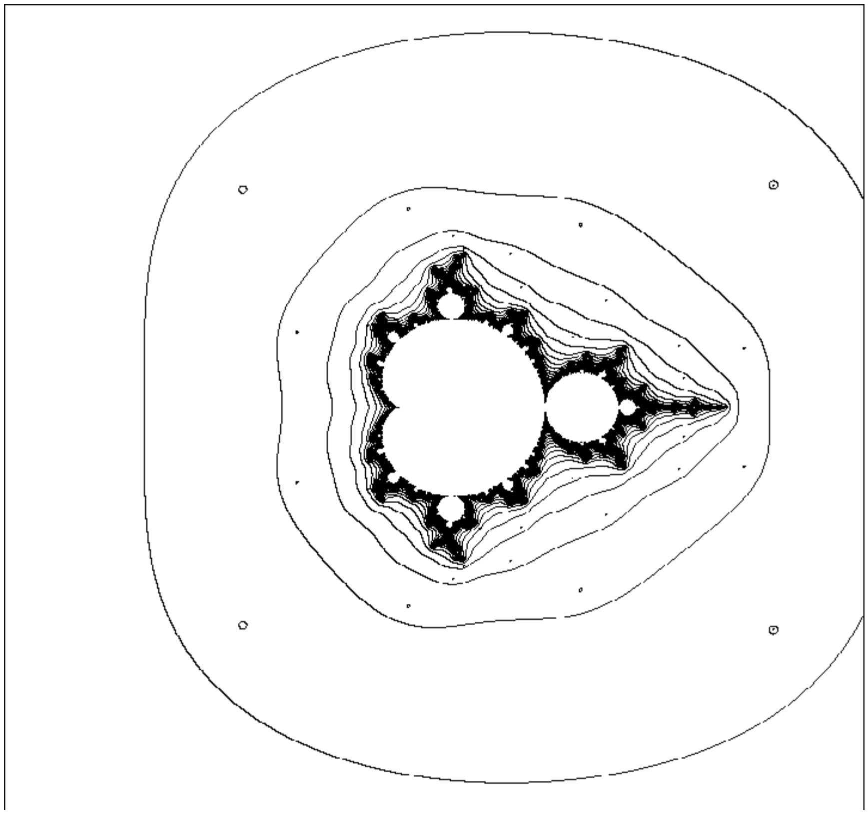

Figure 15: A small slice of constant height $b \equiv 18$ through a Mandelbrot-torus in the plane $\hat{\mathcal{P}}(3)$, using coordinates $(a,\, b)$. Here $a$ varies over a box of width $.04$ centered at $a = 2$. This slice intersects the curve $\mathcal{S}_1$ tranversally at the central point of the figure.

More generally, consider the tree $T$ for an arbitrary component of Type D in $\mathcal{S}_1$. Suppose that the outer critical point $\mathbf{w}_0$ has period $n$, and lies at angle $t$ from the central vertex $\mathbf{v}_0$. For any dyadic angle $\delta$ as above, we can tune to obtain a tree $T * T'(\delta)$ for which the $(nk+1)$-st image $\mathbf{w}_{nk+1}$ of $\mathbf{w}_0$ is periodic of period $n$, and lies in the $2t$-limb. Again we can stretch this $(nk+1)$-st image in towards the central vertex, and thus construct other hyperbolic components. But in general, there does not seem to be a immediately contiguous component which can be constructed in this way.

Similarly, we can consider a completely arbitrary capture component in $\mathcal{S}_1$. The corresponding tree $T$ has outer critical point $\mathbf{w}_0$ lying in a limb which has angle say $t$ from the fixed central vertex $\mathbf{v}_0$. If the $(k+1)$-st forward image $\mathbf{w}_{k+1}$ of $\mathbf{w}_0$ is equal to $\mathbf{v}_0$, then it is not difficult to see that the $k$-th forward image $\mathbf{w}_k$ must lie in the $t$-limb. (Every other limb, at angle say $\alpha$, maps isomorphically into the limb at angle $2\alpha$.) Thus, the edge $\mathbf{e}$ in the $t$-limb which leads out to $\mathbf{w}_k$ must map to a path in the $2t$-limb which leads in to $v_0$. Now suppose that we choose any angle $\alpha \not\equiv 2t$ which is a pre-image of $t$ under doubling modulo 1. Then we can modify this tree, adding an $\alpha$-limb if it does not already exist, so that the image of $\mathbf{e}$, leading from the $2t$-limb into the center, will extend on out into the $\alpha$-limb. In this new tree, the $(k+1)$-st image of $\mathbf{w}_0$ will lie in the $\alpha$-limb, hence some further iterated image will lie back in the $t$-limb. By such constructions, it is not difficult to obtain either a tree in which $\mathbf{w}_0$ is periodic, or a tree in which $\mathbf{w}_0$ eventually maps to the fixed point $v_0$. In either case, the associated hyperbolic component can be described as one which lies in the $\alpha$-direction from our initial capture component with tree $T$.

**Remark 4.1. What does a neighborhood of $\mathcal{S}_1$ look like?** (Compare Remark 1.1.) Understanding the curve $\mathcal{S}_1$ should be a first step towards understanding the dynamics for maps in $\hat{\mathcal{P}}(3)$ which are close to $\mathcal{S}_1$. Perhaps the easiest points to understand are those in the escape locus. According to (Branner and Hubbard 92) or (Branner 93), each escape point in $\mathcal{S}_1$ is the center of a small Mandelbrot set in the transverse direction, with each period $p$ center in this Mandelbrot set corresponding to an intersection with the period $p$ curve $\mathcal{S}_p$. A transverse section, as shown in Figure 15, illustrates such a small Mandelbrot set. Note the small dots outside of the Mandelbrot copy. Each one seems to represent a small Cantor set of maps. The complementary region, outside of these Cantor sets and outside this Mandelbrot set, represents maps in the shift locus.

# 5 Topology and Geometry of the Superattracting Curve $\mathcal{S}_p$.

For any integer $p \geq 1$, let $\mathcal{S}_p \subset \hat{\mathcal{P}}(3)$ be the ***period $p$ superattracting curve*** consisting of all $F \in \hat{\mathcal{P}}(3)$ for which the critical point $+a$ has period exactly $p$. In other words, $\mathcal{S}_p$ can be identified with the affine algebraic variety consisting of all pairs $(a, v) \in \mathbb{C}^2$ such that the critical point $a$ has period exactly $p$ under the map

$$F(z) \;=\; z^3 - 3a^2 z + (2a^3 + v)\,. \tag{12}$$

**Remark 5.1.** It is important to work with this normal form, rather than with $F(z) = z^3 - 3a^2 z + b$, since it will allow a simpler description of the curve $\mathcal{S}_p$. As examples, the equations for $\mathcal{S}_1$ and $\mathcal{S}_2$ in the $(a, v)$-plane take the form

$$v - a \;=\; 0 \qquad \text{and} \qquad v^3 - 3a^2 v + 2a^3 + v - a \;=\; 0\,,$$

with degrees one and three respectively. The corresponding equations in the $(a, b)$-plane, obtained by substituting $b - 2a^3$ in place of $v$, would have degrees three and nine.

**Theorem 5.2.** *Each $\mathcal{S}_p$ is a smooth affine algebraic curve.*

The proof will be given later in this section.

**Question 5.3. Is $\mathcal{S}_p$ connected?** It seems quite possible that all of the curves $\mathcal{S}_p$ are irreducible, or equivalently that they are topologically connected. For example, we will see that $\mathcal{S}_1$ and $\mathcal{S}_2$ are connected curves of genus zero, while $\mathcal{S}_3$ is a connected curve of genus one. However, I don't know how to attack this question in general.

The degree of the affine curve $\mathcal{S}_p$ can be computed as follows. It will be convenient to first consider the disjoint union $\bigcup_{n|p}\mathcal{S}_n \subset \mathbb{C}^2$ of the curves $\mathcal{S}_n$ where $n$ ranges over all divisors of $p$. This will be denoted by $\mathcal{S}_p^{\uplus}$.

**Lemma 5.4.** *The degree of this affine curve $\mathcal{S}_p^{\uplus}$ is*

$$\deg(\mathcal{S}_p^{\uplus}) \;=\; \sum_{n|p}\deg(\mathcal{S}_n) \;=\; 3^{p-1}\,.$$

*Furthermore, the number of hyperbolic components of Type A in $\mathcal{S}_p^{\uplus}$ is also equal to $3^{p-1}$.*

**Remark 5.5.** Given this statement, it is easy to compute the degree of $\mathcal{S}_p$. Assuming inductively that we have computed the degree $\deg(\mathcal{S}_n)$ for all proper divisors of $p$, we simply need to subtract these numbers from $3^{p-1}$ to get the degree of $\mathcal{S}_p$. More generally, it will be convenient to define numbers $\nu_d(p)$ by the equation[3]

$$d^p \;=\; \sum_{n|p}\nu_d(n)\,.$$

For example, $\nu_d(p)$ can be interpreted as the number of period $p$ points for a generic polynomial map of degree $d$, and $\nu_2(p)/2$ can be interpreted as the number of period $p$ centers in the Mandelbrot set. With this notation, our conclusion is that

$$\deg(\mathcal{S}_p) \;=\; \nu_3(p)/3\,.$$

Here is a table listing $\nu_2(p)/2$ and $\nu_3(p)/3$ for small $p$.

| $p$ | 1 | 2 | 3 | 4 | 5 | 6 | 7 | 8 | 9 | 10 |
|---|---|---|---|---|---|---|---|---|---|---|
| $\nu_2(p)/2$ | 1 | 1 | 3 | 6 | 15 | 27 | 63 | 120 | 252 | 495 |
| $\nu_3(p)/3$ | 1 | 2 | 8 | 24 | 80 | 232 | 728 | 2160 | 6552 | 19600 |

**Proof of Lemma 5.4.** Evidently $\mathcal{S}_p^{\uplus}$ can be defined by the polynomial equation $F^{\circ p}(a)-a=0$. Since $F(z)=z^3-3a^2z+2a^3+v$, we can write

$$\begin{aligned} F(a) &= v\,,\\ F^{\circ 2}(a) &= (v^3-3a^2v+2a^3)+v\,, \end{aligned}$$

[3] Equivalently, by the Möbius Inversion Formula, $\nu(p) = \sum_{n|p}\mu(n)\,d^{p/n}$, where the ***Möbius function*** $\mu(n)$ equals $(-1)^k$ if $n=p_1p_2\cdots p_k$ is a product of $k$ distinct prime factors, with $\mu(1)=1$, but with $\mu(n)=0$ whenever $n$ has a squared prime factor.

and in general

$$F^{\circ p}(a) \;=\; (v^3 - 3a^2v + 2a^3)^{3^{p-2}} + \text{ (lower order terms)} \qquad (13)$$

for $p \ge 2$. Thus the equation $F^{\circ p}(a) = a$ has degree $3^{p-1}$ in the variables $a$, $v$, as asserted.

To count hyperbolic components of Type $A$, note that the center of each such component is a polynomial of the form $F(z) = z^3 + v$. More generally, for any degree $d$ we can study the family of maps

$$g_v(z) \;=\; z^d + v, \qquad (14)$$

counting the number of $v$ such that the critical orbit $0 \mapsto v \mapsto v^d + v \mapsto \cdots$ has period $p$. The argument will be based on (Schleicher 04) which studies the connectedness locus for for the family (14), known as the ***Multibrot set***. In particular, Schleicher studies external rays in the $v$ parameter plane. He shows that for each angle which has period $p$ under multiplication by $d$, the corresponding parameter ray lands on the boundary of a hyperbolic component of period $p$. Furthermore, if $p \ge 2$, then exactly $d$ such rays land on the boundary of any given period $p$ component. In the period one case, the corresponding statement is that all $d-1$ of the rays of period one land on the boundary of the unique period one component. Since there are exactly $d^p - 1$ rays which have period dividing $p$, a straightforward argument now shows that the number of period $p$ components in the Multibrot set is $\nu_d(p)/d$, and the conclusion follows. $\square$

**Remark 5.6.** The centers of period dividing $p$ in this Multibrot family are precisely the roots of the polynomial $g_c^{\circ p}(0)$, which has degree $d^{p-1}$. Thus an immediate corollary of Lemma 5.4 is the purely algebraic statement that this polynomial has $d^{p-1}$ distinct roots.

These same numbers $\nu_3(p)/3$ can also be used to count hyperbolic components of Type B and D.

**Definition 5.7.** Let $\mathcal{S}'_p \subset \hat{\mathcal{P}}(3)$ be the ***dual*** superattractive period $p$ curve, consisting of all maps $F(z) = z^3 - 3a^2z + 2a^3 + v$ for which the critical point $-a$ has period exactly $p$.

**Lemma 5.8.** *For each $p$, $r \ge 1$, the curve $\mathcal{S}_p$ intersects $\mathcal{S}'_r$ transversally in $\nu_3(p)\nu_3(r)/3$ distinct points. These intersection points comprise precisely the center points of all hyperbolic components in $\mathcal{C}(3)$ which have Type A, B, or D.*

(On the other hand the center point of a component of Type C lies on only one of these curves $\mathcal{S}_p$ or $\mathcal{S}'_r$.) As examples, for $p = 1, 2, 3$, the intersection $\mathcal{S}_p \cap \mathcal{S}'_1$ consists of 3, 6, and 24 points respectively, while $\mathcal{S}_2 \cap \mathcal{S}'_2$ has 12 points. Representative Hubbard trees are shown in Figures 34 and 35, while Julia sets illustrating three of these trees are shown in Figure 36.

**Proof of Lemma 5.8.** We will use Bezout's theorem, which states that if two curves in the complex projective plane intersect transversally, then the number of intersection points is equal to the product of the degrees of the two curves. As noted above, the curve $\mathcal{S}_p$ has degree $\nu_3(p)/3$. A similar computation shows that the curve $\mathcal{S}'_r$ has degree $\nu_3(r)$. (Note: The asymmetry between these two formulas arises from the fact that we are using coordinates $(a, v)$ which are particularly adapted to studying the orbit of $a$ rather than $-a$. The polynomial

$$F^{\circ r}(-a) - (-a) \;=\; (4a^3 + v)^{3^{r-1}} + (\text{lower order terms})$$

has degree $3^r$ rather than $3^{r-1}$.) The curve $\mathcal{S}_p$ intersects the line at infinity in two (highly multiple) points where the ratios $(a : v : 1)$ take the values $(1 : 1 : 0)$ and $(1 : -2 : 0)$ respectively; while $\mathcal{S}'_r$ intersects the line at infinity in the single point $(0 : 1 : 0)$. Thus there are no intersections at infinity, and the conclusion follows. $\square$

## 5A. Escape Regions.

The complement $\mathcal{S}_p \smallsetminus \mathcal{C}(\mathcal{S}_p)$ of the connectedness locus will be called the ***escape locus*** in $\mathcal{S}_p$. Each connected component $\mathcal{E}$ of the escape locus will be called an ***escape region***.

We will see that each escape region $\mathcal{E}$ is conformally isomorphic to a punctured disk (or equivalently to the region $\mathbb{C} \smallsetminus \overline{\mathbb{D}}$). Thus $\mathcal{S}_p$ can be made into a smooth compact surface $\overline{\mathcal{S}}_p$ by adjoining finitely many ideal points, one for each escape region. We can then think of each connected component of $\mathcal{S}_p$ as a multiply punctured Riemann surface with its connectedness locus as a single connected "continent", and with the escape regions as the complementary "oceans", each centered at one of the puncture points. Assuming that this connected component of $\mathcal{S}_p$ is mapped to itself by the canonical involution $\mathcal{I}$, it is a 2-fold branched covering of the corresponding connected component of $\mathcal{S}_p/\mathcal{I}$.

Here is a precise statement.

**Lemma 5.9.** *Each escape region $\mathcal{E}$ is canonically isomorphic to the $\mu$-fold cyclic covering of $\mathbb{C} \smallsetminus \overline{\mathbb{D}}$ for some integer $\mu \geq 1$.*

By definition, this integer $\mu = \mu(\mathcal{E}) \geq 1$ will be called the ***multiplicity*** of the escape region $\mathcal{E}$.

**Proof of Lemma 5.9.** For any $F = F_{a,v} \in \hat{\mathcal{P}}(3)$, the associated Böttcher coordinate $\beta(z) = \beta_{a,v}$ is defined for all complex $z$ with $|z|$ sufficiently large. It satisfies the equation

$$\beta(F(z)) \;=\; \beta(z)^3\,,$$

with $|\beta(z)| > 1$, and with $\beta(z)/z$ converging to $+1$ as $|z| \to \infty$. In particular the co-critical point $2a$ is just large enough so that $\beta(2a)$ is well defined. Now consider the map

$$\widehat{\beta} :\; \mathcal{E} \to \mathbb{C} \smallsetminus \overline{\mathbb{D}} \quad \text{defined by} \quad \widehat{\beta}(F_{a,v}) \;=\; \beta_{a,v}(2a)\,.$$

It is not hard to check that $\widehat{\beta}$ is holomorphic and locally bijective, and that $|\widehat{\beta}(F)|$ converges to $+1$ as $F$ converges towards the connectedness locus. In order to show that it is a covering map, we must describe its behavior near infinity.

As in the proof of Lemma 3.3 Equation (11), we can estimate the behavior of $\widehat{\beta}$ as $|a|$ or $|v|$ tends to infinity, yielding the asymptotic formula

$$\widehat{\beta}(F_{a,v}) \;\sim\; \sqrt[3]{4}\,a \qquad \text{as} \qquad |a| \to \infty\,.$$

Thus $\widehat{\beta}:\ \mathcal{E} \to \mathbb{C}\smallsetminus\overline{\mathbb{D}}$ is proper and locally bijective. Hence it is a covering map of some degree $\mu \geq 1$, as required. $\square$

In particular, it follows that we can choose a conformal isomorphism $\zeta:\ \mathcal{E} \to \mathbb{D}\smallsetminus\{0\}$ satisfying $\zeta(F)^\mu = 1/\widehat{\beta}(F)$. In fact $\zeta$ is uniquely defined up to multiplication by $\mu$-th roots of unity. If $\mathcal{E}^+$ denotes the Riemann surface which is obtained from $\mathcal{E}$ by adjoining a single ideal point at infinity, then $\zeta$ extends to a conformal isomorphism from $\mathcal{E}^+$ onto the open unit disk $\mathbb{D}$. Now $a$ can be expressed as a meromorphic function on $\mathcal{E}^+$ with a pole of order $\mu$. Writing this as $a = \phi(\zeta)/\zeta^\mu$ where $\phi:\ \mathcal{E} \to \mathbb{D}$ is holomorphic with $\phi(0) \neq 0$, we can choose a smooth $\mu$-th root of $\phi(\zeta)$ near the origin. Hence the formula

$$\xi \;=\; 1/\sqrt[\mu]{a} \;=\; \zeta/\sqrt[\mu]{\phi(\zeta)}$$

provides an alternative parametrization of a neighborhood of the base point $\zeta = 0$ in $\mathcal{E}^+$, with $\xi^\mu$ precisely equal to $1/a$.

**Remark 5.10.** Using Lemma 5.9, we can talk about equipotentials and external rays within any escape region. In particular, we can study the landing points of periodic and preperiodic rays. This provides an important tool for understanding the dynamics associated with nearby points of the connectedness locus.

Here is a more geometric interpretation of the multiplicity. Recall that $\mathcal{S}_p$ can be described as an affine curve in the space $\mathbb{C}^2$ with coordinates $(a,\,v)$.

**Lemma 5.11.** *For any constant $a_0$ with $|a_0|$ large, the number of intersections of the line $a = a_0$ in $\mathbb{C}^2$ with the escape region $\mathcal{E} \subset \mathcal{S}_p$ is equal to the multiplicity $\mu(\mathcal{E})$.*

In fact, using this parameter $\xi$, the $\mu$ intersection points correspond precisely to the $\mu$ possible choices for an $\mu$-th root of $a$. $\square$

**Corollary 5.12.** *The number of escape regions in $\mathcal{S}_p$, counted with multiplicity, is equal to the degree $\nu_3(p)/3$.*

**Proof.** This follows immediately, since a generic line intersects $\mathcal{S}_p$ exactly $\nu_3(p)/3$ times. $\square$

We can make a corresponding count of the number of escape regions in the quotient curve $\mathcal{S}_p/\mathcal{I}$. The easiest procedure is just to define the ***multiplicity*** for an escape region $\mathcal{E}/\mathcal{I} \subset \mathcal{S}_p/\mathcal{I}$ to be the sum of the multiplicities of its preimages in $\mathcal{S}_p$. In other words, for each escape region $\mathcal{E}$ in $\mathcal{S}_p$ we set

$$\mu(\mathcal{E}/\mathcal{I}) \;=\; \begin{cases} \mu(\mathcal{E}) & \text{if} \quad \mathcal{E} = \mathcal{I}(\mathcal{E})\,, \\ 2\mu(\mathcal{E}) & \text{if} \quad \mathcal{E} \neq \mathcal{I}(\mathcal{E})\,. \end{cases}$$

With this definition, we clearly get the following statement.

**Corollary 5.13.** ***The number of escape regions in*** $\mathcal{S}_p/\mathcal{I}$***, counted with multiplicity, is also equal to*** $\nu_3(p)/3$***.***

## 5B. The Kneading Sequence of an Escape Region.

Any bounded hyperbolic component of $\mathcal{S}_p$ can be concisely labeled by two complex numbers: the $a$ and $v$ coordinates of its center point. (Compare §5.) However, it is not so easy to label escape components. This section will describe a preliminary classification based on two invariants: the ***kneading sequence***, which is a sequence of zeros and ones with period $q$ dividing $p$, and the ***associated quadratic map***, which is a critically periodic quadratic map with period $p/q$. For periods $p \le 3$, these invariants suffice to give a complete classification of escape regions in the moduli space $\mathcal{S}_p/\mathcal{I}$, but for larger periods they provide only a partial classification. (A complete classification, based on the Puiseux expansion at infinity, will be described in Part 2 of this paper. Compare (Kiwi 06).)

Let $F = F_{a,\,v}$ be any map such that the marked critical point $a$ belongs to the filled Julia set $K(F)$ while the orbit of $-a$ escapes to infinity. Then the orbit of any point $z \in K(F)$ can be described roughly by a symbol sequence $\sigma(z) \in \{0,\,1\}^{\mathbb{N}}$, as follows. There is a unique external ray, with angle say $t$, which lands at the escaping co-critical point $2a$, while two rays of angles $t \pm 1/3$ land at the escaping critical point $-a$. (Compare Figure 9.) These two rays cut the complex plane into two regions, with $a$ on one side and $-2a$ on the other. In fact the equipotential through $-a$ and $2a$ cuts the plane into two bounded regions $U_0$ and $U_1$, numbered so that $a \in U_0$ and $-2a \in U_1$, together with one unbounded region where orbits escape to infinity more rapidly. Now any orbit $z_0 \mapsto z_1 \mapsto \cdots$ in $K(F)$ determines a symbol sequence

$$\sigma(z_0) \;=\; (\sigma_0,\, \sigma_1,\, \ldots) \quad \text{with} \quad \sigma_j \in \{0,1\} \quad \text{and} \quad z_j \in U_{\sigma_j} \quad \text{for all} \;\; j \ge 0\,.$$

In particular, any periodic point determines a periodic symbol sequence. Thus, if $F$ belongs to an escape region in $\mathcal{S}_p$, then the critical point $a$ determines a periodic sequence $\sigma(a) \in \{0,\,1\}^{\mathbb{N}}$, with $\sigma_{j+p}(a) = \sigma_j(a)$, and with $\sigma_0(a) = 0$.

**Definition 5.14.** The periodic sequence $\sigma_1(a)$, $\sigma_2(a)$, …, starting with the symbol $\sigma_1(a)$ for the critical value, will be called the ***kneading sequence*** for the map. It will be convenient to denote this sequence briefly as $\overline{\sigma_1 \cdots \sigma_{p-1} 0}$, where the overline indicates infinite repetition. Evidently the (minimal) period $q$ of this kneading sequence is always a divisor of the period $p$ of $a$. In particular, $1 \le q \le p$.

For each such $F \in \mathcal{S}_p$, let $K_0(F) \subset K(F)$ be the connected component of $a$ in the filled Julia set. The following result (stated somewhat differently) is due to (Branner and Hubbard 92). It makes use of ***hybrid equivalence*** in the sense of (Douady and Hubbard 84/85)??.

**Theorem 5.15.** *The map $F$ restricted to a neighborhood of $K_0(F)$ is hybrid equivalent to a unique quadratic polynomial, which has periodic critical orbit of period equal to the quotient $p/q$, where $q$ is the period of the kneading sequence $\sigma(a)$.*

In fact, Branner and Hubbard show that every connected component of $K(F)$ is either a copy of $K_0(F)$ or a point.

**Outline Proof of Theorem 5.15.** Consider the open set $U_0$, as illustrated in Figure 9. Let $V_0 \subset U_0$ be the connected component of $F^{-q}(U_0)$ which contains $a$, and let $V_j = F^{\circ j}(V_0)$. Evidently $V_j \subset U_{\sigma_j}$ for $0 \le j \le q$, with $V_q = U_0$. Note that the sets $V_1, V_2, \ldots, V_{q-1}$ cannot contain any critical point. For if $a \in V_j$ then $V_0 \subset V_j$, and it would follow easily that the kneading sequence has period dividing $j$. By definition, this cannot happen for $0 < j < q$. It then follows that $F^{\circ q}$ mapping $V_0$ onto $V_q = U_0$ is a proper map with only one critical point. Thus it is a degree two polynomial-like map with non-escaping critical orbit. Therefore, according to (Douady and Hubbard 85), the filled Julia set $K_0$ of this polynomial-like mapping is hybrid-equivalent to $K(z \mapsto z^2 + c)$ for some unique $c$ in the Mandelbrot set. It is not hard to see that $K_0$ can be identified with the connected component of $a$ in $K(F)$. $\square$

Here is another interpretation of the kneading sequence $\{\sigma_j\}$.

**Theorem 5.16.** *Each point $a_j = F^{\circ j}(a)$ in the periodic critical orbit is asymptotic to either $a$ or $-2a$ as $|a| \to \infty$, with*

$$a_j \;\sim\; \begin{cases} a & \text{if} \quad \sigma_j = 0, \\ -2a & \text{if} \quad \sigma_j = 1, \end{cases}$$

*or briefly $a_j \sim (1 - 3\sigma_j)\, a$. In fact the difference*

$$a_j - (1 - 3\sigma_j)a \tag{15}$$

*extends to a bounded holomorphic function from $\mathcal{E}^+ = \mathcal{E} \cup \infty$ to $\mathbb{C}$.*

**Proof.** Using the defining equation

$$a_{j+1} \;=\; a_j^3 - 3a^2 a_j + 2a^3 + v \qquad \text{with} \quad a_0 = a\,,$$

this difference (15) can clearly be expressed as a meromorphic function on $\mathcal{E} \cup \infty$, holomorphic throughout $\mathcal{E}$. Since it is clearly bounded on the intersection of $\mathcal{E}$

with any compact subset of $\mathcal{S}_p$, the only problem is to prove boundedness as $|a| \to \infty$.

As in the proof of Lemma 5.9, we can parametrize a neighborhood of infinity in $\mathcal{E}$ by a branch of $\sqrt[\mu]{a}$. Hence we can expand each $a_j$ as a Puiseux series of the form

$$\sum_{n \le n_0} k_n a^{n/\mu} \;=\; k_{n_0} a^{n_0/\mu} + \cdots + k_1 a^{1/\mu} + k_0 + k_{-1} a^{-1/\mu} + \cdots ,$$

with leading coefficient $k_{n_0} \neq 0$. (Compare (Kiwi 06).) First consider this expansion for $a_1 = v$. If the leading term had degree $n_0/\mu > 1$, then the $a^{3n_0/\mu}$ term in the series for $F(a_1) = a_2$ would dominate, and it would follow easily that the series for the successive $a_j$ would have leading terms of degree tending rapidly to infinity, which would contradict periodicity. On the other hand, if the leading term of the series for $v = a_1$ had degree $n_0/\mu < 1$, then the $2a^3$ term in the series for $F(a_1)$ would dominate, and again the successive degree would increase rapidly. Thus we must have $n_0 = \mu$. A completely analogous argument now shows that the series for every $a_j$ has leading coefficient of degree $n_0/\mu = 1$. Thus, for each $j$, this series has the form $a_j \;=\; k_\mu a +$ (lower order terms), so that

$$a_{j+1} \;=\; F(a_j) \;=\; (k_\mu^3 - 3k_\mu + 2)a^3 \;+\; (\text{lower order terms})\,.$$

But by the previous argument, the coefficient of $a^3$ must be zero. Therefore

$$k_\mu^3 - 3k_\mu + 2 \;=\; (k_\mu - 1)^2(k_\mu + 2) \;=\; 0\,.$$

*This proves that the leading coefficient $k_\mu$ for the expansion of any $a_j$ must be either $+1$ or $-2$. That is, each $a_j$ must be asymptotic to either $a$ or $-2a$.*

First suppose that $a_j \sim a$. Let $\epsilon = a_j - a$. We must prove that $\epsilon$ remains bounded as $|a| \to \infty$. Otherwise the Puiseux expansion for $\epsilon$ would start with a term of degree $n'/n$ with $0 < n' < \mu$. Using the identity

$$a_{j+1} \;=\; F(z + \epsilon) \;=\; v + 3a\epsilon^2 + \epsilon^3\,,$$

the $3a\epsilon^2$ would dominate, and would have degree $> 1$ which is impossible. Thus $\epsilon = O(1)$ as required.

In the case $a_j \sim -2a$, a completely analogous argument using the identity

$$F(-2a + \epsilon) \;=\; 9a^2\epsilon + 6a\epsilon^2 + \epsilon^3$$

proves the even sharper statement that $\epsilon = O(1/a)$ as $|a| \to \infty$. This completes the proof of Theorem 5.16. $\square$

We can sharpen the count in Lemma 5.11 as follows. Given a kneading sequence $\{\sigma_j\}$ of period dividing $p$, let $n = \sum_1^p (1 - \sigma_j)$ be the number of indices $1 \le j \le p$ with $\sigma_j = 0$. Thus $1 \le n \le p$.

**Lemma 5.17.** *The number of escape regions in $\mathcal{S}_p^{\uplus}$ with kneading sequence $\{\sigma_j\}$, counted with multiplicity, is equal to $2^{n-1}$.*

**Proof.** We can embed $\mathcal{S}_p^{\uplus}$ into $\mathbb{C}^p$ by mapping each point with periodic critical orbit

$$a = a_0 \mapsto a_1 \mapsto \cdots \mapsto a_p = a$$

to the $p$-tuple $(a_1, a_2, \ldots, a_{p-1}, a) \in \mathbb{C}^p$. Such $p$-tuples form a 1-dimensional affine variety, characterized by the polynomial equations:

$$F(a_j) \;=\; a_{j+1} \qquad \text{for} \qquad 1 \le j < p\,,$$

where $F(z) \;=\; z^3 - 3a^2 z + 2a^3 + a_1$ so that

$$a_{j+1} - a_1 \;=\; (a_j - a)^2 (a_j + 2a)\,. \tag{16}$$

Now embed $\mathbb{C}^p$ into the projective space $\mathbb{CP}^p$ by identifying each $(a_1, \ldots, a_{p-1} : a) \in \mathbb{C}^p$ with the point $(1 : a_1 : \ldots : a_{p-1} : a)$ in projective space. Intersect the resulting 1-dimensional projective variety with the $(p-1)$-plane at infinity consisting of all points of the form $(0 : a_1 : \ldots : a_{p-1} : a)$. The resulting intersection can be described by deleting all terms of lower degree from the equations (16), leaving only the cubic equations

$$(a_j - a)^2 (a_j + 2a) \;=\; 0\,. \tag{17}$$

This yields an alternative proof that, as $a$ tends to infinity, the ratio $a_j/a$ must tend to either $+1$ or $-2$. In fact, according to Equation (15), we know that

$$\lim_{a\to\infty} a_j/a \;=\; 1 - 3\sigma_j\,.$$

In other words, the resulting zero-dimensional variety at infinity consists precisely of the points

$$(0 : 1 - 3\sigma_1 : \cdots : 1 - 3\sigma_{p-1} : 1)$$

associated with different possible kneading sequences. The squared factor in equation (17) means that each point with $\sigma_j = +1$, $1 \le j < p$, must be counted double, for a total intersection multiplicity of $2^{n-1}$. Now approximating the plane at infinity by a plane $a =$ large constant, the number of intersections (counted with multiplicity) remains unchanged, and the conclusion follows. □

## 5C. Examples.

Here are more explicit descriptions of $\mathcal{S}_p$ and $\mathcal{S}_p/\mathcal{I}$ for the cases with $p \le 4$. (For the cases with $p \le 3$, each end of the curve $\mathcal{S}_p$ has multiplicity $\mu = 1$, so that there are exactly $\nu_3(p)/3$ ends.) In specifying periodic kneading sequences, recall that infinite repetition is indicated by an overline so that, for example, $\overline{010}$ stands for $010010010\cdots$.

**Period 1.** The curve $\overline{\mathcal{S}}_1 \cong \mathbb{C}$ has genus zero with one puncture of multiplicity one, namely the point at infinity. (Compare Figure 5.) The projection to $\overline{\mathcal{S}}_1/\mathcal{I}$ is a 2-fold branched covering, branched at the puncture point and at the center of the principal hyperbolic component. (Compare Figure 6.)

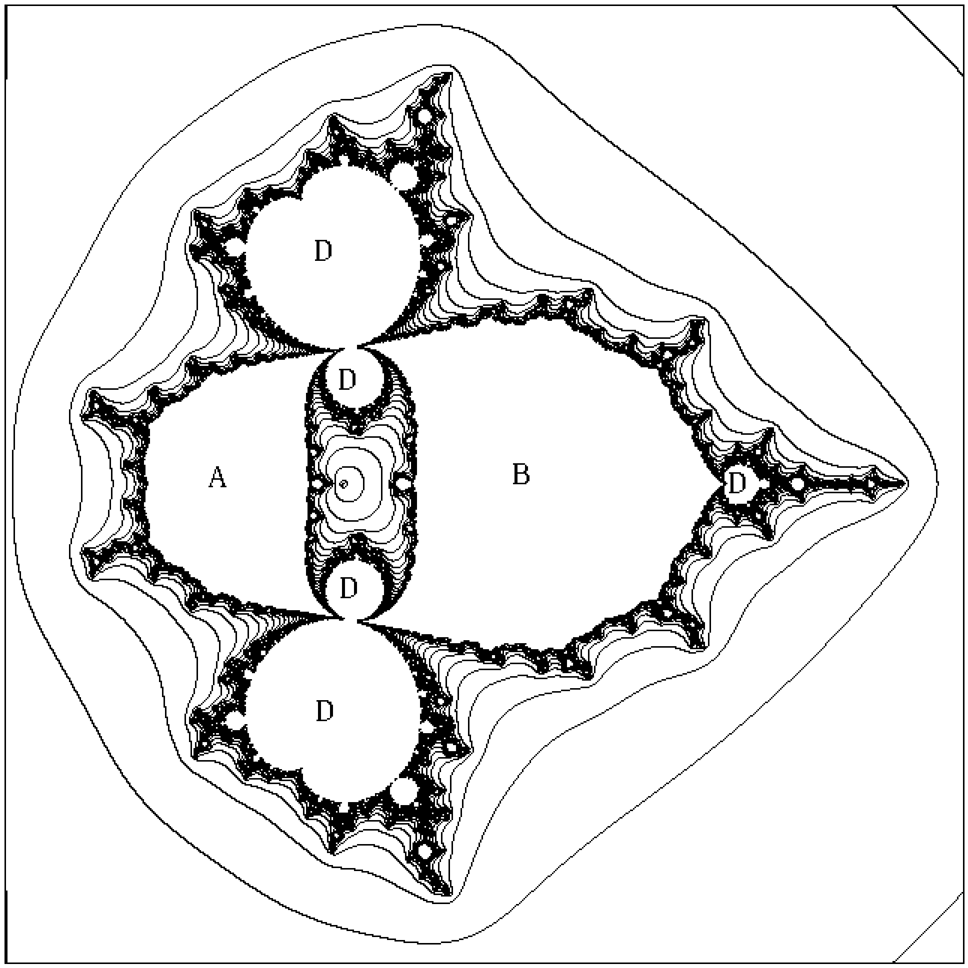


Figure 16: Connectedness locus in $\mathcal{S}_2/\mathcal{I}$, with coordinate $\delta^2 = (F(a) - a)^2$.

**Period 2.** The curve $\mathcal{S}_2$ has genus zero, and two ends of multiplicity one. In fact a polynomial $F \in \mathcal{S}_2$ can be uniquely specified by the "displacement" $\delta = F(a) - a$, which can take any value except zero and infinity. Given $\delta \in \mathbb{C} \smallsetminus \{0\}$, we can solve for $a = -(\delta + \delta^{-1})/3$ and $v = a + \delta$. The projection $\overline{\mathcal{S}}_2 \to \overline{\mathcal{S}}_2/\mathcal{I}$ is branched over the two punctures. Thus $\mathcal{S}_2/\mathcal{I}$ also has genus zero and two ends, with uniformizing parameter $\delta^2 \neq 0$. (See Figures 16–19.) This quotient surface contains one hyperbolic component of type A, one of type B, and infinitely many of types C and D. It contains two "escape regions", consisting of maps for which the orbit of the free critical point $-a$ escapes to infinity. Figure 18 shows a representative Julia set for a point in the inner escape region, centered at the origin, $\delta^2 = 0$. Every connected component of $K(F)$ is either a point or a homeomorphic copy of the filled Julia set for the "basilica"

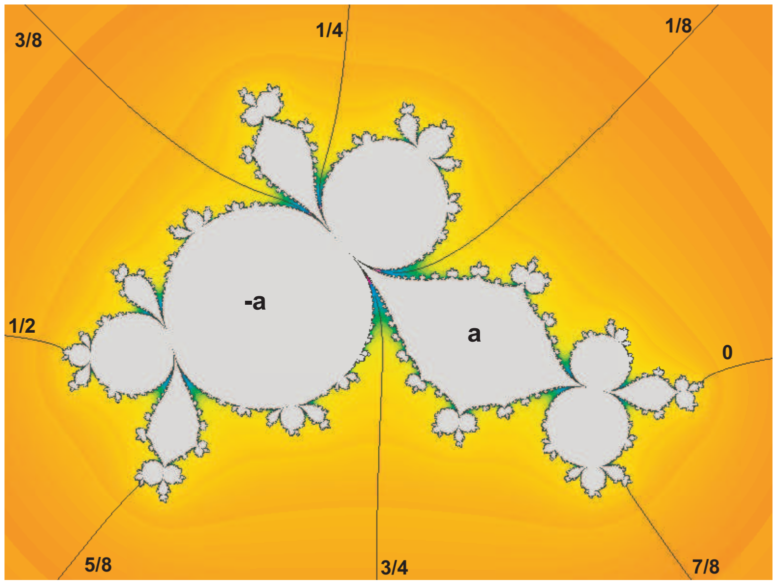


Figure 17: Julia set for a map $F \in \mathcal{S}_2$ which is a limit point of six different hyperbolic components, four bounded and two unbounded, as shown in Figure 16. (This is the higher of the two such maps, with $\delta^2 \approx .0620 + 1.4183\,i$.) Here the rays of angle $1/8$, $1/4$, $3/8$, and $3/4$ land at a common parabolic fixed point of multiplier $-1$. By arbitrarily small deformations, this parabolic point can split up in eight different ways, yielding a new map $F'$ which either belongs to one of four large bounded hyperbolic components, or one of the two escape regions. (The Julia set for the center of the smallest of these hyperbolic components is shown at the top of Figure 36.) Furthermore, $F$ can be deformed into either escape region in two essentially different ways, depending on whether the rays of angle $\{1/8,\ 3/8\}$ or those of angle $\{1/4,\ 3/4\}$ continue to land at a common fixed point.

map $Q(z) = z^2 - 1$. Figure 19 shows a representative Julia set for the outer escape region centered at $\infty$. Here each component of $K(F)$ is either a point or a copy of the closed unit disk (the filled Julia set for $Q(z) = z^2$). In both cases, the filled Julia set is partitioned into two subsets by the two external rays which crash together at the escaping critical point $-a$. These rays are shown in white.

Near either of these two puncture points, the curve $\mathcal{S}_2$ can be described by a Laurent expansion of the form

$$v(a) \;=\; \begin{cases} \;\;a \;-1/(3a) - 1/(3a)^3 - 2/(3a)^5 - 5/(3a)^7 - \cdots & \text{for } \delta \text{ near } 0, \\ -2a + 1/(3a) + 1/(3a)^3 + 2/(3a)^5 + 5/(3a)^7 + \cdots & \text{for } \delta \text{ near } \infty. \end{cases}$$

(Compare (Kiwi 06).)

However, one cannot expect that all hyperbolic Julia sets will be so easy to understand. The interaction between the two critical orbits can lead to

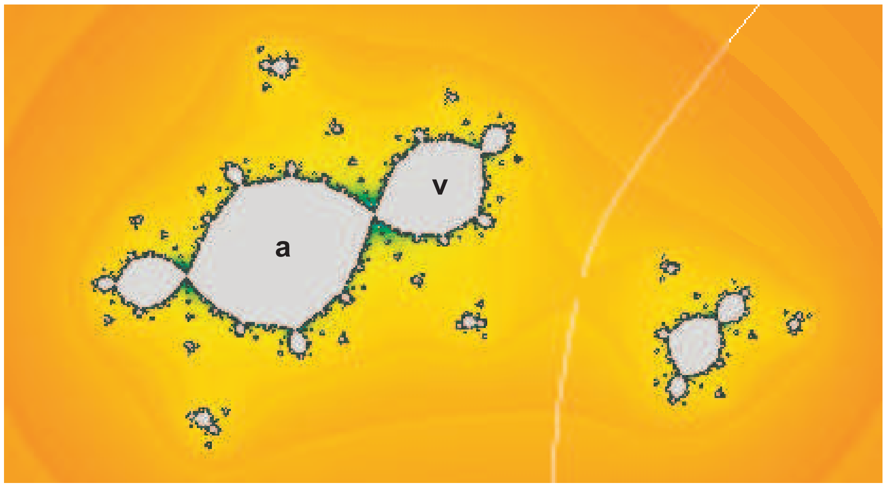


Figure 18: Julia set for a map $F$ in the inner escape region of $\mathcal{S}_2$, with kneading sequence $\overline{0}$ and with associated quadratic map $Q(z) = z^2 - 1$. (Here $\delta = .7 + .3i$.)

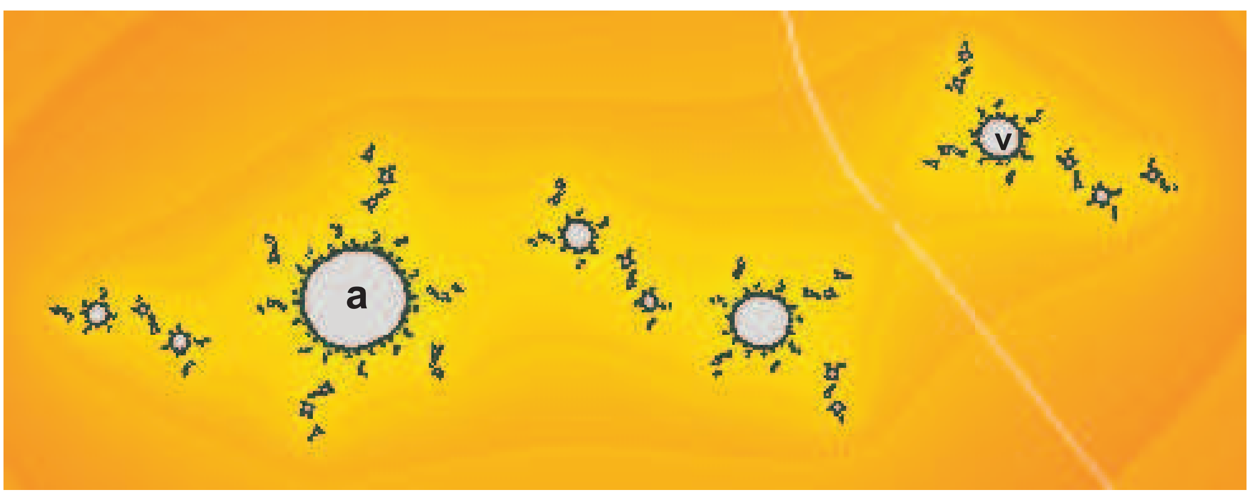


Figure 19: Julia set for a map $F \in \mathcal{S}_2$ in the outer escape region, with kneading sequence $\overline{01}$ and with associated quadratic map $Q(z) = z^2$. (Parameter value $\delta = 2 + .5i$.) In both of these figures, the two external rays which crash together at the escaping critical point $-a$ are shown in white.

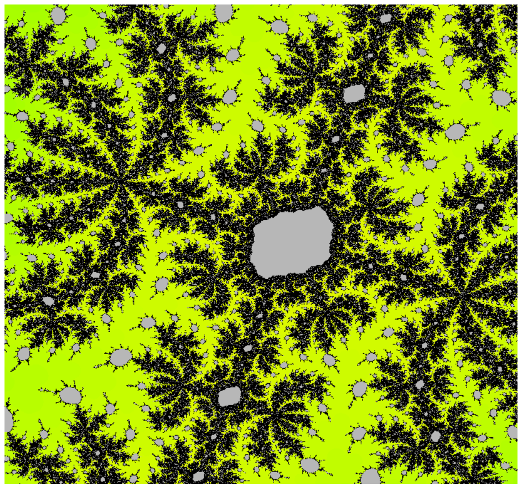

Figure 20: Detail from the Julia set of a hyperbolic map of type D. The Fatou component of the critical point $-a$ (in the center) has period 42, while the critical point $+a$ (far outside to the left) has period 2. Preimages of $-a$ are surrounded by foliage, while preimages of $+a$ are in the open.

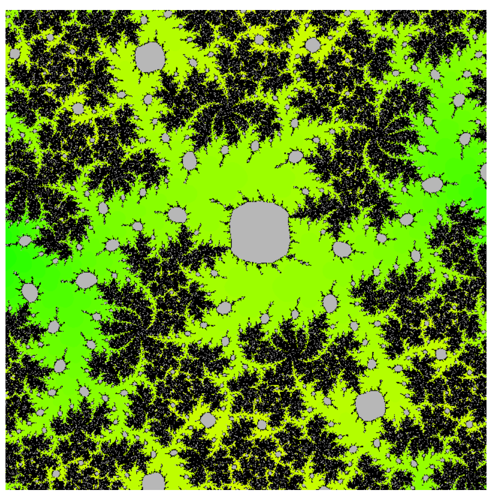

Figure 21: Detail from the Julia set of a hyperbolic map of type C. The critical point $+a$ (far to the left) has period 2, while the Fatou component of $-a$ (in the center) maps to the Fatou component of $+a$ after 85 iterations. Preimages of $-a$ are connected to the foliage on both sides, while the other preimages of $+a$ are connected on one side only.

remarkable richness and complexity, even in the hyperbolic case. The following two examples both represent points of the curve $\mathcal{S}_2$. Figure 20 shows an example of Type D with parameter $\delta = 2.03614{+}0.05431\,i$. The free critical point $-a$ lies on one of the seven branches emanating from a repelling periodic point (below the figure) with period two and rotation number 2/7. Figure 21 shows a nearby example of Type C with $\delta = 2.03540 + 0.05316\,i$.

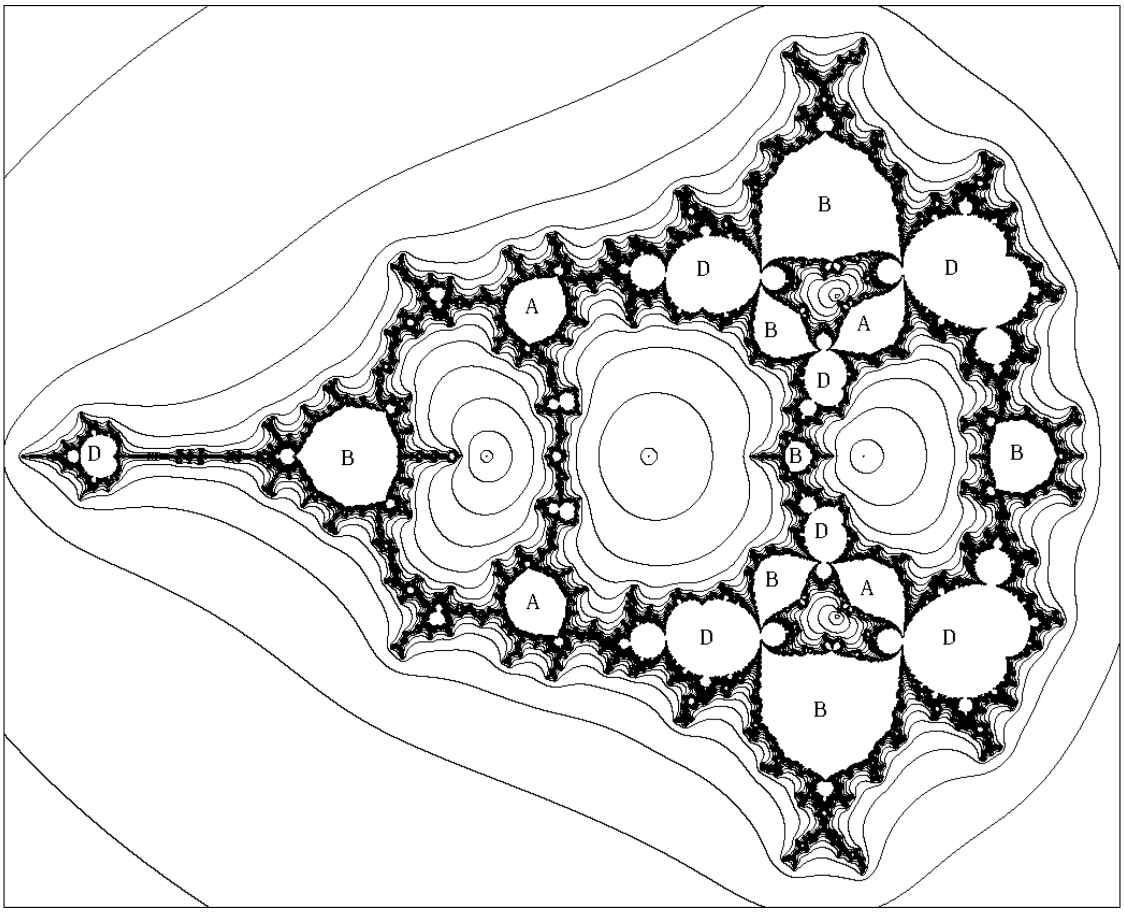


Figure 22: Connectedness locus in $\mathcal{S}_3/\mathcal{I}$, with coordinate $c = (F^{\circ 2}(a) - F(a))/(F(a) - a)$.

**Period 3.** The curve $\mathcal{S}_3$ has genus one, being diffeomorphic to an eight times punctured torus. However, the quotient $\mathcal{S}_3/\mathcal{I}$ has genus zero, with six ends. (Thus the involution $\mathcal{I}$ fixes four of the ends of $\mathcal{S}_3$ but permutes the other four in pairs.) More explicitly, a map in $\mathcal{S}_3$ is determined up to affine conjugation by the "shape" of its superattracting orbit. After an affine conjugation which moves the critical point $a$ to zero and the critical value $F(a)$ to one, our map $F$ will be replaced by something of the form $w \mapsto \alpha w^3 + \beta w^2 + 1$, where say $0 \mapsto 1 \mapsto 1+c \mapsto 0$. Here $c$ is a parameter which specifies the "shape" of the critical orbit. It is not difficult to solve for

$$\alpha \;=\; -\frac{c^3+2c^2+c+1}{c(c+1)^2}\;, \qquad\qquad \beta \;=\; c-\alpha \;=\; \frac{c^4+3c^3+3c^2+c+1}{c(c+1)^2}\quad .$$

Thus the coefficients $\alpha \neq 0$ and $\beta$ are uniquely determined by the shape parameter $c$, which can take any finite value with the exception of $c=0\,,\,-1\,$, where the denominator vanishes, and $c=-0.1225\pm 0.7448\,i$ or $-1.7548$ (to four significant figures), where the numerator of the expression for $\alpha$ vanishes. These five points, together with the point at infinity, represent punctures in the Riemann surface $\overline{\mathcal{S}}_3/\mathcal{I}\approx\widehat{\mathbb{C}}$. The associated connectedness locus in the $c$-plane, or in other words in $\mathcal{S}_3/\mathcal{I}$, is shown in Figure 22. To obtain a corresponding picture for the curve $\mathcal{S}_3$ itself, we would have to form the 2-fold covering of $\widehat{\mathbb{C}}$, ramified at four of the six puncture points. In fact this ramified covering is a (punctured) elliptic curve which can be identified with the Riemann surface of the function

$$c \;\mapsto\; \sqrt{c(c^3+2c^2+c+1)} \;=\; c(c+1)\sqrt{\alpha}\;,$$

ramified at $c=0$ and at the three values of $c$ which represent period three centers in the Mandelbrot set.

**Remark 5.18.** This period three moduli space $\mathcal{S}_3/\mathcal{I}$ has six escape regions, corresponding to maps for which the orbit of the free critical point escapes to infinity. Each of these regions is canonically isomorphic to a punctured disk. The five finite puncture points can be characterized as the five values of $c$ for which the quadratic map $z\mapsto z^2+c$ has critical orbit of period one, two or three. In other words, they are the center points of the five hyperbolic components in the Mandelbrot set which have period $\leq 3$. For $F$ in three of these escape regions, corresponding to the period 3 centers in the Mandelbrot set, the Julia set $J(F)$ contains infinitely many copies of the associated quadratic Julia set. (This is similar to the situation in Figure 18.) For $F$ in the other three escape regions, the Julia set is made up out of points and circles, as in Figures 20 and 21. (Compare (Branner and Hubbard 92).)

This curve $\mathcal{S}_3/\mathcal{I}$ has four hyperbolic components of Type A. These are the images of the eight Type A centers in $\mathcal{S}_3$, representing maps of the form $F(z)=z^3+v$ which have critical orbits of period three. The corresponding shape parameters are given by $c=v^2\approx -1.598\pm .6666\,i$ or $.0189\pm .6026\,i$ (the four points where $\beta(c)=0$). It has eight hyperbolic components of Type B, that is four with $F(a)=-a$, and four with shape parameter $c'=-1-1/c$ satisfying $F(-a)=a$. There are infinitely many components of Types C and D.

**Period 4.** The curve $\mathcal{S}_4$ will be studied in (Bonifant and Milnor ) (the continuation of this paper). Let me simply mention that the situation is more complicated in period 4. In particular, four of the twenty ends of $\mathcal{S}_4$ have multiplicity two, or in other words are ramified over the $a$-plane.

**Outline Proof of Theorem 5.2.** To prove that the curve $\mathcal{S}_p$ is smooth, we proceed as follows. For any $F \in \hat{\mathcal{P}}(3)$ which is sufficiently close to $\mathcal{S}_p$, it follows from the implicit function theorem that there is a unique periodic point close to $a$. Evidently the multiplier $\lambda = \lambda(F)$ of this periodic point depends holomorphically on $F \in \hat{\mathcal{P}}(3)$. We must prove that the partial derivatives $\partial\lambda/\partial a$ and $\partial\lambda/\partial v$ are not simultaneously zero.

At hyperbolic points, the proof is relatively easy. For each hyperbolic component of $\mathcal{C}(3)$ is canonically biholomorphic to one of four standard models. (See (Milnor 92b).) Within each of these standard models, the locus of those maps for which a specified one of the critical points is precisely periodic is transparently a smooth complex submanifold.

In a neighborhood of a non-hyperbolic map, we make use of a surgery argument as follows. Evidently the critical point $-a$ cannot belong to the attractive basin of $+a$, hence the immediate basin of $a$ is isomorphic to the open unit disk, parametrized by its Böttcher coordinate. Using quasiconformal surgery, it is not difficult to replace this superattractive basin by a basin with multiplier $\lambda$.

This yields a new map $F_\lambda$, where $\lambda$ varies over the open unit disk, which depends smoothly on $\lambda$ and coincides with the original map when $\lambda = 0$. Since the composition $\lambda \mapsto F_\lambda \mapsto \lambda(F_\lambda)$ is the identity map, this proves Theorem 5.2. □

Some of the ends in the curve $\mathcal{S}_p$ can be described quite explicitly as follows.

**Lemma 5.19.** *Each end of the cubic superattracting locus $\mathcal{S}_p$ can be described, for large $|a|$, by a Laurent series having one of the following two forms*

$$\left.\begin{array}{c} v-a \\ v+2a \end{array}\right\} = k_0 + k_1/a^{1/\mu} + k_2/a^{2/\mu} + \cdots ,$$

*where $\mu$ is the multiplicity. Among these, there are $\nu_2(p)/2$ ends with trivial kneading sequence. These correspond to the $\nu_2(p)/2$ period $p$ centers $z \mapsto z^2 + c_0$ in the Mandelbrot set, and have Laurent series of the form*

$$v - a = c_0/3a + k_3/a^3 + k_5/a^5 + \cdots .$$

*For these special ends, the non-trivial components of the corresponding filled Julia sets $K(F)$ are homeomorphic to the filled Julia sets of the associated quadratic map $z \mapsto z^2 + c_0$. These ends have the property that, for large $|a|$, the orbit of the periodic critical point $a$ under the associated cubic map $F$ always stays within the $1/|a|$ neighborhood of $a$. On the other hand, if $F$ belongs to an end of $\mathcal{S}_p$ which is not of this form, with $|a|$ large, then the orbit of $a$ under $F$ must also pass close to the co-critical point $-2a$.*

The proof is not difficult, and will be omitted. □

It follows easily that each of these special ends is carried into itself by the involution $\mathcal{I}$. Using the identity $g(\mathcal{S}_p) = 2g(\mathcal{S}_p/\mathcal{I}) + r/2 - 1$, where $g$ is the

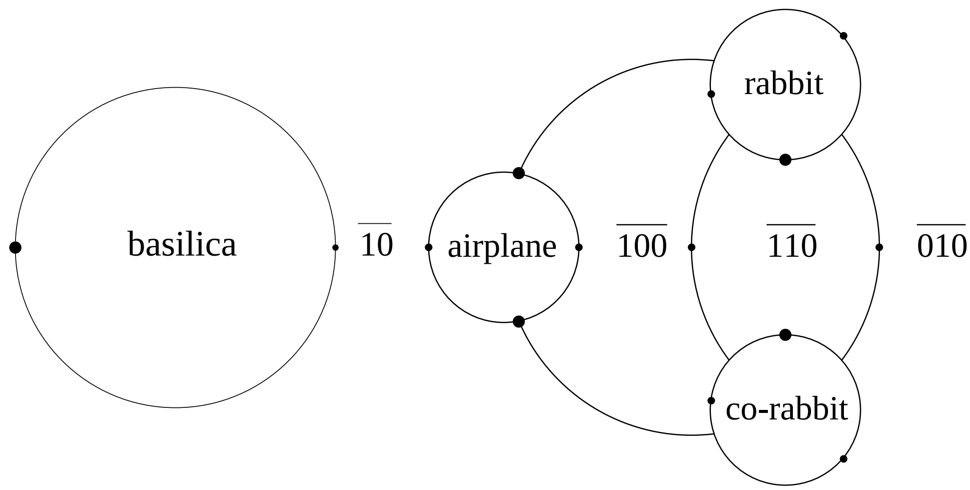


Figure 23: Sketch of the cell subdivision for $\mathcal{S}_2/\mathcal{I}$ and the conjectured cell subdivision for $\mathcal{S}_3/\mathcal{I}$. (Compare Figures 16 and 22.) Here the centers of components of Types A and B have been indicated by heavy and light dots respectively. Each of the complementary 2-cells in $\overline{\mathcal{S}}_p/\mathcal{I}$ is labeled, either with its kneading sequence, or with the nickname for its associated quadratic map if the kneading sequence is $\overline{0}$.

genus and $r$ the number of ramification points, this yields the crude inequality $g(\mathcal{S}_p) \ge r/2 - 1 \ge \nu_2(p)/4 - 1$, which implies the following: *The genus of $\mathcal{S}_p$ is non-zero for $p \ge 3$, and tends to infinity as $p \to \infty$.*

## 5D. A Conjectured Cell Subdivision of $\mathcal{S}_p$.

How can we understand the topology of the curve $\mathcal{S}_p$? Even if we could verify the conjecture that $\mathcal{S}_p$ is connected, this would leave open the problem of computing its genus. This is not a trivial question, since this curve in $\mathbb{C}^2$ has complicated singularities when extended to a variety in the complex projective plane. Here is one approach to understanding the topology of $\mathcal{S}_p$ and of its non-singular compactification $\overline{\mathcal{S}}_p$. We will usually assume that $p \ge 2$, since the structure of $\mathcal{S}_1$ is much simpler.

Since each bounded hyperbolic component in $\mathcal{S}_p$ is conformally isomorphic to the unit disk, with a preferred center point, we can define the concept of a ***regulated path*** in the connectedness locus $\mathcal{C}(\mathcal{S}_p)$. (Compare the Appendix. Of course, since we don't know whether $\mathcal{C}(\mathcal{S}_p)$ is locally connected, there may be real difficulties in proving the existence of such regulated paths.)

**Conjecture 5.20.** *For each escape region $\mathcal{E}_\iota \subset \mathcal{S}_p$ with $p \ge 2$, there is a unique simple closed regulated curve $\Gamma_\iota$ which separates $\mathcal{E}_\iota$ from the other escape regions. This curve $\Gamma_\iota$ bounds a topological cell $U_\iota$ within the compactified* *curve $\overline{\mathcal{S}}_p$, so that $U_\iota$ contains $\mathcal{E}_\iota$ but is disjoint from the other escape regions. Furthermore, there is a cell subdivision of $\overline{\mathcal{S}}_p$ with the union $\Gamma$ of the $\Gamma_\iota$ as 1-skeleton, and with the $U_\iota$ as 2-cells. In particular, the union of the closures $\overline{U}_\iota = U_\iota \cup \Gamma_\iota$ of these 2-cells is the entire curve $\overline{\mathcal{S}}_p$.*

We can describe this 1-skeleton $\Gamma$ as the "***core***" of $\mathcal{S}_p$, since all of the most interesting dynamics seems to be centered around it. In particular, it is conjectured that the center points of all hyperbolic components of Types A and B are contained in $\Gamma$.

For the special case $p = 1$, the situation is much simpler. Define the ***core*** of $\mathcal{S}_1$ to be the center point of its unique hyperbolic component of Type A, so that we obtain a cell subdivision with a single vertex (corresponding to the map $z \mapsto z^3$), with the rest of $\mathcal{S}_1$ as 2-cell.

If this conjecture is true, then it follows easily that the quotient $\overline{\mathcal{S}}_p/\mathcal{I}$ has a corresponding cell structure, with the quotient graph $\Gamma/\mathcal{I}$ as 1-skeleton. See Figure 23, which illustrates the period two and three cases.

For $p \geq 2$, we can divide the bounded hyperbolic components in $\mathcal{S}_p$ into two classes as follows. Call $V$ a ***core component*** if there are two or more escape regions $\mathcal{E}_\iota$ such that the intersection $\overline{V} \cap \overline{\mathcal{E}}_\iota$ contains more than one point. (In terms of this conjectured cell structure, this means that $V$ is cut into two or more pieces by $\Gamma$.) Call $V$ a ***peripheral component*** otherwise. We can define the ***thick core*** $\Gamma^+ \subset \mathcal{S}_p$ to be the closure of the union of all core components. Then the complement $\mathcal{S}_p \smallsetminus \Gamma^+$ is a disjoint union of open sets $\mathcal{E}_\iota^+$, one contained in each cell $U_\iota$. By a ***limb*** of the connectedness locus within $U_\iota$ we mean a connected component of $\mathcal{C}(\mathcal{S}_p) \cap \mathcal{E}_\iota^+$. Thus every peripheral hyperbolic component must be contained in some unique limb. *Conjecturally every limb $L$ is attached to $\Gamma^+$ at a unique parabolic point $F_0 \in \overline{L} \cap \Gamma^+$, and is separated from the rest of the connectedness locus by two external rays in $\mathcal{E}_\iota$ which land at $F_0$.*

Again the case $p = 1$ is simpler. The thick core $\Gamma^+ \subset \mathcal{S}_1$ is defined to be the closure of the principal hyperbolic component, and its complement is defined to be $\mathcal{E}^+$.

There are completely analogous descriptions within $\mathcal{S}_p/\mathcal{I}$. The reader should have no difficulty in distinguishing core components and limbs among the reasonably large components in Figures 6, 16, and 22.

# 6 Quadratic Julia Sets in Cubic Parameter Space.

Assuming that the cell subdivision of §5 exists, we can get a good idea of the structure of the connectedness locus $\mathcal{C}(\mathcal{S}_p)$ by studying its intersection with each of the conjectured 2-cells. This section will attempt to provide an explicit description for those complementary 2-cells which have trivial kneading sequence, and hence are associated with quadratic polynomials of critical period $p$.

Let $g$ be a quadratic polynomial with period $p$ critical point, and let $\mathcal{E}_g \subset \mathcal{S}_p/\mathcal{I}$ be the associated escape region. Thus, for every $F \in \mathcal{E}_g$, the filled Julia set $K(F)$ contains infinitely many copies of $K(g)$. Let $U_g \supset \mathcal{E}_g$ be the 2-cell which contains $\mathcal{E}_g$ in the conjectured cell subdivision of §5.

**Basic Construction.** Let $K^\sharp(g)$ be the compact set which is obtained by cutting open[4] the filled Julia set $K(g)$ along its minimal Hubbard tree $T_g$. Thus the preimage $T_g^\sharp = \eta^{-1}(T_g)$, under the natural projection $\eta : K^\sharp(g) \to K(g)$ is a topological circle, which can be described as the ***inner boundary*** of $K^\sharp(g)$. (Compare Figure 24.) Let $J^\sharp(g) = \eta^{-1}(J(g))$ be the preimage of the Julia set in $K^\sharp(g)$.

**Conjecture 6.1.** *There exists a dynamically defined canonical embedding $\phi$ from the cut-open filled Julia set $K^\sharp(g)$ into the parameter cell $\overline{U}_g$ which turns $K^\sharp(g)$ inside-out so that the inner boundary circle $T_g^\sharp$ of $K^\sharp(g)$ maps to the outer boundary circle $\Gamma_g = \partial U_g$.*

Alternatively, for periods $\leq 3$, since $\mathcal{S}_p/\mathcal{I}$ has genus zero, we can turn $\mathcal{S}_p/\mathcal{I}$ inside out by mapping it onto the Riemann sphere so that the puncture point in $\mathcal{E}_g$ goes to the point at infinity. The resulting picture can be compared directly with $K^\sharp(g)$. As an example, for the case $Q(z) = z^2 - 1$ we can compare Figure 24 with Figure 25. Evidently there is a strong resemblance between the region outside the white circle $T_g^\sharp$ in Figure 24 and the region outside the black circle $\Gamma_g$ in Figure 25. The most striking difference is the presence of many copies of the Mandelbrot set in Figure 25, and also in the right half of Figure 26. (Compare Conjecture 6.2 below.) Figures 27 and 28 provide a similar example for period three.

The embedding $\phi : K^\sharp(g) \to U_g$ can be described intuitively as follows. Each point $\widehat{z} \in K^\sharp(g) \smallsetminus J^\sharp(g)$ corresponds to a cubic map $\phi(\widehat{z}) \in \overline{U}_g$ which is constructed starting with the quadratic map $g$ by altering the dynamics so that $\widehat{z}$ will be an additional critical point (or a double critical point in the special case that $\widehat{z}$ is already critical). Thus:

**Case A.** If $\widehat{z}$ belongs to the Fatou component $V_0$ containing 0 then we will obtain a cubic map of Type A, with both critical points in the same Fatou component.

**Case B.** If $\widehat{z}$ belongs to some forward image $g^{\circ j}(V_0)$ with $0 < j < p$, then we will obtain a component of Type B, with both critical points in the same cycle of Fatou components.

**Case C.** For all other $\widehat{z}$ in $K^\sharp(g) \smallsetminus J^\sharp(g)$, we will obtain a component of Type C.

This provides a very rough description of the map $\phi$ within the Fatou region of $K^\sharp(g)$. It is conjectured that $\phi$ extends continuously over all of $K^\sharp(g)$.

To deal with components of Type D, the following supplementary statement is needed. A point in the cut-open Julia set $J^\sharp(g)$ will be called ***periodic*** if it is the image of a periodic point of $J_g$.

[4]In the special case $p = 1$, so that $Q(z) = z^2$, no cutting is necessary, and $K^\sharp(g)$ should be identified with the unit disk $K(g)$.

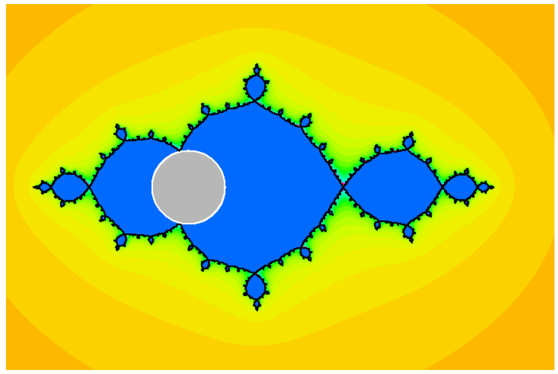

Figure 24: The cut-open filled Julia set $K^\sharp(g)$ for the "basilica" map $Q(z) = z^2 - 1$. Here the Julia set $J^\sharp(g)$ is colored black.

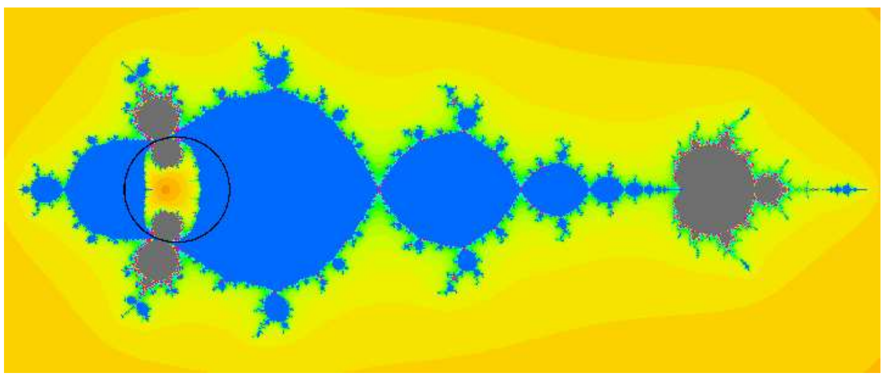

Figure 25: The curve $\mathcal{S}_2$ inverted so that the "basilica" escape region will be on the outside. The black circle approximates the core $\Gamma_g$ of $\mathcal{S}_2$.

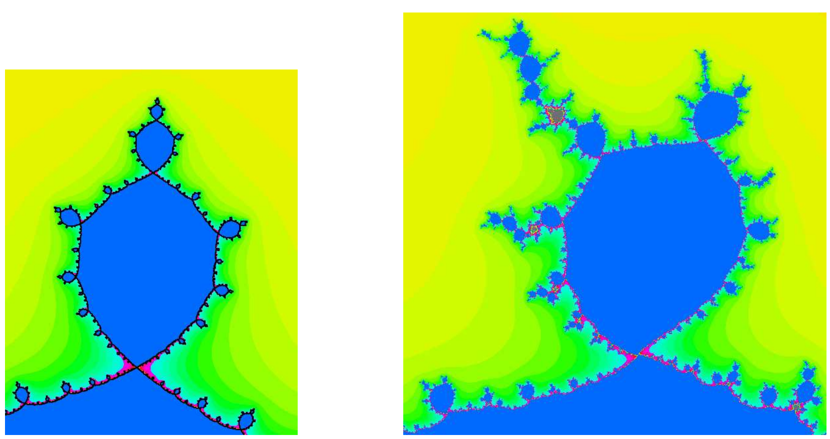

Figure 26: Details near the top of Figures 24 and 25 respectively.

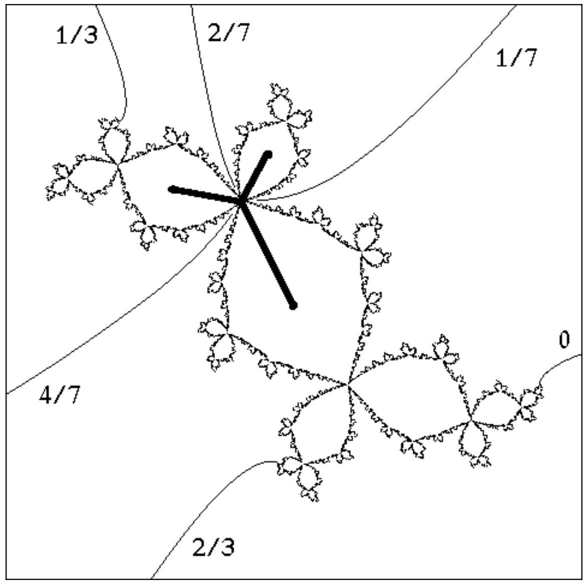


Figure 27: Julia set for the Douady rabbit, with minimal Hubbard tree emphasized.

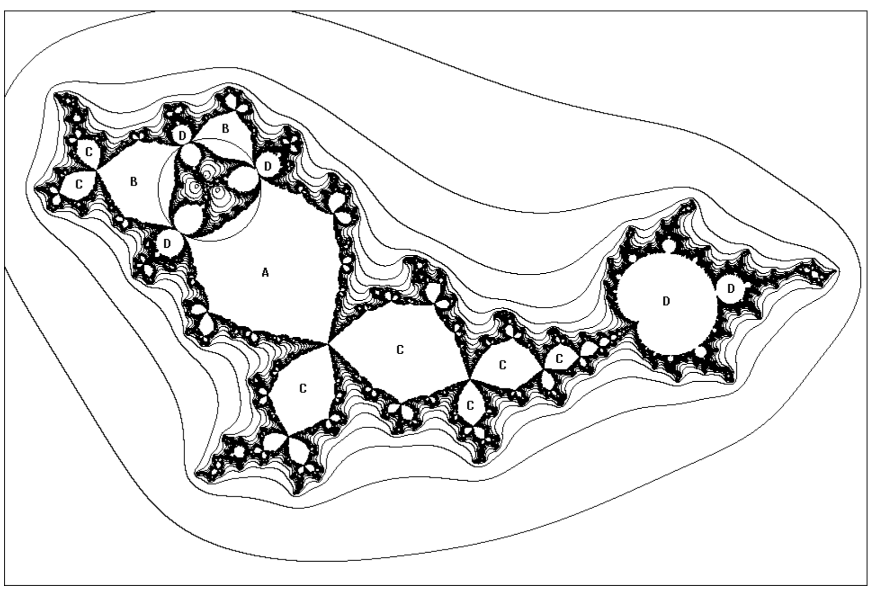


Figure 28: This is Figure 22, inverted in a small circle about the upper right puncture point and then rotated $90^\circ$. Our claim is that the region outside of the small circle is homeomorphic to the Figure 27, cut open along its minimal tree, and with further decorations, including Mandelbrot sets or portions of Mandelbrot sets.

**Conjecture 6.2.** *For every Julia periodic point $\widehat{z} \in J^\sharp(g)$, a copy of the Mandelbrot set is attached to $\phi(K^\sharp(g))$ at the point $\phi(\widehat{z})$ within the curve $\mathcal{S}_p/\mathcal{I}$. More precisely, if $\widehat{z}$ is a periodic point with combinatorial rotation number $m/n \neq 0$, then the $(m/n)$-limb of the Mandelbrot set is attached within $U_g$, with the rest of the Mandelbrot set attached in the complementary parameter region $\mathcal{S}_p/\mathcal{I} \smallsetminus U_g$. On the other hand, for periodic points of rotation number zero, the entire Mandelbrot set will be attached within $U_g$. In all cases, this attached Mandelbrot set intersects $\phi(K^\sharp(g))$ only at the point $\phi(\widehat{z})$ itself; and in all cases there are further decorations added to these Mandelbrot sets.*

There is a very close connection between periodic points in the Julia set $J_g$ and external rays which are periodic under angle doubling. The connection becomes even closer if we pass to the cut-open Julia set $J^\sharp(g)$. In fact:

**Lemma 6.3.** *Every periodic external ray lands on a periodic point in $J^\sharp(g)$, and every periodic point in $J^\sharp(g)$ is the landing point of exactly one external ray. Hence, if Conjecture 6.2 is correct, there is a one-to-one correspondence between periodic external rays for $K(g)$ and Mandelbrot copies attached to $\phi(K^\sharp(g))$.*

Evidently this provides a simple way of labeling those Mandelbrot copies which are attached in regions $U_g$.

**Outline of the Construction.** This conjectured embedding $\phi$ from $K^\sharp(g)$ into $U_g \subset \mathcal{S}_p$ will be described in the following four subsections. §6A will describe $\phi(\widehat{z})$ in the case where $\widehat{z}$ corresponds to the center of a Fatou component in $K(g)$. The image $\phi(\widehat{z})$ will then be the center of a hyperbolic component in $\mathcal{S}_p/\mathcal{I}$. As in §4, a representative cubic map is most easily described by means of its Hubbard tree. In §6, we extend to the case of an arbitrary $\widehat{z}$ in the Fatou subset $K^\sharp(g) \smallsetminus J^\sharp(g)$. §6 will study the case where $\widehat{z}$ belongs to the Julia set $J^\sharp(g)$ but is not periodic, and §6 will consider the case of a periodic point in the Julia set.

# 6A. Enramification: The Hubbard Tree.

The rather ungainly word "***enramification***" will be used for the operation of constructing a cubic polynomial map $F$ from some given quadratic polynomial map $g$ by artificially introducing a new critical point (or by replacing the simple critical point by a double critical point). Here three cautionary points should be emphasized:

- Although the construction is known to make sense in many cases, its existence in general is conjectural.
- The construction is not always uniquely defined. More precisely if $\widehat{z}$ belongs to the minimal tree $T_g$, and is not an endpoint of this tree, then multiple choices are possible; hence the necessity of cutting-open along $T_g$ in the discussion above.

- This new map $F$ is well defined only up to affine conjugation, so that we cannot distinguish between $F$ and its image $\mathcal{I}(F) : z \mapsto -F(-z)$. For this reason, we will work with $\mathcal{S}_p/\mathcal{I}$ rather than $\mathcal{S}_p$.

We first discuss enramification as an operation on abstract Hubbard trees. Here is a brief outline to fix notations. (See the Appendix for a more detailed presentation.) Let $F$ be a post-critically finite polynomial of degree $d \geq 2$, and let $S \supset F(S)$ be a forward invariant set containing the critical points. The associated ***Hubbard tree*** $T = T(S)$ is a finite acyclic simplicial complex which has dimensional one, except in the special case where $S = T(S)$ consist of a single point. Its underlying topological space $|T| \subset K(F)$ is the smallest subset of $K(F)$ which contains $S$ and is connected by regulated paths. By the ***valence*** $n(z)$ of a point $z \in |T|$ I will mean the number of connected components of $|T| \setminus \{z\}$. The set $V$ of vertices of $T$ consists of $S$ together with the finitely many points $\mathbf{v}$ of valence $n(\mathbf{v}) \geq 3$. Note that $F$ maps vertices into vertices. Furthermore, if $\mathbf{e}$ is an edge with $\mathbf{v}$ as one of its two boundary points and if $U$ is a small neighborhood of $\mathbf{v}$, then $F$ maps $U \cap \mathbf{e}$ into a unique edge which will be denoted by $F_{\mathbf{v}}(\mathbf{e})$. Similarly, any iterate $F^{\circ k}$ induces a map $F^{\circ k}_{\mathbf{v}}$ from edges at $\mathbf{v}$ to edges at $F^{\circ k}(\mathbf{v})$. As part of the structure of $T$ we include the following:

**(1)** The map $F$ restricted to the set $V$ of vertices.

**(2)** The ***local degree*** function which assigns an integer $d(\mathbf{v}) \geq 1$ to each vertex, with

$$\sum_{\mathbf{v}} (d(\mathbf{v}) - 1) = d - 1\,.$$

Here $d(\mathbf{v}) > 1$ if and only if $\mathbf{v}$ is a critical point.

**(3)** The ***angle function*** $\angle(\mathbf{e}_1,\, \mathbf{e}_2) \in \mathbb{Q}/\mathbb{Z}$, where $\mathbf{e}_1$ and $\mathbf{e}_2$ are any two edges meeting at a common vertex $\mathbf{v}$. This vanishes if and only if $\mathbf{e}_1 = \mathbf{e}_2$. The map $F$ multiplies all angles at $\mathbf{v}$ by $d(\mathbf{v})$, in the sense that

$$\angle\big(F_{\mathbf{v}}(\mathbf{e}_1),\, F_{\mathbf{v}}(\mathbf{e}_2)\big) \;=\; d(\mathbf{v})\, \angle(\mathbf{e}_1,\, \mathbf{e}_2)\,.$$

Recall that any periodic point $z$ of period $p \geq 1$ in the Julia set has a well defined ***rotation number*** in $\mathbb{Q}/\mathbb{Z}$ which describes the way that the external rays landing at $z$ are rotated by $F^{\circ p}$. (See for example (Milnor 00).) If we choose a Hubbard tree having $z$ as a vertex, then this rotation number also describes the way in which the edges incident to $z$ are rotated by the correspondence $F^{\circ p}_z$.

For any critically finite polynomial $F$, there is a unique ***minimal tree*** $T_{\min}(F)$ which is obtained by taking the union of critical orbits as the generating set $S$. Our preliminary goal can be described roughly as follows:

> ***Given a post-critically finite quadratic polynomial*** $Q(z) = z^2 + c$***, to study cubic polynomials*** $F$ ***such that the minimal Hubbard tree for*** $F$ ***can be constructed by minor modifications of some Hubbard tree for*** $g$***.***

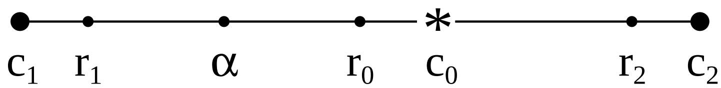


Figure 29: A Hubbard tree for the "airplane" map $Q(z) = z^2 - 1.754866\cdots$, with critical orbit $\{\mathbf{c}_j\}$ of period three. The associated root points $\{\mathbf{r}_j\}$ form a period three orbit in the Julia set with rotation number zero, while the fixed point $\alpha$ has rotation number $1/2$.

To this end, we start with the minimal Hubbard tree $T_{\min} = T_{\min}(g)$ for the quadratic map. Given any periodic or pre-periodic point $\mathbf{w}_0 \in K(F)$, let $T(\mathbf{w}_0)$ be the Hubbard tree for $g$ which has as its generating set $S$ the union of the critical orbit and the orbit of $\mathbf{w}_0$.

**Theorem 6.4.** *In most cases the extended tree $T = T(\mathbf{w}_0)$, as described above, can be made into the Hubbard tree $\widehat{T}$ of a cubic polynomial simply by replacing the local degree function $d(\mathbf{v})$ by*

$$\widehat{d}(\mathbf{v}) \;=\; \begin{cases} d(\mathbf{v}) & \text{if} \quad \mathbf{v} \neq \mathbf{w}_0 \\ d(\mathbf{v}) + 1 & \text{if} \quad \mathbf{v} = \mathbf{w}_0\,, \end{cases}$$

*and by carefully modifying the angle function at $\mathbf{w}_0$ and at all vertices which are iterated pre-images of $\mathbf{w}_0$. In fact, if $\mathbf{w}_0$ has valence $n(\mathbf{w}_0) \geq 1$, then there are precisely $n(\mathbf{w}_0)$ distinct ways of carrying out this angle modification. However, there is one special case where a different construction is necessary, namely the case when $\mathbf{w}_0$ is a periodic point in the Julia set with rotation number zero but with valence $n(\mathbf{w}_0) = 2$.*

For an example of this special case, see Figure 29, and for its resolution see Remark 6.7 and Figure 31.

**Note.** If $n(\mathbf{w}_0) \leq 1$, then the construction is uniquely defined and no angle modification is necessary. In particular, this will be the case whenever $\mathbf{w}_0$ lies strictly outside of the minimal tree. (Compare Figure 30.)

The proof of Theorem 6.4 will be based on two lemmas. Let $Q(z) = z^2 + c$ be a critically finite quadratic polynomial, and let

$$0 = \mathbf{c}_0 \mapsto \mathbf{c}_1 \mapsto \cdots \mapsto \mathbf{c}_k$$

be the distinct points in the critical orbit, with $\mathbf{c}_1 = c$. (We are mainly interested in the critically periodic case where $k = p - 1$ and $Q(\mathbf{c}_{p-1}) = \mathbf{c}_0$; but it is no more difficult to consider the preperiodic case at the same time.)

**Lemma 6.5.** *Let $Q(z) = z^2 + c$ be a critically finite quadratic polynomial, as above. If $k > 0$ then, in the minimal tree $T_{\min}$, we have $n(\mathbf{c}_1) = 1$ and $n(\mathbf{c}_0) \leq 2$. In fact, in the critically periodic case of period $p$ we have*

$$1 = n(\mathbf{c}_1) \leq n(\mathbf{c}_2) \leq \cdots \leq n(\mathbf{c}_{p-1}) \leq n(\mathbf{c}_0) \leq 2\,.$$

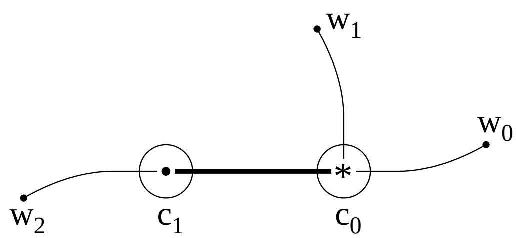


Figure 30: The extended tree $T(\mathbf{w}_0)$ for the "basilica" map $Q(z) = z^2 - 1$, together with the period three orbit $\{\mathbf{w}_0, \mathbf{w}_1, \mathbf{w}_2\}$. The minimal tree $T_{\min} \subset T(\mathbf{w}_0)$ has been emphasized. Note that the edge from $\mathbf{c}_0$ to $\mathbf{w}_0$ maps to the path from $\mathbf{c}_1$ through $\mathbf{c}_0$ to $\mathbf{w}_1$.

*If $\mathbf{w}_0$ is a periodic or preperiodic point which lies strictly outside of $T_{\min}$, then a similar argument applied to the extended tree $T(\mathbf{w}_0)$ shows that $n(\mathbf{w}_0) = 1$.*

**Proof.** Every non-degenerate tree must have at least two vertices $\mathbf{v}$ with $n(\mathbf{v}) = 1$. For otherwise, starting with any edge we could keep finding successive edges on one end or the other until we generate a closed loop, which is impossible. Since every vertex outside the critical orbit has valence $n(\mathbf{v}) \geq 3$ by the definition of the minimal tree, it follows that there are at least two of the $\mathbf{c}_j$ with $n(\mathbf{c}_j) = 1$.

Therefore, since $F$ is injective in the neighborhood of any non-critical point, we have

$$1 = n(\mathbf{c}_1) = n(\mathbf{c}_2) \leq \cdots \leq n(\mathbf{c}_k) \leq n(Q(\mathbf{c}_k)).$$

Furthermore, since $F$ is at most 2-to-1 in a neighborhood of the critical point $\mathbf{c}_0$, it follows that $n(\mathbf{c}_0) \leq 2$. In the critically periodic case, since $Q(\mathbf{c}_{p-1}) = \mathbf{c}_0$, it follows that $n(\mathbf{c}_i) \leq 2$ for all points of the critical orbit.

Now consider the extended tree $T(\mathbf{w}_0)$ in the case that $\mathbf{w}_0 \notin |T_{\min}|$. If $\mathbf{w}_0 \mapsto \mathbf{w}_1 \mapsto \cdots$, then a similar argument shows that $n(\mathbf{w}_h) \leq n(\mathbf{w}_{h+1})$ provided that $\mathbf{w}_h \neq 0$. On the other hand, this extended tree must have at least one endpoint outside of $|T_{\min}|$. For otherwise, starting with any edge $\mathbf{e}$ outside of $|T_{\min}|$ and extending in both directions, we could either construct a closed loop outside of $T_{\min}$, or else construct a path from $|T_{\min}|$ to itself which passes through $\mathbf{e}$. Since both cases are impossible, it follows easily that $\mathbf{w}_0$ is an endpoint of $T(\mathbf{w}_0)$, as asserted. (Note that this last argument works even in the degenerate case $Q(z) = z^2$.) $\square$

**Lemma 6.6.** *Let $\mathbf{w}_0$ be periodic of period $p \geq 1$ in the quadratic Julia set $J(g)$. If $n(\mathbf{w}_0) \geq 3$, then the map $g^{\circ p}_{\mathbf{w}_0}$ permutes the $n(\mathbf{w}_0)$ incident edges cyclically.*

**Proof.** An analogous statement for external rays landing at $\mathbf{w}_0$ is proved in (Milnor 00, Lemma 2.7); and the corresponding statement for the tree $T(\mathbf{w}_0)$ follows easily. $\square$

**Proof of Theorem 6.4.** We distinguish six cases.

**Case 1.** Suppose that $\mathbf{w}_0$ is an ***endpoint*** of the tree $T(\mathbf{w}_0)$, in the sense that $n(\mathbf{w}_0) \le 1$. Then we need only replace the local degree $d(\mathbf{w}_0)$ by

$$\widehat{d}(\mathbf{w}_0) = d(\mathbf{w}_0) + 1.$$

The given angle function is consistent without any change. Evidently this construction is uniquely defined. Using Poirier's Theorem (stated as Theorem A.3 in the Appendix), it yields a cubic map which is uniquely defined up to affine conjugation.

By Lemma 6.5 this includes all cases where the point $\mathbf{w}_0$ does not belong to $|T_{\min}|$. *For the rest of the proof, it will be tacitly understood that* $\mathbf{w}_0 \in |T_{\min}|$, *and that* $n(\mathbf{w}_0) \ge 2$.

**Case 2.** Suppose $g$ is critically periodic, and that $\mathbf{w}_0$ is one of the points $\mathbf{c}_h$ in the critical orbit, but is not the critical point $\mathbf{c}_0 = 0$. Since we have assumed that $n(\mathbf{w}_0) \ge 2$, it follows by Lemma 6.5 that $n(\mathbf{w}_0) = 2$, and it is not hard to check that the angle $\angle(\mathbf{e}_1, \mathbf{e}_2)$ between the two edges which meet at $\mathbf{w}_0$ must be equal to $1/2$. To make a cubic tree, we must first redefine the local degree at $\mathbf{w}_0$ to be $\widehat{d}(\mathbf{w}_0) = 2$. Let $\mathbf{e}'_1$ and $\mathbf{e}'_2$ be the two edges which meet at $Q(\mathbf{w}_0)$. Since the cubic map $\widehat{F}_{\mathbf{w}_0}$ must double angles, the angles for the cubic map must satisfy

$$2\angle(\mathbf{e}_1, \mathbf{e}_2) \;=\; \angle(\mathbf{e}'_1, \mathbf{e}'_2) \;=\; 1/2\,.$$

In other words, we must change the angle at $\mathbf{w}_0$ to either $\angle(\mathbf{e}_1, \mathbf{e}_2) = \frac{1}{4}$ or $\angle(\mathbf{e}_1, \mathbf{e}_2) = \frac{3}{4}$. Furthermore, we must make exactly the same change at every iterated pre-image $\mathbf{c}_j$, $0 < j \le h$, for which $n(\mathbf{c}_j) = 2$. Thus, in this case there are just two essentially distinct ways of carrying out the construction.

As an example, if we start with a *real* quadratic map in Case 2, then the construction will yield two different cubic maps which are complex conjugate to each other, but are not affinely conjugate to any real map.

**Case 3.** Now suppose that $\mathbf{w}_0$ the critical point 0. Then we must replace $d(\mathbf{w}_0) = 2$ by $\widehat{d}(\mathbf{w}_0) = 3$. Whether $\mathbf{w}_0$ is periodic or pre-periodic, there are just two incident edges. Again there are two possible choices for the modified angles, but in this case the possible choices are $\frac{1}{3}$ and $\frac{2}{3}$.

**Case 4.** Next suppose that $\mathbf{w}_0$ is strictly preperiodic. (Compare (Bielefeld 89).) Then the local map from a neighborhood of $\mathbf{w}_0$ to a neighborhood of $Q(\mathbf{w}_0)$ preserves the angles between neighboring edges, say $\theta_1, \ldots, \theta_n$. The angles at $Q(\mathbf{w}_0)$ will not change; but we must choose new angles $\widehat{\theta}_j$ at $\mathbf{w}_0$ satisfying $2\widehat{\theta}_j \equiv \theta_j \pmod{\mathbb{Z}}$. In order to satisfy the condition that $\sum \widehat{\theta}_j = \sum \theta_j = 1$, we must choose $\widehat{\theta}_j = (\theta_j + 1)/2$ for one of the $n$ angles, and $\widehat{\theta}_j = \theta_j/2$ for the $n - 1$ remaining angles. Again, any choice of angles at $\mathbf{w}_0$ must be propagated backwards to any vertices which eventually map to $\mathbf{w}_0$; and hence again there are exactly $n$ allowable choices. If $\mathbf{w}_0 = 0$ hence $n(\mathbf{w}_0) = 2$, the argument is similar, but now the allowable angles are $\frac{1}{3}$ and $\frac{2}{3}$.

**Case 5.** Finally, suppose that $\mathbf{w}_0 \in |T_{\min}|$ is periodic of period $q \ge 1$ and belongs to the Julia set. If $n(\mathbf{w}_0) \ge 3$, then by Lemma 6.6 the first return map $g^{\circ q}$ permutes the $n = n(\mathbf{w}_0)$ edges which meet at $\mathbf{w}_0$ cyclically. The same will be true for $n(\mathbf{w}_0) = 2$, proved that the rotation number at $\mathbf{w}_0$ is equal to $1/2$. Number these edges as $\{\mathbf{e}_j\}$ with $j \in \mathbb{Z}/q$ so that $g^{\circ q_{\mathbf{w}_0}}(\mathbf{e}_j) = \mathbf{e}_{j+1}$. Since $\mathbf{w}_0$ is in the Julia set, the angle $\theta_j$ between $\mathbf{e}_j$ and the next edge in positive cyclic order is equal to $1/n$ by definition. However, in order to make $T(\mathbf{w}_0)$ into a cubic tree, we must choose new angles $\widehat{\theta}_j$. Since $g^{\circ n}$ has degree two at $\mathbf{w}_0$, the required condition on these new angles is that

$$\widehat{\theta}_{j+1} \equiv 2\widehat{\theta}_j \qquad (\mathrm{mod}\ \mathbb{Z})\,.$$

Iterating $q$ times, this yields $\widehat{\theta}_j \equiv 2^q\widehat{\theta}_j$ (mod $\mathbb{Z}$), so that each $\widehat{\theta}_j$ must have the form $k/(2^q - 1)$. The only possible solution is that these angles form some cyclic permutation of the sequence

$$1/(2^q-1)\,,\quad 2/(2^q-1)\,,\quad 2^2/(2^q-1)\,,\quad \ldots\,,\quad 2^{q-1}/(2^q-1)\,.$$

In fact, using the requirement that $0 < \widehat{\theta}_j < 1$ with $\sum \widehat{\theta}_j = 1$, we can write $2\widehat{\theta}_j = \widehat{\theta}_{j+1} + \epsilon_j$ with $\epsilon_j \in \{0,\, 1\}$. Summing over $j$, it follows that $\sum \epsilon_j = 1$; and the conclusion follows easily. Thus there are exactly $n$ distinct solutions. Evidently, any choice of angles for $\mathbf{w}_0$ can easily be propagated backward to any vertices of $T(\mathbf{w}_0)$ which eventually map to $\mathbf{w}_0$ (including all vertices on its periodic orbit).

Since this covers all possibilities (except the case of rotation number zero and valence two, which has been excluded), it completes the proof of Theorem 6.4. $\square$

**Remark 6.7.** In the exceptional case of rotation number zero and valence two, this construction cannot work, since we would have to find a non-zero solution to the equation $\theta \equiv 2\theta$ (mod $\mathbb{Z}$), which is impossible. However this does not cause any real difficulty. It merely requires a somewhat different modification in which extra branches are added to the tree. As a typical example, if we start with the airplane tree of Figure 29 and want to enramify the point $\mathbf{r}_1$ of period three, then we must add three short branches to the tree, as shown in Figure 31. (Here, to follow the conventions of the Appendix, the angles between consecutive edges at the periodic Julia vertices of valence three should all be 120°.) In such examples, there are always two possible choices since we can put new critical point to either side of the original tree.

It is interesting to ask which trees contain such a vertex of valence two and rotation number zero. Conjecturally, the Hubbard tree for $Q(z) = z^2 + c$ contains such an exceptional periodic orbit if and only if the induced mapping from $T$ to itself has positive topological entropy, or if and only if $c$ belongs to the central "cactus" in the Mandelbrot set. (For a study of Hubbard tree entropy, see (LiTao 07). Following (Cvitanović and Myrheim 89), the central ***cactus*** is the smallest compact subset of the Mandelbrot set which contains the central cardioid component and all of its iterated satellites. )

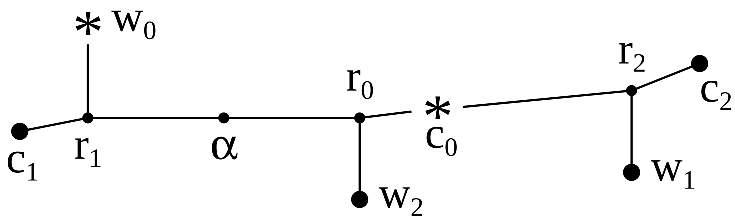


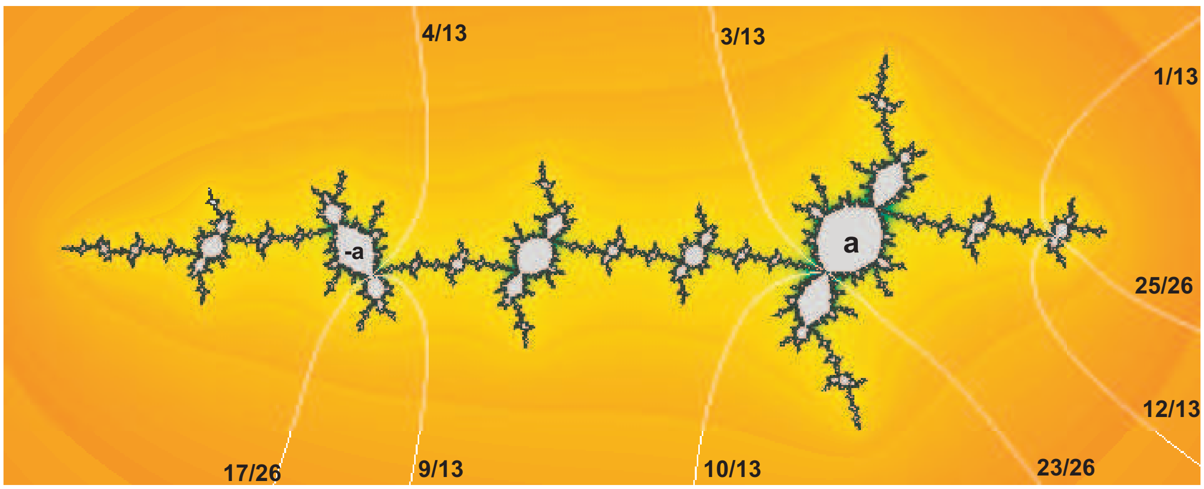


Figure 31: Above: the airplane tree of Figure 29, with a new period 3 critical orbit added. Below: the corresponding Julia set. (Here $a = \mathbf{c}_0 \cong .828 + .019\,i$ and $v = \mathbf{c}_1 \cong -.758 - .152\,i$, with $\mathbf{w}_0 = -a$.) Note that the Fatou components containing $\mathbf{c}_j$ and $\mathbf{w}_{j-1}$ have the repelling point $\mathbf{r}_j$ as a common boundary point.

## 6B. Components of Type A, B, C.

Now consider an arbitrary point $\widehat{z} \in K^\sharp(g) \smallsetminus J^\sharp(g)$. The corresponding Fatou component in $K(g)$ contains a unique precritical point. According to Theorem 6.4 we can construct an associated cubic Hubbard tree, and hence an associated cubic map which is postcritically finite and hyperbolic. We want to find a map in the same hyperbolic component $W$ which corresponds to $\widehat{z}$.

Now consider the case of an interior point $w \in K(q)$. Within the component $U$ of $w$, there will always be one and only one pre-critical point $\mathbf{w}_0$. As in §4, we can make the extended Hubbard tree $T'(\mathbf{w}_0)$ into a cubic Hubbard tree. (In the special case where $\mathbf{w}_0 \in T$, there are $n(\mathbf{w}_0)$ different ways of carrying out this construction.) Each such cubic Hubbard tree determines a post-critically finite hyperbolic cubic polynomial $F_0$, and we can now obtain the required polynomial $F$ by "tuning" $F_0$.

To understand this tuning construction, first look at an arbitrary component $U$ of the interior of $K(q)$. Then some iterate $q^{\circ m}$ maps $U$ diffeomorphically onto the component $U_0$ which contains the critical point. Since the first return map from $U_0$ to itself has degree two, there is a canonical Böttcher diffeomorphism $\beta$ from $U_0$ onto the open unit disk. Hence $U$ itself is canonically diffeomorphic to the open unit disk under $\beta \circ q^{\circ m}$.

To study the corresponding open set in cubic parameter space, let $W$ be the component of the polynomial $F_0$ within the open set of hyperbolic polynomials within $\mathcal{S}_p$. We will prove the following.

**Lemma 6.8.** *This open set $W$ in the parameter curve $\mathcal{S}_p$ is either a one-, two- or three-fold branched cover of the corresponding open set $U$ in $K(q)$, branched at the central point $F_0 \mapsto \mathbf{w}_0$. More explicitly, the degree of this covering is two if $\mathbf{w}_0$ coincides with the quadratic critical point, three if $\mathbf{w}_0$ is one of the $p-1$ post-critical points, and $W \xrightarrow{\approx} U$ in all other cases.*

Note that we have avoided this branching, in the formulation of the Period $p$ Conjecture, by cutting $K(F)$ open along its Hubbard tree.

**Outline Proof.** First note that each bounded Fatou component $U \subset K(g)$ of the quadratic filled Julia set is canonically biholomorphic to the open unit disk $\mathbb{D}$. To see this, let $U_0 = g^{\circ n}(U)$, $n \geq 0$, be the first forward image of $U$ which contains the critical point. Then we can first map $U$ biholomorphically onto $U_0$ by $g^{\circ n}$, and then map $U_0$ biholomorphically onto $\mathbb{D}$, using the Böttcher coordinate associated with the degree two self-map $g^{\circ p} : U_0 \to U_0$.

Similarly, for any bounded hyperbolic component $W \subset \mathcal{S}_p$, there is a canonical holomorphic map from $W$ to $\mathbb{D}$. The composition $W \to \mathbb{D} \leftrightarrow U$ then yield the required holomorphic covering map from $W$ onto $U \subset K(g)$.

For components of Type $A$, $B$ or $C$ one proceeds as follows.[5]

For $F \in W$, let $n \geq 0$ be the smallest integer such that $F^{\circ n}(-a)$ belongs to the Fatou component $U_a$ of the periodic point $+a$. If $W$ is of Type C, then the Böttcher coordinate for the degree two map $F^{\circ p} : U_a \to U_a$ is well defined, and we can simply define $\beta(F)$ to be the Böttcher coordinate of $F^{\circ n}(-a)$. Evidently $\beta$ maps $W$ biholomorphically onto $\mathbb{D}$.

For Type A (with $n = 0$) or Type B (with $0 < n < p$), we have to work a little harder. For the central point $F_0 \in W$, the image $F_0^{\circ n}(-a)$ is precisely equal to $+a$, and we set $\beta(F_0) = 0$. For $F \neq F_0$, we will see that the Böttcher coordinate for the map $F^{\circ p} : U_a \to U_a$ can be defined in a neighborhood of $+a$ which is large enough to contain $F^{\circ n}(-a)$. The Böttcher coordinate of $F^{\circ n}(-a)$ will then be the required invariant $\beta(F)$; and it is not hard to check that the correspondence $F \mapsto \beta(F)$ from the open set $W \subset \mathcal{S}_p$ to $\mathbb{D}$ is proper and holomorphic, and is locally bijective except at $F_0$. We will prove that it has degree two (for Type A) or degree three (for Type B) by studying local behavior near the central point $F_0$. (Compare the proof of Lemma 3.6.)

First consider a component $W \subset \mathcal{S}_p$ of Type A. It will be convenient to set $z = a + w$, and $v = F(a) = a + \delta$. Using $w$ as independent variable, we obtain a polynomial map

$$\Psi(w) \ = \ \delta + 3aw^2 + w^3$$

[5] For Type D one would use a quite different construction, mapping $F \in W$ to the multiplier of the periodic orbit associated with $-a$; but that will not concern us here.

which is affinely conjugate to $F$, with critical points $w = 0$ and $-2a$. A brief computation shows that the $n$-th iterate of $\Psi$ has the form

$$\Psi^{\circ n}(w) \;=\; \delta_n \,+\, 3ac_n w^2 \,+\, c_n w^3 \,+\, O(w^4)\,.$$

where $\delta_n$ and $c_n$ are polynomial functions of $\delta$ and $a$, with $\delta_n = \Psi^{\circ n}(0)$. In particular, if the critical point 0 has period $p$, then $\delta_p = 0$ so that

$$\Psi^{\circ p}(w) \;=\; 3ac_p w^2 \,+\, c_p w^3 \,+\, O(w^4)\,.$$

Here the coefficient $c_p$ must be non-zero, since the orbit of zero has period exactly $p$.

The Böttcher coordinate associated with $\Psi^{\circ p}$ has a power series expansion of the form

$$\beta(w) \;=\; 3ac_p w \,+\, (\text{higher order terms})\,,$$

and converges for $|w| < |2a|$. Hence we have the asymptotic estimate

$$\beta(w) \;\sim\; 3ac_p w \qquad \text{as} \quad w/a \;\to\; 0\,.$$

We can apply this estimate to the critical value

$$\Psi^{\circ p}(-2a) \;=\; 3ac_p(-2a)^2 \,+\, c_p(-2a)^3 \,+\, O(a^4) \;=\; 4c_p a^3 \,+\, O(a^4)\,.$$

Using the identity $\beta(\Psi^{\circ p}(w)) = \beta(w)^2$, since

$$\beta(\Psi^{\circ p}(-2a)) \;\sim\; 3ac_p(4c_p a^3) \quad \text{we obtain} \quad \beta(-2a) \;\sim\; \sqrt{12c_p^2 a^4} \;=\; \pm 2\sqrt{3}\, c_p\, a^2$$

as $a \to 0$. This is the required asymptotic estimate, proving that $\beta : W \to \mathbb{D}$ has degree two.

For Type B components, the construction is as follows. Suppose that

$$F^{\circ m}(U_a) = U_{-a} \;\text{ and }\; F^{\circ n}(U_{-a}) = U_a\,, \;\text{ where }\; m + n = p.$$

Let $F^{\circ m}(a) = -a + \epsilon$, where $|\epsilon|$ is small. It will be convenient to say that two variables have the same ***order*** as $\epsilon \to 0$ if each one is asymptotic to a constant multiple of the other.

Since $-a$ is a simple critical point, it follows that $F(-a + \epsilon) - F(-a)$ has the order of $\epsilon^2$ as $\epsilon \to 0$, and that the first derivative $F'(-a + \epsilon)$ has the order of $\epsilon$. It follows easily that $a - F^{\circ n}(-a)$ also has the order of $\epsilon^2$ as $\epsilon \to 0$. Furthermore, the second derivative of $F^{\circ p}$ at $a$ has the order of $\epsilon$. Hence the Böttcher coordinate of $a + w$ has the order of $\epsilon w$ as both $\epsilon$ and $w/\epsilon$ tend to zero. Taking $a + w$ equal to $F^{\circ n}(-a)$, so that $w$ has the order of $\epsilon^2$, it follows that the corresponding Böttcher coordinate has the order of $\epsilon^3$, as required. □

As an immediate consequence of Lemma 6.8, it follows that the Poincaré geodesic joining the critical point of $g$ to its root point, lifts to a pairs of curves in a component of type A, or a tripod of components in a component of Type B. One of the sectors which is cut by these Poincaré geodesics will correspond to the intersection of this component with the conjectured cell $U_g$.

## 6C. The Non-Periodic Julia Case.

This is perhaps the easiest case to understand. (Compare Figure 2.) If $\widehat{z} \in J^\sharp(g)$ is not periodic, then there is a canonical embedding $\iota : K(g) \hookrightarrow K(F)$ which satisfies $\iota \circ g = f \circ \iota$. The set $K(F)$ can be obtained from the embedded image $\iota(K(g))$ by adjoining a limb $L_z$ homeomorphic to $K(F)$ at $\iota(z)$ for every $z \in K(g)$ which is either equal to $\widehat{z}$ or to some iterated preimage of $\widehat{z}$. This limb $L_z$ maps homeomorphically onto $L(Q(z))$ for $z \neq \widehat{z}$, while $L_{\widehat{z}}$ maps homeomorphically onto all of $K(F)$. There is a canonical retraction $K(F) \to \iota(K(g))$ which maps each $L_z$ to its attaching point $\iota(z)$. In fact we can construct a simple topological model for $K(F)$ as follows: An orbit $z_0 \mapsto z_1 \mapsto \cdots$ in $K(F)$ is uniquely determined by its image

$$(r(z_0),\ r(z_1),\ \ldots) \quad \in \quad \iota(K(g))^{\mathbb{N}} .$$

Furthermore, a given sequence can occur if and only if $r(z_j) \mapsto r(z_{j+1})$ for all $j$ such that $r(z_j) \neq \iota(\widehat{z})$.

Thus $K(F)$ can be uniquely described as a topological dynamical system. However, this analysis does not specify just how $K(F)$ is embedded in $\mathbb{C}$. In fact, if the image of the point $\widehat{z}$ under the projection $K^\sharp(g) \to K(g)$ cuts $K(g)$ into $n$ distinct components, or equivalently if there are $n$ distinct external rays landing at this image point in $K(g)$, then there are $n$ essentially distinct ways of embedding the dynamical system $K(F)$ into $\mathbb{C}$. In fact if we cut $\mathbb{C}$ open along any one of these $n$ rays which land on $K(g)$, then we can paste the entire limb $L_{\widehat{z}}$ into the resulting gap. These $n$ choices correspond precisely to the $n$ ways of lifting the image in $K(g)$ up to the cut-open set $K^\sharp(g)$.

## 6D. The Periodic Julia Case.

If $\widehat{z} \in J^\sharp(g)$ corresponds to a periodic point in $J(g)$, then the situation is similar but more complicated, as illustrated in Figure 3. The repelling periodic point $\widehat{z}$ will be replaced by a parabolic periodic point in $K(F)$, on the boundary of a new parabolic Fatou component. Perhaps the easiest construction is to use the Hubbard tree argument of Theorem 6.4 or Remark 6.7 to construct an associated hyperbolic map. The required $\phi(\widehat{z})$ will then be the root point of the corresponding hyperbolic component.

## Appendix. Hubbard Trees.

This will be an exposition of Hubbard trees, as originally described in (Douady and Hubbard 84/85, §IV), with more precise statements due to Alfredo Poirier. It also describes slightly modified "puffed-out" Hubbard trees.

The ***Hubbard tree*** $T$ associated with a post-critically finite polynomial $F$ can be defined as follows. Each component of the Fatou set $\widehat{\mathbb{C}} \smallsetminus J(F)$ contains a unique periodic or pre-periodic point which will be called its ***center***. A path in the filled Julia set $K(F)$ is ***regulated*** if its intersection with each Fatou component consists of at most two Poincaré geodesics, each joining the center to a boundary point. Now let $S \subset K(F)$ be a finite set which contains all critical points and satisfies $F(S) \subset S$. The ***associated tree*** $T = T_S$ is the regulated convex closure: that is the smallest set containing a regulated path between any two points of $S$. This is a topological tree, and can be triangulated so that the set of vertices consists of the given set $S$, together with a finite number of points where three or more edges come together. The given mapping $F$ carries each edge of $T$ homeomorphically onto some union of edges, namely the unique regulated path joining the images of its two endpoints within $T$.

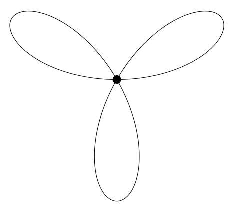

For a polynomial map with a superattracting cycle, there is a modified version of this definition which is sometimes helpful, since it more closely resembles the Julia set. Let $F_T$ be the union of all Fatou components in $K(F)$ which contain vertices of $T$ (or which contain points of the finite set $S$). Then the boundary $\mathcal{P}(T)$ of the union $T \cup F_T$ will be called the ***puffed-out Hubbard tree***. It consists of $\partial F_T$ (the union of the boundary circles of these Fatou components), together with $T \smallsetminus F_T$ (that part of the tree which lies outside of $F_T$). As an example, the minimal tree $T$ for the Douady rabbit is the dark tripod shown in Figure 27, while the puffed-out tree $\mathcal{P}(T)$ is homeomorphic to the above sketch. Other examples of puffed-out trees are shown in Figures 34 and 35. We will see that $T$ and $\mathcal{P}(T)$ contain the same information; so that we can use whichever one seems more convenient.

In this paper we will usually concentrate on the ***minimal*** Hubbard tree, taking $S$ to be the union of the orbits of the critical points. However, the construction works equally well taking a larger finite set, for example by also including one or more periodic orbits. If $T \subset K(F)$ is an arbitrary Hubbard tree, then each iterated preimage is also a Hubbard tree, so that we form an ascending sequence

$$T \subset F^{-1}(T) \subset F^{-2}(T) \subset \cdots \subset K(F).$$

If we exclude the case where $T$ is a single point (the minimal tree for $F(z) = z^d$), then the union of the $F^{-n}(T)$ is everywhere dense in the filled Julia set $K(F)$. Similarly, the puffed-out trees $\mathcal{P}(F^{-n}(T)) \subset K(F)$ provide better and better approximations to the Julia set as $n \to \infty$.

We will ignore complications in the geometry of $T$ and think of it simply as a one-dimensional acyclic simplicial complex. Three additional elements of structure are immediately apparent:

**(1)** There is a prescribed map (the restriction of $F$) from the set $V$ of vertices to itself. This carries the two endpoints of any edge to distinct points, so that it can be extended to a map from $T$ to itself which is one-to-one on each edge.

**(2)** We must specify which vertices are critical points, and with what multiplicity. It will be convenient to describe this by the ***local degree function*** $d : V \to \{1, 2, 3, \ldots\}$, where we set $d(\mathbf{v}) = 1$ if the vertex $\mathbf{v}$ is non-critical and $d(\mathbf{v}) = m + 1 \geq 2$ if $\mathbf{v}$ is a critical point of multiplicity $m$.

($\mathbf{3_0}$) If three or more edges meet at a vertex, then the cyclic order of these edges in the positive direction around this vertex must be specified. Note that this cyclic order determines, up to isotopy, how the tree is to be embedded into $\mathbb{C}$.

However, this data is not sufficient to uniquely determine the affine conjugacy class of $F$. For example Figures 32 and 33 illustrate Julia sets which are not affinely conjugate to their mirror images, although this fact cannot be deduced if we are given only the data above. Similarly, the three puffed-out trees at the top of Figure 35 cannot be distinguished without further information. For this reason we introduce the ***angles*** between edges of the tree as an essential part of the structure.

Let $\mathbf{e}_1, \mathbf{e}_2, \ldots, \mathbf{e}_n$ be the edges incident to a single vertex, listed in positive cyclic order, where the subscripts are interpreted as integers modulo $n$ so that $\mathbf{e}_0 = \mathbf{e}_n$. Then the angles between successive edges $\mathbf{e}_j$ and $\mathbf{e}_{j+1}$ are to be positive rational numbers with sum

$$\angle(\mathbf{e}_0, \mathbf{e}_1) \;+\; \angle(\mathbf{e}_1, \mathbf{e}_2) \;+\; \cdots \;+\; \angle(\mathbf{e}_{n-1}, \mathbf{e}_n) = 1\,.$$

More generally, the angle (in the positive direction) between any two edges meeting at a common vertex is well defined. We will think of this angle as an element of the circle $\mathbb{Q}/\mathbb{Z}$, and replace the hypothesis ($\mathbf{3_0}$) by the following sharper hypothesis. It will be convenient to use the notation $F_{\mathbf{v}}(\mathbf{e})$ for the unique edge which contains $F(U \cap \mathbf{e})$, where $U$ is a small neighborhood of $\mathbf{v}$.

(**3**) This angle $\angle(\mathbf{e}, \mathbf{e}') \in \mathbb{Q}/\mathbb{Z}$ is well defined for any two edges meeting at a common vertex $\mathbf{v}$, and satisfies

$$\angle(\mathbf{e}, \mathbf{e}') + \angle(\mathbf{e}', \mathbf{e}'') \;\equiv\; \angle(\mathbf{e}, \mathbf{e}'')\ (\mathrm{mod}\ \mathbb{Z})\,,$$

with $\angle(\mathbf{e}, \mathbf{e}') \equiv 0$ only if $\mathbf{e} = \mathbf{e}'$. Furthermore, for the image of two such edges near $\mathbf{v}$, we have

$$\angle\Big(F_{\mathbf{v}}(\mathbf{e}),\, F_{\mathbf{v}}(\mathbf{e}')\Big) \;\equiv\; d(\mathbf{v})\, \angle(\mathbf{e}, \mathbf{e}') \qquad (\mathrm{mod}\ \mathbb{Z})\,. \tag{A1}$$

For the definition of the angle between two edges, we must distinguish two cases, as follows.

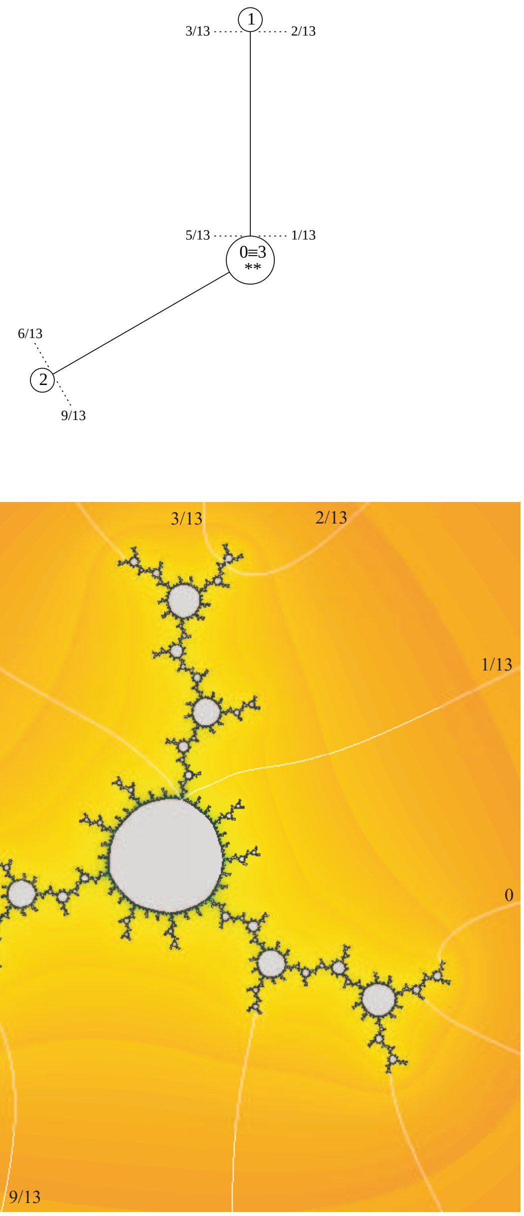


Figure 32: The top sketch shows a cubic Hubbard tree with a double critical point at which the two adjacent branches form an angle of $1/3$ $(= 120°)$. External angles along the root orbit have been indicated. The lower figure shows the corresponding Julia set. All external rays with angles of the form $k/13$ are shown in white.

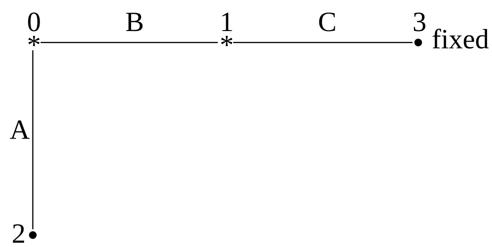


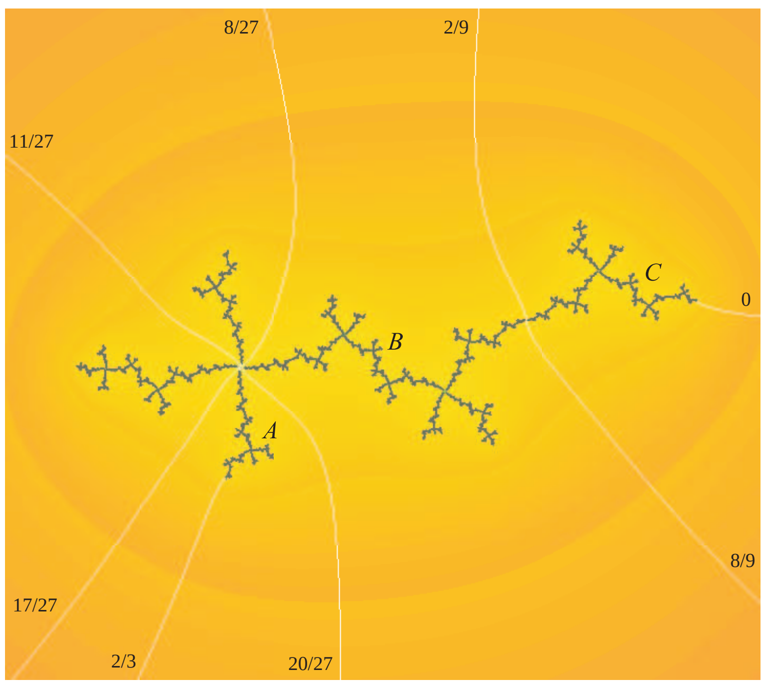


Figure 33: The top sketch shows a Hubbard tree with a right angle. The critical orbit maps as $0 \mapsto 1 \mapsto 2 \mapsto 3 \circlearrowleft$, where $0$ and $1$ are simple critical points, while the edges of the tree map as $A \mapsto C \mapsto A \cup B \cup C$, $B \mapsto \overline{B} \cup \overline{A}$, where the overline stands for reversal of orientation. The corresponding cubic Julia set is shown below. Here 0 and 1 are the landing points of the 8/27 and 2/9 rays.

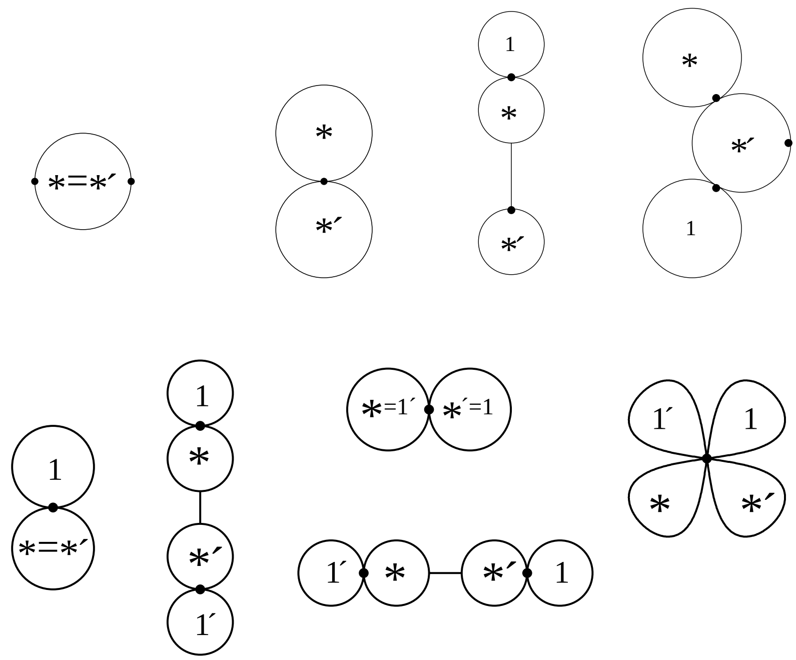


Figure 34: Puffed-out Hubbard tree representations for the nine essentially distinct maps with both critical orbits periodic of period $\leq 2$. The top row illustrates four maps which have a critical fixed point, denoted by $*'$. The first two represent points in $\mathcal{S}_1 \cap \mathcal{S}'_1$, namely the map $z \mapsto z^3$ with a fixed double critical point, and the map $z \mapsto z^3 + \frac{3}{2}z$ with two critical fixed points. The next two maps correspond to points in $\mathcal{S}_2 \cap \mathcal{S}'_1$, with a period two critical orbit, indicated by $* \leftrightarrow 1$, as well as the fixed critical point $*'$. The remaining five diagrams represent in $\mathcal{S}_2 \cap \mathcal{S}'_2$ with both critical orbits of period 2, labeled by $* \leftrightarrow 1$ and $*' \leftrightarrow 1'$. The dots on the boundary circles represent periodic points of minimal period on the boundary of the corresponding Fatou component. (When two such Fatou components touch each other, the associated edge of the tree has been collapsed to a point in these two figures.) In each case we can obtain representatives for all maps in the corresponding $\mathcal{S}_p \cap \mathcal{S}'_q$ from the illustrated examples by making use of conjugation by $z \leftrightarrow -z$ $(180^\circ$ degree rotation), together with complex conjugation (reflection in a horizontal line).

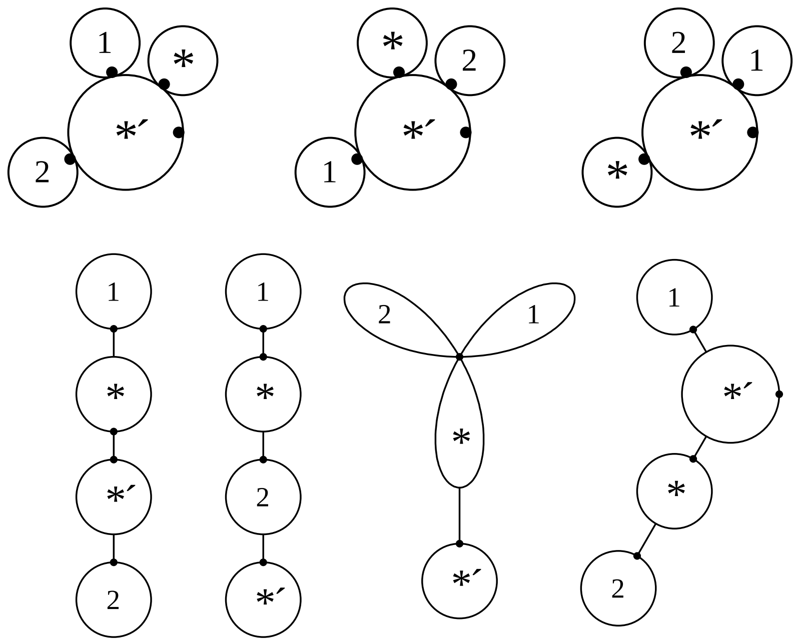


Figure 35: Trees for the seven essentially different maps in $\mathcal{S}_3 \cap \mathcal{S}'_1$. Here the period three critical orbit is labeled by the symbols $* \mapsto 1 \mapsto 2 \mapsto *$, while the fixed critical point is labeled by $*'$. Note the $1/7$, $2/7$, $4/7$ internal angles for the top three examples, and the $1/3$, $2/3$ internal angles for the last example.

**Definition A.1.** Call a vertex $\mathbf{v} \in T \subset K(F)$ either a ***Fatou vertex*** or a ***Julia vertex*** according as it belongs to the Fatou set or the Julia set of $F$. In fact we can make this distinction just from the structures **(1)** and **(2)** described above: *It is easy to check that* $\mathbf{v}$ *is a Fatou vertex if and only if some forward image of* $\mathbf{v}$ *is a periodic critical point.* In the figures, we will usually emphasize this distinction by replacing each Fatou vertex by a small circle.

In the case of two edges of $T$ which meet at the center of a Fatou component $U$ of $F$, the definition of this angle is straightforward. There is an essentially unique conformal diffeomorphism taking $U$ to the unit disk and taking each edge intersected with $U$ to a radius. We can then use the usual angle, as measured within the unit disk. Since the map $F$ from $U$ to $F(U)$ corresponds to the map $w \mapsto w^{d(\mathbf{v})}$ between disks, the identity (A1) follows easily.

In the case of edges meeting at a Julia vertex $\mathbf{v}$, Poirier defines this angle as follows. If $\mathbf{v}$ is periodic under $F$, and if $n$ edges meet at $\mathbf{v}$, then we simply define the angle between two edges which are consecutive in cyclic order to be $1/n$. In the more general case where $\mathbf{v}$ is not periodic, we must choose these angles so that Equation (A1) is satisfied. However, it may happen that there is more than one possible choice. In that case, we can resolve the difficulty as follows. Suppose that $F^{\circ m}(\mathbf{v})$ is periodic. Then $F^{-m}(T)$ will have a full complement of edges meeting at $\mathbf{v}$. If there are $n$ such edges, then we again define the angle between two which are consecutive in cyclic order to be $1/n$. As an example, in Figure 33, the angle $\angle(A, B)$ could a priori be either $1/4$ or $3/4$. In this case, it suffices to pass to $F^{-1}(T)$ which has four edges meeting at this point, in order to determine that the correct angle is $1/4$.ß

**Definition A.2.** By an ***abstract tree*** we will mean a topological tree which has been provided with a mapping from vertices to vertices, a local degree function, and an angle function satisfying the conditions **(1)**, **(2)** and **(3)** above. Note that the cyclic order ($\mathbf{3_0}$) is uniquely determined by the angular structure **(3)**.

The problem is now to characterize which abstract trees can actually be realized as the Hubbard trees of polynomials. Poirier provides a very simple answer as follows.

**Theorem A.3. (Poirier).** An abstract tree can be realized as the Hubbard tree of a polynomial if an only if two conditions are satisfied:

1. **Expansiveness.** For every edge $\mathbf{e}$, either at least one of its two boundary points is a Fatou vertex, or else some forward image $F^{\circ k}(\mathbf{e})$ covers two or more edges.[6]
2. **Normalization.** The consecutive angles around any periodic Julia vertex are all equal.

When these conditions are satisfied, the resulting polynomial is unique up to affine conjugation, and has degree $d$ satisfying $d-1 = \sum_{\mathbf{v}} \Big(d(\mathbf{v})-1\Big)$.

For the proof, the reader is referred to (Poirier 93). □

We can also use these ideas to construct the puffed-out Hubbard tree, starting only with the abstract tree. Simply replace each Fatou vertex by a small circle. Now for any edge $\mathbf{e}$ which does not contain a pre-critical point in its interior (or in other words , any edge such that no forward image crosses through a critical point), collapse that portion $\mathbf{e}_0$ of $\mathbf{e}$ which is outside of the small circles to a single point. It is not difficult to check that the result is homeomorphic to the puffed-out tree as described above. As an example, in Figure 12a, neither edge has an interior pre-critical point, hence both edges must be collapsed, yielding the top right diagram of Figure 34.

To conclude this appendix, here are a few elementary remarks.

As in §6, define the ***valence*** $n(\mathbf{v})$ to be the number of edges of $T$ which are incident at the vertex $\mathbf{v}$. Thus $n(\mathbf{v}) \geq 1$, except in the trivial case of a

[6] An equivalent expansivity condition, used by (Bruin and Schleicher 01), is the following: ***For every edge*** $\mathbf{e}$ ***there must be some forward image*** $F^{\circ k}(\mathbf{e})$ ***which contains a critical point (perhaps on its boundary).*** It is not difficult to show that this Bruin-Schleicher condition is completely equivalent to Poirier's condition.

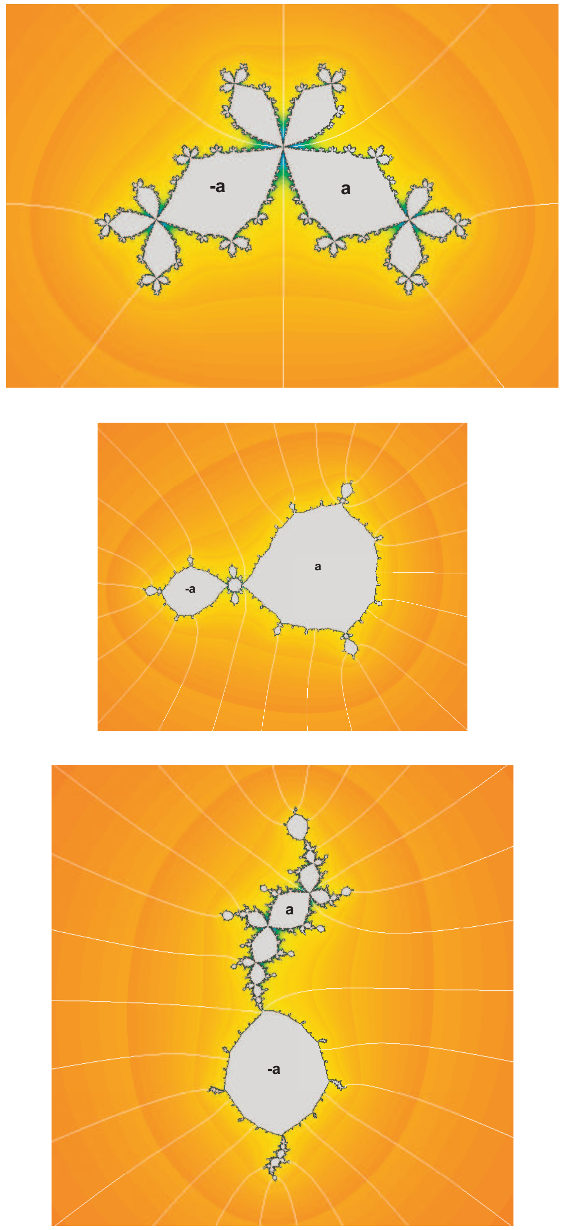


Figure 36: Julia sets for three representative examples. The "bow tie" Julia set above, with polynomial $z^3 - \frac{3}{4}z + i\sqrt{7}/4$, corresponds to the last tree in Figure 34. All rays with denominator $3^2 - 1 = 8$ are shown. The next, on the left, corresponds to the top right tree in Figure 35, and the last "dancing rabbit" example corresponds to the next to last tree in Figure 31. All rays of denominator $3^3 - 1 = 26$ are shown in these two cases.

tree consisting of a single vertex. The tree $T$ is said to be ***minimal*** if every vertex with $n(\mathbf{v}) \le 2$ is critical or post-critical. It is not hard to check that every Hubbard tree contains a unique minimal one.

Note the inequality

$$n(F(\mathbf{v})) \;\ge\; n(\mathbf{v})/d(\mathbf{v})\,, \tag{A2}$$

which follows easily from formula ($A1$). As an example, in the case of a periodic Julia vertex it follows that $n(\mathbf{v})$ takes the same value at all vertices of the cycle. (This was assumed earlier when we assigned the angle $\angle(\mathbf{e},\,\mathbf{e}') = 1/n(\mathbf{v})$ between consecutive edges at a periodic Julia vertex $\mathbf{v}$.)

A vertex $\mathbf{v}$ is said to be an ***endpoint*** (or a ***free vertex***) of $T$ if $n(\mathbf{v}) \le 1$. As noted in the proof of Lemma 6.5, *every tree has at least one endpoint.* (For otherwise, starting with any edge, we could pass to an adjacent edge. Continuing inductively, we could then construct a closed loop, which is impossible.)

Closely related is the Euler characteristic formula $2\,\chi(T) = \sum_{\mathbf{v}\in V}\ (2 - n(\mathbf{v}))$, which holds for any one dimensional simplicial complex. In the case of a tree, we have $\chi(T) = 1$, so that

$$\sum_{\mathbf{v}} \Big(2 - n(\mathbf{v})\Big) \;=\; 2\,. \tag{A3}$$

This clearly implies that there is at least one vertex with $n(\mathbf{v}) \le 1$.

# References


P. Atela 1992, *Bifurcations of dynamic rays in complex polynomials of degree two*, Ergodic Theory Dynam. Systems **12**, 401–423.

B. Bielefeld 1989, *Changing the order of critical points of polynomials using quasiconformal surgery*, Thesis, Cornell University.

P. Blanchard 1984, *Complex analytic dynamics on the Riemann sphere*, Bull. A. M. S. **11**, 85-141.

P. Blanchard, R. Devaney and L. Keen 1991, *The dynamics of complex polynomials and automorphisms of the shift*, Invent. Math. 104, 545–580.

A. Bonifant and J. Milnor, *Cubic polynomial maps with periodic critical orbit, Part 2*, in preparation.

B. Branner 1986, *The parameter space for cubic polynomials*, pp. 169-179 of "Chaotic Dynamics and Fractals", edit. Barnsley and Demko, Acad. Press.

B. Branner and J. H. Hubbard 1988, *The iteration of cubic polynomials I, The global topology of parameter space*", Acta Math. **160**, 143–206.

B. Branner and J. H. Hubbard 1992, *The iteration of cubic polynomials II, patterns and parapatterns,* Acta Math. **169**, 229–325.

B. Branner 1993, *Cubic polynomials, turning around the connectedness locus,* pp. 391–427 of "Topological Methods in Mathematics" (edit. Goldberg and Phillips), Publish or Perish.

M. Brown 1960, *A proof of the generalized Schoenflies theorem*, Bulletin A.M.S. **66**, 74-76. (See also "*The monotone union of open n-cells is an open n-cell*", Proc.A.M.S. **12** (1961) 812-814.)

H. Bruin and D. Schleicher 2001, *Symbolic Dynamics of Quadratic Polynomials,* Preprint, Institut Mittag-Leffler, (2001/02) 128 pages.

X. Buff and C. Henriksen 2001, *Julia sets in parameter spaces,* Comm. Math. Phys. **220**, 333–375.

P. Cvitanović and J. Myrheim 1989, *Complex universality*, Comm. Math. Phys. **121**, 225–254.

A. Douady and J. H. Hubbard 1982, *Itération des polynômes quadratiques complexes*, CRAS Paris **294**, 123-126.

A. Douady and J. H. Hubbard 1984/85, *Étude dynamique des polynômes complexes, Parts I and II*, Publ. Math. d'Orsay.

A. Douady and J. H. Hubbard 1985, *On the dynamics of polynomial-like mappings*, Ann. Sci. Ec. Norm. Sup. (Paris) **18**, 287-343.

D. Faught 1992, *Local connectivity in a family of cubic polynomials*, Thesis, Cornell University.

L. Goldberg and J. Milnor 1993, *Fixed points of polynomial maps. II. Fixed point portraits,* Ann. Sci. École Norm. Sup. **26**, 51–98.

J.H. Hubbard 1993, *Local connectivity of Julia sets and bifurcation loci, three theorems of J.-C. Yoccoz*, pp. 467–511 of "Topological Methods in Mathematics" (edit. Goldberg and Phillips), Publish or Perish.

J. Kiwi 2006, *Puiseux series polynomial dynamics and iteration of complex cubic polynomials*, Ann. Inst. Fourier (Grenoble) **56**, 1337–1404.

P. Lavaurs 1989, *Systèmes dynamiques holomorphes: explosion de points periodiques paraboliques,* Thesis, Université Paris-Sud.

T. Li (Tao Li) 2007, *A monotonicity conjecture for the entropy of Hubbard trees*, Thesis, Stony Brook University.

J. Luo 1995, *Combinatorics and holomorphic dynamics: captures, matings, Newton's method,* Thesis, Cornell University.

J. Milnor 1989, *Self-similarity and hairiness in the Mandelbrot set*, pp. 211-257 of "Computers in Geometry", edit. M. Tangora, Lect. Notes Pure Appl. Math. **114**, Dekker.

J. Milnor 1992a, *Remarks on iterated cubic maps,* Experiment. Math. **1**, 5–24.

J. Milnor 1992b, *Hyperbolic components in spaces of polynomial maps,* with an appendix by A. Poirier, Stony Brook IMS preprint 1992-3.

J. Milnor 1993, *Geometry and dynamics of quadratic rational maps,* Experimental Math. **2**, 37–83.

J.Milnor 2000, *Periodic orbits, external rays, and the Mandelbrot set*, in "Géometrie Complexe et Systèmes Dynamiques," Astérisque **261**, 277–333.

J. Milnor 2006, "Dynamics in One Complex Variable," 3rd edition, Princeton University Press.

C. L. Petersen and Tan Lei 2004, *The central hyperbolic component of cubic polynomials*. See http://www.u-cergy.fr/rech/pages/tan/ .

A. Poirier 1993, *On Postcritically Finite Polynomials, Part 2: Hubbard Trees,* Stony Brook IMS preprint 1993-7.

M. Rees 1990, *Components of degree two hyperbolic rational maps,* Invent. Math. **100**, 357-382.

M. Rees 1992, *A partial description of parameter space of rational maps of degree two*, Part I: Acta Math. **168**, 11–87.

M. Rees 1995, *A partial description of parameter space of rational maps of degree two*, Part II: Proc. London Math. Soc. **70**, 644–690.

P. Roesch 1999, *Puzzles de Yoccoz pour les applications à allure rationnelle*, L'Enseign. Math. **45**, 133-168.

P. Roesch 2006, *Hyperbolic components of polynomials with a fixed critical point of maximal order*, arXiv:math/0612172. (Published version to appear.)

D. Schleicher 2004, *On fibers and local connectivity of Mandelbrot and Multibrot sets*, Proc. Symp. Pure Math. **72, I**, Fractal Geometry and Applications, AMS, 477–517.

Tan L. and Yin, Y. 1996, *Local connectivity of the Julia set for geometrically finite rational maps.* (English summary) Sci. China Ser. A **39**, 39–47.

Tan L. (Tan Lei) 1997, *Branched coverings and cubic Newton maps,* Fund. Math. **154**, 207–260.

B. Wittner 1988, *On the bifurcation loci of rational maps of degree two*, Thesis, Cornell University.